UNIVERSITY OF CALIFORNIA SAN DIEGO

BIOPHYSICAL MECHANISMS OF DISTURBANCES TO SYNOVIAL JOINT LUBRICANT HOMEOSTASIS IN POST-TRAUMATIC OSTEOARTHRITIS

A dissertation submitted in partial satisfaction of the

requirements for the degree Doctor of Philosophy

in

Bioengineering

by

Aimee R. Raleigh

Committee in Charge:

Professor Robert L. Sah, Chair
Professor Gary S. Firestein, Co-Chair
Professor Koichi Masuda
Professor Geert W. Schmid-Schönbein
Professor Liangfang Zhang

2018

The Dissertation of Aimee R. Raleigh is approved, and it is acceptable in quality and form for publication on microfilm and electronically:

_____

_____

_____

_____

Co-Chair

_____

Chair

University of California San Diego
2018

TABLE OF CONTENTS

LIST OF FIGURES

LIST OF TABLES

ACKNOWLEDGMENTS

I would first like to greatly acknowledge my graduate research advisor and dissertation committee Chair, Dr. Robert Sah, as well as my dissertation committee Co-Chair, Dr. Gary Firestein. Thank you both for the opportunity to learn from your expertise, for challenging me to extend my experiments, and for the many hours of research planning and discussions. Dr. Sah, thank you especially for the countless hours spent working on projects, proposals, and papers, and for the continuing education on topics ranging from troubleshooting experiments to efficient data presentation to statistics. I am truly grateful for the growth I have experienced over the past five years, and will forever cherish my time in the Cartilage Tissue Engineering lab.

I would also like to thank the other members of my dissertation committee: Dr. Koichi Masuda, Dr. Geert Schmid-Schönbein, and Dr. Liangfang Zhang for their valuable input over the past few years at UCSD. Thank you for the insightful questions, feedback, and suggestions.

I am incredibly grateful to Dr. Koichi Masuda for the many long hours in his lab he dedicated to teaching me molecular biology and rabbit surgery techniques, for letting me use his state-of-the-art equipment, and for the countless discussions we have shared during my time here. Thank you for your generosity and insight.

I would like to thank the members (both current and former) of the CTE lab who have helped me in countless ways over the years. Michele, thank you for welcoming me into the lab and teaching me many of the biochemical techniques used in my studies. Barb, thank you for your ingenious ideas and suggestions and your encouragement with all things PRG4-related over the years. Albert, thank you for introducing me to PCR and for the collaboration and discussion. Van, thank you for all of your help troubleshooting issues (especially those technology-related).

Finally, I am so grateful for the support of friends, siblings, parents, and relatives during my time at UC San Diego. Thank you for your patience and encouragement.

Chapter 2 will be submitted to *Nature Biomedical Engineering*. The dissertation author was the primary author and thanks co-authors Michele M. Temple-Wong, Yang Sun, Dongfang Qian, Kenji Kato, Koichiro Murata, Gary S. Firestein, Koichi Masuda, and Robert L. Sah. This work was supported by research grants from the National Institutes of Health (R01 AR055637, T32 AR060712), the Department of Defense (DOD OR13085), the UC San Diego Frontiers of Innovation Scholarship Program, and the San Diego Fellowship.

Chapter 3 will be submitted to *European Cells and Materials*. The dissertation author was the primary author and thanks co-authors Julian J. Garcia, Maegen J. Cravotta, Barbara L. Schumacher, Kenjo Kato, Gary S. Firestein, Koichi Masuda, and Robert L. Sah. This work was supported by research grants from the National Institutes of Health (R01 AR055637, T32 AR060712), the Department of Defense (DOD OR13085), the UC San Diego Frontiers of Innovation Scholarship Program, and the San Diego Fellowship.

Chapter 4 will be submitted to *Arthritis & Rheumatology*. The dissertation author was the primary author and thanks co-authors Julian J. Garcia, Barbara L. Schumacher, Shingo Miyazaki, Junichi Yamada, Gary S. Firestein, Koichi Masuda, and Robert L. Sah. This work was supported by research grants from the National Institutes of Health (R01 AR055637, T32 AR060712), the Department of Defense (DOD OR13085), the UC San Diego Frontiers of Innovation Scholarship Program, and the San Diego Fellowship.

Chapter 5 will be submitted to *Osteoarthritis and Cartilage*. The dissertation author was the primary author and thanks co-authors Julian J. Garcia, Barbara L. Schumacher, Junichi Yamada, Shingo Miyazaki, Raeek Rahman, Rebecca L. Drake, Gary S. Firestein, Robert L. Sah,

and Koichi Masuda. This work was supported by research grants from the National Institutes of Health (R01 AR055637, T32 AR060712) and the Department of Defense (DOD OR13085).

I would also like to acknowledge support by the National Institute of Health, Department of Defense, UC San Diego Frontiers of Innovation Scholarship Program, the San Diego Fellowship, and the ARCS Foundation, without which my studies would not have been possible.

VITA

2013	B.S.E, Biomedical Engineering Duke University, Durham, North Carolina
2013-2018	Graduate Student Researcher Cartilage Tissue Engineering Laboratory University of California San Diego, La Jolla, California
2014	M.S., Bioengineering University of California San Diego, La Jolla, California
2018	Ph.D., Bioengineering University of California San Diego, La Jolla, California

Book Chapter

Raleigh AR, McCarty WJ, Chen AC, Meinert C, Klein TJ, Sah RL. Synovial joints: Mechanobiology and tissue engineering of articular cartilage and synovial fluid. In: Comprehensive Biomaterials, Ducheyne P, Healey KE, Hutmacher DE, Grainger DE, Kirkpatrick CJ Eds.: Elsevier 2017:107-134.

Journal Articles

Raleigh AR, Temple-Wong MM, Sun Y, Qian D, Kato K, Murata K, Firestein GS, Masuda K, Sah RL. Fluctuation of synovial fluid hyaluronan concentration in post-traumatic osteoarthritis joints depends on the dynamic balance between biosynthesis, loss, and dilution. *Nature Biomedical Engineering. Submitted.*

Raleigh AR, Garcia JJ, Schumacher BL, Miyazaki S, Yamada J, Firestein GS, Masuda K, Sah RL. Synovial fluid: Serum ratio of protein concentration is increased in experimental osteoarthritis and inversely correlated with synovial fluid hyaluronan concentration. *In preparation*.

Raleigh AR, Garcia JJ, Cravotta MJ, Schumacher BL, Kato K, Firestein GS, Masuda K, Sah RL. Decreased synovial fluid proteoglycan-4 concentration in ACL-transected knee joints is due to dynamic imbalance in biosynthesis, clearance, and effusion. *In preparation*.

Raleigh AR, Garcia JJ, Schumacher BL, Yamada J, Miyazaki S, Rahman R, Drake RL, Firestein GS, Sah RL, Masuda K. Select viscosupplement therapies decrease experimental & theoretical measures of lubricant loss from the synovial joint. *In preparation*.

Temple-Wong MM, Raleigh AR, Frisbie DD, Sah RL, McIlwraith CW. Articular cartilage lubrication with polyglycan: Effects in vitro and with in vivo supplementation following osteochondral fracture in the horse. *Osteoarthritis Cartilage. Submitted*.

Vernekar VN, Wallace CS, Wu M, Chao JT, O'Connor SK, Raleigh AR, Liu X, Haugh JM, Reichert WM. Bi-ligand surfaces with oriented and patterned protein for real-time tracking of cell migration. *Colloids Surf B*. 123:225-35, 2014.

Selected Abstracts

Raleigh AR, Cravotta MJ, Garcia JJ, Schumacher BL, Kato K, Firestein GS, et al. Decreased synovial fluid proteoglycan-4 concentration in ACL-transected knee joints is due to dynamic imbalance in biosynthesis, clearance, and effusion. *OARSI World Congress* 2018: 204.

Raleigh AR, Garcia JJ, Schumacher BL, Firestein GS, Masuda K, Sah RL. Synovial fluid: Serum ratio of protein concentration is increased in experimental osteoarthritis and inversely correlated with synovial fluid hyaluronan concentration. *Trans Orthop Res Soc* 2018; 43: 509.

Raleigh AR, Sun Y, Qian D, Temple-Wong MM, Kato K, Murata K, Firestein GS, Masuda K, Sah RL. Synovial tissue gene expression following acute injury: Implications for lubricant secretion. *Trans Tiss Eng Regen Med Intnl Soc-North America*, 2016.

Raleigh AR, Sun Y, Qian D, Temple-Wong MM, Kato K, Murata K, et al. Synovial fluid hyaluronan fluctuation in post-traumatic osteoarthritis: Dependence on the dynamic balance between biosynthesis, loss, and fluid flux *Trans Orthop Res Soc* 2017; 42: 1506.

ABSTRACT OF THE DISSERTATION

BIOPHYSICAL MECHANISMS OF DISTURBANCES TO SYNOVIAL JOINT LUBRICANT HOMEOSTASIS IN POST-TRAUMATIC OSTEOARTHRITIS

by

Aimee R. Raleigh

Doctor of Philosophy in Bioengineering

University of California San Diego, 2018

Professor Robert L. Sah, Chair

Professor Gary S. Firesein, Co-Chair

Post-traumatic osteoarthritis (PTOA) progression in synovial joints involves the individual and interactive responses of multiple cell types in articular cartilage (AC) and synovial lining (SL), resulting in alterations in the concentration of functional lubricant

molecules, hyaluronan (HA) and proteoglycan 4 (PRG4) in synovial fluid (SF). We hypothesize that changes in lubricant concentration during disease progression are due to both biophysical and biological processes in the synovial joint. This dissertation aimed to analyze these processes, in a rabbit model of PTOA and in response to selected therapies, using a multi-scale mathematical model, using estimates for *in vivo* lubricant secretion and macromolecular transport properties.

Previous mass balance analyses were extended to model the dependence of SF HA and PRG4 concentrations on rates of lubricant generation, loss, clearance, and SF volume fluxes. Compared to contralateral non-operated (Non-OP) and healthy control (CTRL) joints, ACL-transected (ACLT) knees had lower SF concentrations of both HA and PRG4 at extended times following injury, attributable to distinct biological and biophysical phenomena. Despite increased HA generation by cells in the SL, HA concentration was decreased at both acute and chronic times in ACLT knees due to increased loss and clearance rates, as well as increased SF volume (diluting the HA in SF). PRG4 concentrations were decreased only at extended times post-injury, due to a substantial reduction in the rates of PRG4 synthesis by cells in the SL and AC, in addition to dilution effects of SF effusions. One potential mechanism of increased lubricant loss following acute injury is altered SL transport. An increase in the ratio of protein in SF to that in serum, $k^{SF:S}$, was correlated with a decreased HA concentration, and particularly with decreased HA of high molecular mass. The increases in $k^{SF:S}$ suggest that changes to SL architecture following injury (such as that stemming from increased cellular proliferation, matrix reorganization, and stretching due to joint swelling) may impact its permeability to large molecules, such as HA and PRG4. When viscosupplement therapies were applied in three serial injections following ACLT, the decreases in lubricant concentrations were reversed, due to

increased lubricant secretion as well as maintenance of SL macromolecular retention (attenuated $k^{SF:S}$).

The refinement of a multi-scale model that mechanistically describes variations in SF lubricant concentrations using *in vivo* rabbit data can serve as a foundation for better understanding the basis for SF dynamics, as well as elucidating timeframes in which an intervention may reverse progressive joint degradation. The modeling indicates that metrics and markers of synovial joint health need to include not only biological indices at the levels of cells (biosynthesis) and molecules (causing degradation), but also physical properties of tissues (membrane permeability) and organs (fluid flux).

CHAPTER 1

INTRODUCTION

1.1 General Introduction to the Dissertation

The complex synovial fluid (SF) milieu, containing fluid and macromolecular components that are continuously turned over, has important implications for joint nutrition and lubrication. Following an acute injury, there is often a progressive deterioration of synovial joints during osteoarthritis progression, a process influenced by multiple tissue and cell types. A key metric for SF lubrication is the concentration of the molecules hyaluronan (HA) and proteoglycan-4 (PRG4), which reflect dynamic synthesis and loss within the SF but which also correlate with SF function in reducing friction and wear during joint loading and articulation. To investigate the specific biophysical and biological processes governing lubricant turnover in the synovial joint, it is helpful to use a mass balance analysis that allows for evaluation of HA and PRG4 dynamics across various time scales.

The overall motivation of this dissertation was to analyze these processes, in a rabbit model of post-traumatic osteoarthritis and in response to selected therapies, using a multi-scale mathematical model, validated for *in vivo* and *in vitro* lubricant secretion and macromolecular transport properties. The objectives of the studies in this dissertation were: (1) develop, calibrate, and validate a mathematical model for the normal and post-traumatic rabbit synovial joint, reflecting key biological and biophysical properties (Aim 1, Chapters 2-4) and (2) use this model

to evaluate the effect of IA therapies in the rabbit joint, especially with regards to SL changes (Aim 2, Chapter 5).

Chapter 1 begins with an introduction to the structure, composition, and function of the key components of the synovial joint: the synovial fluid, synovial lining and underlying synovial subintima (together comprising the synovium), and the articular cartilage. Key lubricating molecules in SF (hyaluronan and proteoglycan 4) are outlined. A discussion of post-traumatic osteoarthritis, animal models to evaluate disease progression, and the motivation to fully understand its pathogenesis, follows. Finally, the chapter concludes with a discussion of joint transport and its importance for SF function.

Chapter 2, which is currently being prepared for submission to *Nature Biomedical Engineering*, continues the introduction of the lubricant hyaluronan, with a discussion of known information from past literature and a special focus on the difficulty of studying its dynamics *in vivo*. An updated mass balance model for studying hyaluronan dynamics following ACL transection in the rabbit knee is presented, and *in vivo* data is used to calibrate the model. Variables measured, calculated, or estimated from the model are presented, as are the implications for the role of c^{SF}_{HA} in the progression of PTOA.

Chapter 3, which is currently being prepared for submission to *European Cells and Materials*, continues the introduction of the lubricant proteoglycan-4, with a discussion of the various joint cell populations that secrete the molecule, and with a special focus on the difficulty of studying its dynamics *in vivo*. The mass balance model introduced in Chapter 2 is used to evaluate proteoglycan-4 dynamics following ACL transection in the rabbit knee. The variable c^{SF}_{PRG4} following injury is evaluated, and the key mechanisms governing its magnitude at acute and chronic times is presented.

Chapter 4, which is currently being prepared for submission to *Arthritis & Rheumatology*, continues the introduction of the protein content in the synovial fluid, and discusses its relevance as a biomarker for arthritis progression when compared to serum protein content. The ratio of protein in SF to serum ($k^{SF:S}$) across a continuous molecular mass range is evaluated in the rabbit model of PTOA. The total protein content, as well as $k^{SF:S}$ in specific molecular mass bins, is used to assess changes to protein transport from the serum to the SF following acute injury, and is compared to $c^{SF}{}_{HA}$ to evaluate potential implications of increased joint protein influx on SF lubricant function.

Chapter 5, which is currently being prepared for submission to *Osteoarthritis and Cartilage*, uses the mass balance model introduced and used in Chapters 2 and 3, as well as the novel SL permeability metric introduced in Chapter 4, to evaluate the effect of viscosupplement therapies on PTOA progression in the rabbit knee. Changes in variables pertaining to SF and SL dynamics are presented, as are implications for the early administration of IA therapy to mitigate lubricant loss from the synovial cavity.

Chapter 6 summarizes the major findings of the studies presented here, and discusses the implications for research of early mediators of synovial joint lubricant dysregulation following injury.

1.2 Structure, Composition, and Function of Healthy Synovial Joints

In diarthrodial joints, articular cartilage (AC) surfaces are bordered by subchondral bone and synovial fluid (SF, **Figure 1**). SF is an ultrafiltrate of plasma that contains lubricating molecules such as hyaluronan (HA) and proteoglycan-4 (PRG4) that are synthesized by resident cells within the joint tissues [38, 76]. SF is encapsulated by both AC and a thin synovium (SYN), and its volume (V^{SF}) and molecular content are continually recirculating, providing nutrients, signaling proteins, and removing waste products for cells in the SYN, AC, meniscus, and anterior and posterior cruciate ligaments [93]. Because it provides lubrication for apposing joint surfaces and functions to reduce the friction coefficient, the SF is functionally important in joint articulation. The metabolism of cells in the joint, as well as influx of plasma proteins, influences the biochemical composition of the SF.

1.2.1. Synovial Fluid

SF is normally a straw-colored, viscous fluid contained within the synovial cavity by the SL. The key functions of SF are as a biomechanical lubricant and as a conduit for metabolites, cellular waste products, and soluble signaling factors. The metabolism of cells in the joint, as well as influx of plasma proteins, influences the biochemical composition of the SF. In the normal human knee joint, the volume of SF is on the order of 1 mL [98], of which the fluid and protein content is turned over in ~1-2 hrs [19]. In healthy joints, the SF molecular components (including lubricants, proteins, and soluble mediators) and fluid volume give rise to its unique properties and functions in maintaining joint homeostasis.

The SF, in addition to serving as a reservoir for nutrients and signaling molecules for resident joint cells, also contains high-M_r molecules that are retained in the synovial cavity due to their large size, contributing to maintenance of SF volume during joint flexion [114, 115]. The composition of SF reflects its origin as a plasma ultrafiltrate. The protein composition of SF is similar to that of plasma [101, 102], though SL selectively restricts large plasma proteins in the vasculature from entering the joint space. In normal human SF, the total protein concentration ($c^{SF}_{protein}$) is 25-28 mg/mL, ~30% of the total protein concentration in serum ($c^{S}_{protein}$) [37, 98]. The most abundant SF macromolecule is albumin (~10mg/mL), which serves as a primary contributor to SF oncotic pressure and as a minor contributor to SF viscosity [70]. The SF molecular content is supplemented with lubricating molecules secreted by resident joint cells. These lubricants are HA [85] and PRG4 [106, 124, 125], which are discussed in more detail below.

1.2.2. Synovium

The SYN consists of two layers: a thin intimal synovial lining (SL), which interfaces with the SF and contains both fibroblast-like and macrophage-like synoviocytes (FLS, MLS), and a thicker synovial subintima (SS), which interfaces with vascular and lymphatic structures. The thin SL serves as a joint border, retaining SF and preventing excessive fluid and molecular loss during joint movement [7, 28]. This lining is roughly 50-60 μm thick in humans and 15-40 μm thick in rabbits [49, 91]. The SL is often described as a "membrane," and allows for selective transport of molecules and fluids into and out of the joint space. The flux of molecules and fluids through the SL and into the SF has been modeled using an approach analogous to that taken for trans-capillary flow [61, 62]. The SS consists of a loose network of extracellular matrix

molecules [50, 92], including collagen fibrils (type I, III, and V), microfibrils (type VI), HA, chondroitin and heparan sulfate, fibronectin, and laminin [70]. The SS includes penetrating vasculature (from capillaries, C) and lymphatics (L), but as a loose and disorganized tissue provides little resistance to flux of fluids or solutes either into or out of the synovial cavity [50, 92, 99, 116].

Flux of fluid into the joint occurs as blood plasma is filtered through the size-selective capillary and synovial membranes in series [116]. This filtering of blood plasma is a product of both diffusive and advective fluxes, driven by concentration, hydrostatic pressure, and oncotic pressure gradients between the SF and SS compartments [63, 77]. Transport of molecules from the capillaries to the interstitial space and into the SF depends on SL and capillary "membrane" properties, as well as the properties of the solute. The SL permeability to solutes depends on the solute size (given by molecular mass (M_r) or hydrodynamic radius), charge, and concentration. Diffusive and advective transport into and out of the SL occurs through apparent pores (~20-90nm in diameter) in the synoviocyte- and ECM-dense SL tissue [35, 99], making SL permeability to solutes inversely related to their size. High-M_r lubricant molecules are preferentially retained in the joint, as the reflected fraction of high-M_r HA by SL is ~60-75% [100].

1.2.3. Articular Cartilage

AC is an alymphatic, avascular connective tissue that covers the ends of long bones and functions as a low-friction, wear-resistant surface to facilitate joint movement and load-bearing. In AC, articular chondrocytes (ACH) are encapsulated within a water-rich specialized extracellular matrix (ECM) comprised mostly of collagen type II and proteoglycan (PG) [73,

122]. The AC has a high compressive strength due to the negatively charged glycosaminoglycan (GAG) chains in the PG network, which creates an osmotic swelling pressure. In addition, the collagen network provides AC with tensile and shear strength, allowing it to resist the swelling pressure of the PG network [81]. The AC displays zonal architecture and cell and matrix content, with distinguished superficial, middle, and deep zones. The superficial zone of cartilage contains a relatively high cell density (~1-10% by volume), low fixed charge density, and collagen fibrils arranged in parallel to the AC surface [81]. With distance from the AC surface, cell density decreases, cell organization becomes more columnar, water content decreases, and the concentration of PGs (increased) and distribution of collagen fibrils (perpendicular to surface) are altered, so that the mechanical properties of cartilage vary with depth [16].

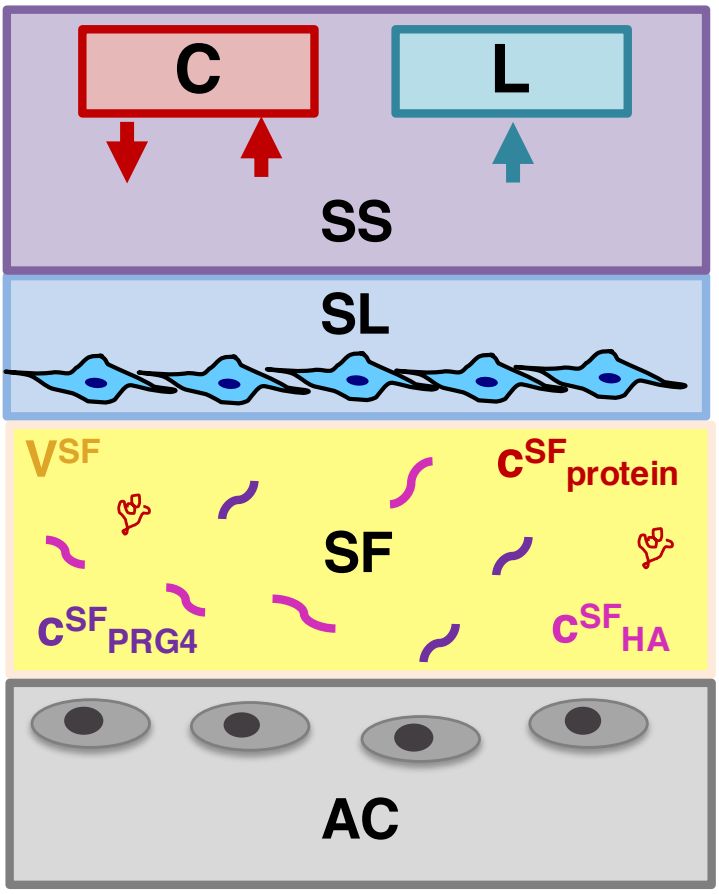

Figure 1.1: Modeling the synovial joint as a series of interconnected compartments. The synovial joint can be modeled as well-mixed tissue compartments (AC, SF, SL, SS) connected at their boundaries. The dynamics of any molecule *i* can be modeled using a mass balance equation relating generation and loss within a compartment of interest. Articular cartilage (AC), synovial fluid (SF), synovial lining (SL), and synovial subintima (SS) compartments are shown, as well as the capillaries (C) and lymphatics (L).

1.3 Role of Joint Lubricants Hyaluronan and Proteoglycan-4

1.3.1. Hyaluronan

One important component of SF is the lubricant HA (**Figure 2**) [38, 93]. HA is a non-sulfated, anionic glycosaminoglycan consisting of repeating disaccharide units of D-glucuronic acid and D-N-acetylglucosamine [32]. The normal concentration of HA in SF (c^{SF}_{HA}) is 1-4 mg/mL, of which most (>70%) is of high molecular mass (M_r, 2-7 MDa) [3, 4, 74]. HA is produced by HA synthases (HAS), which exist as three different isoforms, HAS1, HAS2, and HAS3 [95, 119]. These synthases span the plasma membrane, where they produce and secrete HA into the extracellular matrix. In transfected cells, HAS1 and HAS2 produce high M_r forms of HA, whereas HAS3 produces lower M_r HA [40]. HA production has been attributed to *HAS2* in healthy rabbit FLS, whereas *HAS1* and *HAS3* expression were not or were barely detected in rabbit FLS [79, 86]. The relative contributions of each synthase to the total HA content differs based on cell type and biochemical environment [23, 123]. SF HA is produced primarily by FLS within the SL, with its relatively large surface area and high cell density [39]. FLS HA secretion can be increased *in vitro* with the application of TGF-β1, IL-1β, or TNF-α [9] or the application of static stretch [80], and *in vivo* with stretch of the SL induced by increased V^{SF} [19].

In comparison to the fluid and small solute components of the SF, which turn over in ~1 hour in healthy joints, the turnover time for HA is larger by an order of magnitude, ranging from ~13-34 hours depending on M_r, joint motion, and injury state [14, 24, 52, 70]. HA plays an important role in the maintenance of SF volume and protein content in the presence of pressure gradients, such as during consecutive knee flexion and extension [17, 72]. At c^{SF}_{HA} greater than 1 mg/mL, HA molecular networks interact and form a mesh-like structure that restricts solute and fluid flux at the boundary of the SF and the SL [17, 18, 114, 115]. Due to this high-M_r HA

outflow buffering in joints, SL permeability is a function of c^{SF}_{HA} [64]. Decreases in c^{SF}_{HA}, and especially that of high M_r, have functional implications not only for decreased joint lubrication and viscosity, but also for the maintenance (or lack thereof) of normal V^{SF} and $c^{SF}_{protein}$.

1.3.2. Proteogycan-4

PRG4, also known as superficial zone protein (SZP), lubricin, and megakaryocyte stimulating factor (MSF, all products of the *PRG4* gene), is a ~345 kd mucinous glycoprotein containing multiple O-linked β(1-3)Gal-GalNAc oligosaccharides, which serve as lubricating domains (**Figure 2**) [42, 43, 103, 109, 110, 124]. PRG4 is found at concentrations (c^{SF}_{PRG4}) ranging from 50-450 μg/mL in knee joints [26, 104], and is secreted by chondrocytes in the superficial zone of AC [109], FLS in the SL [110], as well as cells in the meniscus [111, 129] and joint ligaments [58].

PRG4 secretion by superficial zone ACH and SL FLS are modulated by both soluble signaling and biomechanical factors. *In vitro*, the application of TGF-β1 served as a stimulator of AC PRG4 secretion, while IL-1α and TNF- α reduced its secretion by ACH [30, 44, 46, 105]. Biomechanically, PRG4 gene expression and secretion were induced by dynamic compression and shear, as well as continuous passive motion [82-84]. In FLS, PRG4 secretion is increased by *in vitro* supplementation with TGF-β1, but secretion is attenuated with IL-1β [9].

As a lubricant, PRG4 reduces the interaction of articulating cartilage surfaces, especially when these surfaces are in close contact [34, 41, 106, 107]. The values of c^{SF}_{HA} and c^{SF}_{PRG4} are functionally important, as HA and PRG4 lower the friction coefficient and mechanical interaction of articulating cartilage surfaces in a concentration-dependent manner.[1, 57, 74, 106]

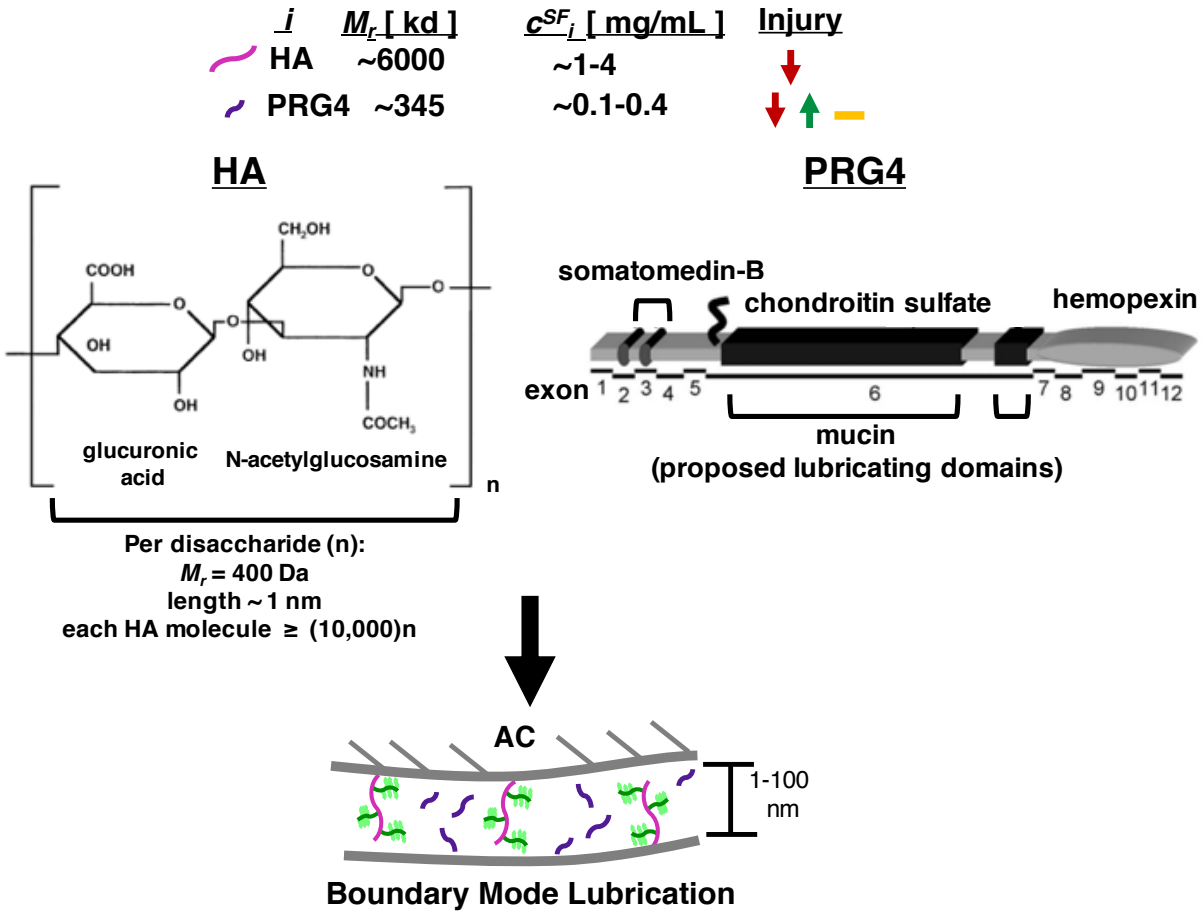

Figure 1.2: Role of synovial fluid constituents in joint lubrication. The lubricating molecules hyaluronan (HA) and proteoglycan-4 (PRG4) play an important role in boundary mode lubrication, when articular cartilage surfaces are in close contact. Hyaluronan is formed by consecutive addition of repeating disaccharides (shown). PRG4 is a glycoprotein consisting of different binding motifs and lubrication domains, some of which are shown. Adapted from [32, 97].

1.4 Synovial Joint Changes in Osteorthritis

1.4.1. Joint Changes in Osteoarthritis

Osteoarthritis (OA) is the most common form of arthritis and as a term encompasses a group of chronic, incapacitating joint diseases that affect over 27 million people in the United States [54]. Commonly affected joints are the knees, hips, and hands and common risk factors include age, obesity, prior traumatic joint injury, and joint malalignment [71]. The disease is often diagnosed radiographically (narrowing joint space or osteophyte formation), clinically (localized joint pain increased with activity, restricted joint motion, functional impairment), or pathologically [13, 54]. Although previously defined as non-inflammatory, OA is increasingly being recognized as an inflammatory condition [20, 22].

Following joint injury[1, 5, 96] or joint surgery [36], as well as during aging and OA progression [74, 127], c^{SF}_{HA} decreases, while variable c^{SF}_{PRG4} have been reported [1, 2, 5, 25, 26]. $c^{SF}_{protein}$ is generally increased in arthritis, especially for high molecular mass (M_r) proteins [53, 60]. In addition, inflammation often induces joint swelling, SL hyperplasia, and SL immune cell infiltration [60, 75]. Resultant changes to V^{SF}, SF hydrostatic and osmotic pressures, and SL architecture may alter membrane properties of the SL, such as those related to solute transport (see below). Changes to the SL in rabbits have been induced experimentally via manipulation of matrix content via enzymatic digestion of protein or GAG components [112, 113] or via manipulation of SF hydrostatic and osmotic pressure by intra-articular (IA) injection of exogenous solutions [51, 59, 90]. In response to these changes, flux of fluid and solute into or out of the joint cavity is increased, suggesting a decrease in the ability of the SL to selectively retain molecules (such as high-M_r lubricants) in the SF.

1.4.2. Animal Models of Post-Traumatic Osteoarthritis

Injury to knee joint tissues (cartilage, subchondral bone, ligament, or meniscus) increases the likelihood of initiation and progression of osteoarthritis (OA) [33, 128]. Animal models of post-traumatic OA (PTOA) allow analysis of SF composition and metabolism over acute-to-chronic (<1, >4 wk) periods [11, 12, 55, 56, 89]. SF lubricant concentration is altered following cases of acute injury, due to changes in rates of biosynthesis and degradation, influx and efflux, and total intra-articular volume [1, 5, 10, 25]. The pathophysiological basis of altered tribological properties following acute injury is unknown and may involve a variety of factors, including altered lubricant synthesis by resident joint cells [9, 10], altered fluid and molecular turnover due to changes in influx and/or efflux, or altered degradation of molecules within the SF.

One such model of PTOA is the rabbit model of ACL transection (ACLT) [15, 75, 94]. Following ACLT in rabbit knees, HA residence time is decreased while synovial proliferation and neovascularization are drastically increased [31, 75], while SL apparent permeability is variably increased [75]. These changes are time-dependent and vary based on model system. Immediately following injury, there is an acute inflammatory response that results in the transient reorganization of the SL due to influx of immune cells [8, 75]. At more chronic time points following injury, a re-organization of the SL barrier influences solute and fluid transport [117, 118]. In addition, effusions raise joint pressure, stretching out the SL tissue and diluting the matrix biopolymers, changing the effective pore size and surface area of the SL [65, 68, 90]. A likely factor in the injury-induced increase in SL transport is altered matrix content and organization, and thus altered membrane permeability, during arthritis progression.

1.4.2. Changes to SF Soluble Signaling Molecules in Early Osteoarthritis

During the onset of chronic inflammatory diseases, imbalances between cell growth, death, and an increase in the production of catabolic cytokines can lead to the development of a pro-inflammatory cascade in the joint. FLS in particular can develop activated phenotypes (defined by a lack of contact inhibition and the ability to grow in anchorage-free conditions), which is associated with further cytokine and protease production [6, 27, 78]. *In vivo*, transient perturbations in the native cellular milieu can drive the development of a pro-inflammatory positive feedback loop, although the exact mechanism is incompletely understood [29]. GM-CSF, M-CSF, TNF-α, and IL-1 stimulate joint macrophages to produce elevated levels of IL-1, TNF-α, and IL-18, which are believed to "activate" FLS (inducing proliferation within the SL) as well as ACH (inducing secretion of degradative proteases such as MMPs) [6, 28, 78, 126]. The feedback cycle is amplified when these "activated" FLS in turn secrete IL-8, IL-6, and GM-CSF, which further stimulate macrophages to continue producing pro-inflammatory stimulants [6, 28, 78, 126]. It is important to consider that the soluble signaling environment of SF also has implications for secretion of lubricants by resident joint cells, as FLS [9] and chondrocytes [47, 108] respond to growth factors and cytokines to either increase or decrease their secretion of HA and PRG4, sometimes in a synergistic fashion.

Because many signaling pathways are involved in the development of inflammatory joint diseases, treatment modalities have evolved to target overall inflammation as well as specific cell receptors and cytokines involved in catabolic processes that are believed to play a role in whole joint degradation. While the paracrine signaling between cells and across different synovial tissues is complex and dynamically evolves during osteoarthritis progression, the outcomes of

such signaling (such as increased FLS proliferation or increased lubricant degradation) are essential to predicting SF lubricant composition and function.

1.5 Theoretical Modeling of Synovial Joint Transport

SF turnover via filtration of blood plasma through the size-selective capillary and synovial lining (SL) "membranes" in series is important for maintaining healthy SF fluid and molecular content [63, 77, 116]. Plasma volume (and therefore associated solute) is driven down hydrostatic pressure gradients from the vasculature to the SF (via advective fluxes), and solute is separately driven down concentration gradients in the same direction (via diffusive fluxes). Therefore, molecular transport across membranes (such as those between the vasculature and SF or between SF and lymphatics) is driven by both advective and diffusive fluxes [21, 45, 66, 67, 69, 87, 88, 93, 121]. In healthy joints, the SF biomolecular composition is in dynamic equilibrium, with molecules entering the SF via transport from plasma to SF and by local cell synthesis, and molecules leaving the SF via transport from SF to the lymphatics or by local degradation [10].

Equations governing fluid transport across biological membranes were originally formulated as a function of hydrostatic and oncotic pressure gradients between the vasculature and adjacent interstitial tissue [120]. Starling's laws have since been tested and adapted for trans-membrane transport by incorporating variables to describe membrane characteristics [45, 87, 121]. Fluid flow into or out of SF (a type of interstitial tissue) can be described by a version of Starling's law modified for a leaky membrane [66, 67, 69, 93]:

$$v_{H_2O}^{\alpha|\beta} = A^{\alpha|\beta} \cdot k^{\alpha|\beta} \cdot \left[\left(P^{\alpha} - P^{\beta} \right) - \sigma_i^{\alpha|\beta} \cdot \left(\pi^{\alpha} - \pi^{\beta} \right) \right], \quad (1)$$

where i is the molecule of interest, α and β represent compartments separated by a membrane, from and to which occurs the flux of water, $v^{\alpha|\beta}{}_{H2O}$. The hydraulic conductance, $k^{\alpha|\beta}$, is a measure of the ease of fluid filtration flow through a membrane. $\Delta P^{\alpha|\beta}$ and $\Delta\pi^{\alpha|\beta}$ are the

hydrostatic and oncotic pressure differences between compartments, $\sigma^{\alpha/\beta}{}_i$ is the reflection coefficient of the membrane, and $A^{\alpha|\beta}$ is the area over which the solute is being transported [93].

$v^{\alpha/\beta}{}_{H2O}$ drives the advective flux of a solute i, $J^{\alpha/\beta}{}_i$, which is described as follows [21, 88]:

$$J_{i,adv}^{\alpha|\beta} = v_{H2O}^{\alpha|\beta} \cdot \left(1 - \sigma_i^{\alpha|\beta}\right) \cdot c_i^{\alpha}, \qquad (2)$$

where $\sigma^{\alpha|\beta}{}_i$ is as described above and $c^{\alpha}{}_i$ is the concentration of i in the source compartment α. The total flux of a solute i across a membrane is the sum the solute flux due to advective fluid flow, $J^{\alpha|\beta}{}_{i,adv}$, and that due to diffusion, $J^{\alpha|\beta}{}_{i,diff}$. $J^{\alpha|\beta}{}_{i,diff}$ is a function of the concentration gradient of i between α and β:

$$J_{i,diff}^{\alpha|\beta} = p_i^{\alpha|\beta} \cdot A^{\alpha|\beta} \cdot \Delta c_i^{\alpha|\beta}, \qquad (3)$$

where $p^{\alpha|\beta}{}_i$ is the permeability of the membrane to i and $\Delta c^{\alpha|\beta}{}_i$ is the concentration gradient.

Combining advective and diffusive fluxes, the total flux of i between α and β is:

$$J_{i,total}^{\alpha|\beta} = \left[p_i^{\alpha|\beta} \cdot A^{\alpha|\beta} \cdot \Delta c_i^{\alpha|\beta}\right] + \left[A^{\alpha|\beta} \cdot k^{\alpha|\beta} \cdot \left[\left(\Delta P^{\alpha|\beta}\right) - \sigma_i^{\alpha|\beta} \cdot \left(\Delta \pi^{\alpha|\beta}\right)\right] \cdot \left(1 - \sigma_i^{\alpha|\beta}\right) \cdot c_i^{\alpha}\right]. \qquad (4)$$

Thus, the flux of a molecule i (such as protein) from α (blood plasma) to β (SF) depends on variables governing fluid flow (e.g. $\Delta P^{\alpha|\beta}$, $\Delta \pi^{\alpha|\beta}$) and also on variables describing the characteristics of the capillary and SL "membranes" (e.g. $\sigma^{\alpha|\beta}{}_i$, $p^{\alpha|\beta}{}_i$).

The combination of transport theory and experiment can elucidate how the concentration of the SF lubricants HA and PRG4, as well as total protein, are altered dynamically following initiation of post-traumatic osteoarthritis. For lubricants, there is no influx from the plasma since HA and PRG4 are secreted by resident joint cells. Therefore, transport equations can be used to model the efflux of these lubricants from the SF to the lymphatics. In the case of lubricant efflux (where α is the SF and β is the lymphatics (L), with the SL as a semi-permeable membrane

separating the two compartments), **eqn. 4** can be simplified by assuming that $c^{L}_{lubricant} << c^{SF}_{lubricant}$:

$$J^{SF|L}_{lubricant} = c^{SF}_{lubricant} \cdot \left(\left[p^{SF|L}_{lubricant} \cdot A^{SF|L} \right] + \left[v^{SF|L}_{H_2O} \cdot \left(1 - \sigma^{SF|L}_{lubricant} \right) \right] \right), \quad (5)$$

These transport equations elucidate the importance of evaluating dynamic changes to SF composition (such as $c^{SF}_{protein}$, which affects π^{SF}) and volume (which affects P^{SF}),[48, 69] as well as SL membrane properties (such as σ, k, and p) in estimating changes to joint transport following injury or during osteoarthritis progression.

Term	Description	Units
$A^{\alpha \mid \beta}$	area	cm^2
c^{α}_{i}	concentration	mg / mL
i	solute	-
$J^{\alpha \mid \beta}_{i}$	flux of solute	mg / min
$k^{\alpha \mid \beta}$	hydraulic conducance	cm/(min · cmH_2O)
P^{α}	hydrostatic pressure	cm H_2O
$p^{\alpha \mid \beta}_{i}$	permeability	cm / min
π^{α}	osmotic pressure	cm H_2O
$\sigma^{\alpha \mid \beta}_{i}$	reflection coefficient	-
V^{α}	volume	mL
$v^{\alpha \mid \beta}_{H2O}$	flux of water	µL / min

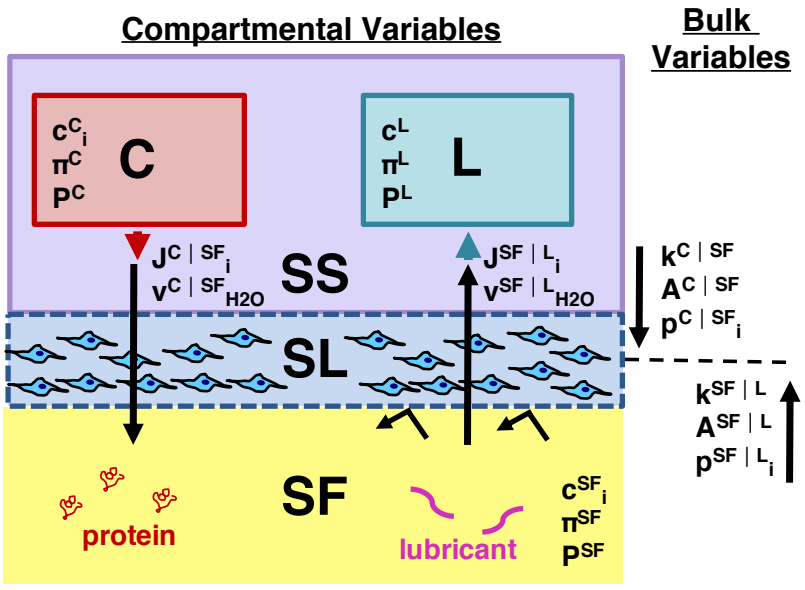

Figure 1.3: Influx of fluids and solutes (from capillaries, C, to SF) and efflux (from SF to lymphatics, L) can be modeled using **eqn. 4** with variables as shown.

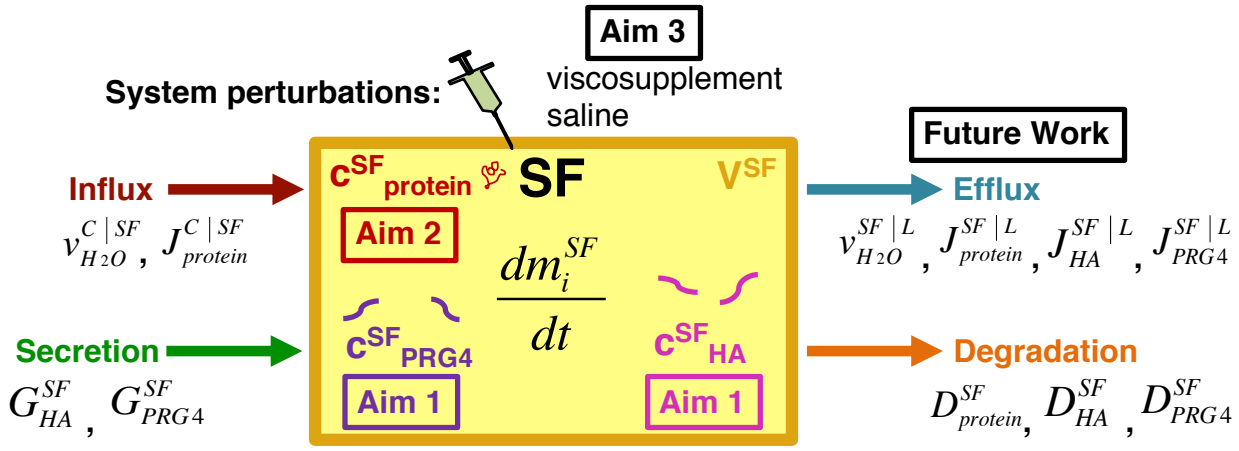

Figure 1.4: Summary of the aims of the dissertation by chapter. In Aim 1, a mathematical model describing macromolecular dynamics in SF is updated to include contributions from fluid fluxes. c^{SF}_{HA}, c^{SF}_{PRR4}, and $c^{SF}_{protein}$ are evaluated in healthy and PTOA knees as functions of generation (influx, secretion) and loss (efflux, degradation). In Aim 2, an index of SL transport, relating the relative protein in SF to that in serum, is described and used to evaluate PTOA progression in the rabbit model. In Aim 3, the effect of viscosupplement IA therapy on lubricant dynamics is evaluated.

1.6 References

1. Antonacci JM, Schmidt TA, Serventi LA, Cai MZ, Shu YL, Schumacher BL, McIlwraith CW, Sah RL: Effects of equine joint injury on boundary lubrication of articular cartilage by synovial fluid: role of hyaluronan. *Arthritis Rheum* 64:2917-26, 2012.

2. Atarod M, Ludwig TE, Frank CB, Schmidt TA, Shrive NG: Cartilage boundary lubrication of ovine synovial fluid following anterior cruciate ligament transection: a longitudinal study. *Osteoarthritis Cartilage* 23:640-7, 2015.

3. Balazs EA: The physical properties of synovial fluid and the special role of hyaluronic acid. In: *Disorders of the Knee,* ed. by AJ Helfet, Lippincott Co., Philadelphia, 1974, 63-75.

4. Balazs EA, Watson D, Duff IF, Roseman S: Hyaluronic acid in synovial fluid. I. Molecular parameters of hyaluronic acid in normal and arthritis human fluids. *Arthritis Rheum* 10:357-76, 1967.

5. Ballard BL, Antonacci JM, Temple-Wong MM, Hui AY, Schumacher BL, Bugbee WD, Schwartz AK, Girard PJ, Sah RL: Effect of tibial plateau frracture on lubrication function and composition of synovial fluid. *J Bone Joint Surg Am* 94:e64(1-9), 2012.

6. Bartok B, Firestein GS: Fibroblast-like synoviocytes: key effector cells in rheumatoid arthritis. *Immunological reviews* 233:233-55, 2010.

7. Bartok B, Firestein GS: Fibroblast-like synoviocytes: key effector cells in rheumatoid arthritis. *Immunol Rev* 233:233-55, 2010.

8. Benito MJ, Veale DJ, FitzGerald O, van den Berg WB, Bresnihan B: Synovial tissue inflammation in early and late osteoarthritis. *Ann Rheum Dis* 64:1263-7, 2005.

9. Blewis ME, Lao BJ, Schumacher BL, Bugbee WD, Sah RL, Firestein GS: Interactive cytokine regulation of synoviocyte lubricant secretion. *Tissue Eng Part A* 16:1329-37, 2010.

10. Blewis ME, Nugent-Derfus GE, Schmidt TA, Schumacher BL, Sah RL: A model of synovial fluid lubricant composition in normal and injured joints. *Eur Cell Mater* 13:26-39, 2007.

11. Bluteau G, Conrozier T, Mathieu P, Vignon E, Herbage D, Mallein-Gerin F: Matrix metalloproteinase-1,-3,-13 and aggrecanase-1 and-2 are differentially expressed in experimental osteoarthritis. *Biochim Biophys Acta* 1526:147-58, 2001.

12. Bluteau G, Gouttenoire J, Conrozier T, Mathieu P, Vignon E, Richard M, Herbage D, Mallein-Gerin F: Differential gene expression analysis in a rabbit model of osteoarthritis induced by anterior cruciate ligament (ACL) section. *Biorheology* 39:247-58, 2002.

13. Bonnet CS, Walsh DA: Osteoarthritis, angiogenesis and inflammation. *Rheumatology (Oxford)* 44:7-16, 2005.

14. Brown TJ, Laurent UB, Fraser JR: Turnover of hyaluronan in synovial joints: elimination of labelled hyaluronan from the knee joint of the rabbit. *Exp Physiol* 76:125-34, 1991.

15. Chang DG, Iverson EP, Schinagl RM, Sonoda M, Amiel D, Coutts RD, Sah RL: Quantitation and localization of cartilage degeneration following the induction of osteoarthritis in the rabbit knee. *Osteoarthritis Cartilage* 5:357-72, 1997.

16. Chen SS, Falcovitz YH, Schneiderman R, Maroudas A, Sah RL: Depth-dependent compressive properties of normal aged human femoral head articular cartilage: relationship to fixed charge density. *Osteoarthritis Cartilage* 9:561-9, 2001.

17. Coleman PJ, Scott D, Mason RM, Levick JR: Characterization of the effect of high molecular weight hyaluronan on trans-synovial flow in rabbit knees. *J Physiol* 514 (Pt 1):265-82, 1999.

18. Coleman PJ, Scott D, Mason RM, Levick JR: Role of hyaluronan chain length in buffering interstitial flow across synovium in rabbits. *J Physiol* 526 Pt 2:425-34, 2000.

19. Coleman PJ, Scott D, Ray J, Mason RM, Levick JR: Hyaluronan secretion into the synovial cavity of rabbit knees and comparison with albumin turnover. *J Physiol* 503 (Pt 3):645-56, 1997.

20. Conrozier T, Chappuis-Cellier C, Richard M, Mathieu P, Richard S, Vignon E: Increased serum C-reactive protein levels by immunonephelometry in patients with rapidly destructive hip osteoarthritis. *Revue du rhumatisme (English ed)* 65:759-65, 1998.

21. Curry F: Mechanics and thermodynamics of transcapillary exchange. In: *Handbook of Physiology,* ed. by ERaC Michel, American Physiological Society, Bethesda, 1984, 309-74.

22. D'Agostino MA, Conaghan P, Le Bars M, Baron G, Grassi W, Martin-Mola E, Wakefield R, Brasseur J-L, So A, Backhaus M: EULAR report on the use of ultrasonography in painful knee osteoarthritis. Part 1: prevalence of inflammation in osteoarthritis. *Annals of the rheumatic diseases* 64:1703-9, 2005.

23. David-Raoudi M, Deschrevel B, Leclercq S, Boumediene K, Pujol JP: Chondroitin sulfate increases hyaluronan production by human synoviocytes through differential regulation of hyaluronan synthases: Role of p38 and Akt. *Arthritis Rheum* 60:760-70, 2009.

24. Denlinger JL. Metabolism of sodium hyaluronate in articular and ocular tissues. Lille, France: University of Science and Technology; 1982.

25. Elsaid KA, Fleming BC, Oksendahl HL, Machan JT, Fadale PD, Hulstyn MJ, Shalvoy R, Jay GD: Decreased lubricin concentrations and markers of joint inflammation in the synovial fluid of patients with anterior cruciate ligament injury. *Arthritis Rheum* 58:1707-15, 2008.

26. Elsaid KA, Jay GD, Warman ML, Rhee DK, Chichester CO: Association of articular cartilage degradation and loss of boundary-lubricating ability of synovial fluid following injury and inflammatory arthritis. *Arthritis Rheum* 52:1746-55, 2005.

27. Firestein GS: Invasive fibroblast-like synoviocytes in rheumatoid arthritis. Passive responders or transformed aggressors? *Arthritis & Rheumatism* 39:1781-90, 1996.

28. Firestein GS: Etiology and pathogenesis of rheumatoid arthritis. In: *Kelley's Textbook of Rheumatology,* ed. by GS Firestein, Saunders/Elsevier, Philadelphia, PA, 2009, 1035-86.

29. Firestein GS, Zvaifler NJ: How important are T cells in chronic rheumatoid synovitis? *Arthritis & Rheumatism* 33:768-73, 1990.

30. Flannery CR, Hughes CE, Schumacher BL, Tudor D, Aydelotte MB, Kuettner KE, Caterson B: Articular cartilage superficial zone protein (SZP) is homologous to megakaryocyte stimulating factor precursor and Is a multifunctional proteoglycan with potential growth-promoting, cytoprotective, and lubricating properties in cartilage metabolism. *Biochem Biophys Res Commun* 254:535-41, 1999.

31. Fraser JR, Kimpton WG, Pierscionek BK, Cahill RN: The kinetics of hyaluronan in normal and acutely inflamed synovial joints: observations with experimental arthritis in sheep. *Semin Arthritis Rheum* 22:9-17, 1993.

32. Fraser JR, Laurent TC, Laurent UB: Hyaluronan: its nature, distribution, functions and turnover. *J Intern Med* 242:27-33, 1997.

33. Gelber AC, Hochberg MC, Mead LA, Wang NY, Wigley FM, Klag MJ: Joint injury in young adults and risk for subsequent knee and hip osteoarthritis. *Ann Intern Med* 133:321-8, 2000.

34. Gleghorn JP, Bonassar LJ: Lubrication mode analysis of articular cartilage using Stribeck surfaces. *J Biomech* 41:1910-8, 2008.

35. Granger HJ, Taylor AE: Permeability of connective tissue linings isolated from implanted capsules; implications for interstitial pressure measurements. *Circ Res* 36:222-8, 1975.

36. Grissom MJ, Temple-Wong MM, Adams MS, Tom M, Schumacher BL, McIlwraith CW, Goodrich LR, Chu CR, Sah RL: Synovial fluid lubricant properties are transiently deficient after arthroscopic articular cartilage defect repair with platelet-enriched fibrin alone and with mesenchymal stem cells. *Orthop J Sports Med* 2:2325967114542580, 2014.

37. Holley HL, Patton FM, Pigman W, Platt D: An electrophoretic study of normal and post-mortem human and bovine synovial fluids. *Arch Biochem Biophys* 64:152-63, 1956.

38. Hui AY, McCarty WJ, Masuda K, Firestein GS, Sah RL: A systems bIology approach to synovial joint lubrication in health, injury, and disease. *Wiley Interdiscip Rev Syst Biol Med* 4:15-37, 2012.

39. Ingram KR, Wann AK, Angel CK, Coleman PJ, Levick JR: Cyclic movement stimulates hyaluronan secretion into the synovial cavity of rabbit joints. *J Physiol* 586:1715-29, 2008.

40. Itano N, Sawai T, Yoshida M, Lenas P, Yamada Y, Imagawa M, Shinomura T, Hamaguchi M, Yoshida Y, Ohnuki Y, Miyauchi S, Spicer AP, McDonald JA, Kimata K: Three isoforms of mammalian hyaluronan synthases have distinct enzymatic properties. *J Biol Chem* 274:25085-92, 1999.

41. Jay GD: Characterization of a bovine synovial fluid lubricating factor. I. Chemical, surface activity and lubricating properties. *Connect Tissue Res* 28:71-88, 1992.

42. Jay GD, Harris DA, Cha CJ: Boundary lubrication by lubricin is mediated by O-linked beta(1-3)Gal-GalNAc oligosaccharides. *Glycoconj J* 18:807-15, 2001.

43. Jay GD, Tantravahi U, Britt DE, Barrach HJ, Cha CJ: Homology of lubricin and superficial zone protein (SZP): products of megakaryocyte stimulating factor (MSF) gene expression by human synovial fibroblasts and articular chondrocytes localized to chromosome 1q25. *J Orthop Res* 19:677-87, 2001.

44. Jones AR, Flannery CR: Bioregulation of lubricin expression by growth factors and cytokines. *Eur Cell Mater* 13:40-5; discussion 5, 2007.

45. Kedem O, Katchalsky A: Thermodynamic analysis of the permeability of biological membranes to non-electrolytes. *Biochim Biophys Acta* 27:229-46, 1958.

46. Khalafi A, Schmid TM, Neu C, Reddi AH: Increased accumulation of superficial zone protein (SZP) in articular cartilage in response to bone morphogenetic protein-7 and growth factors. *J Orthop Res* 25:293-303, 2007.

47. Klein TJ, Schumacher BL, Blewis ME, Schmidt TA, Voegtline MS, Thonar EJ, Masuda K, Sah RL: Tailoring secretion of proteoglycan 4 (PRG4) in tissue-engineered cartilage. *Tissue Eng* 12:1429-39, 2006.

48. Knight AD, Levick JR: Pressure-volume relationships above and below atmospheric pressure in the synovial cavity of the rabbit knee. *J Physiol* 328:403-20, 1982.

49. Knight AD, Levick JR: The density and distribution of capillaries around a synovial cavity. . *Q J Exp Physiol* 68:629-44, 1983.

50. Knight AD, Levick JR: Morphometry of the ultrastructure of the blood-joint barrier in the rabbit knee. *Q J Exp Physiol* 69:271-88, 1984.

51. Knight AD, Levick JR, McDonald JN: Relation between trans-synovial flow and plasma osmotic pressure, with an estimation of the albumin reflection coefficient in the rabbit knee. *Q J Exp Physiol* 73:47-65, 1988.

52. Knox P, Levick JR, McDonald JN: Synovial fluid--its mass, macromolecular content and pressure in major limb joints of the rabbit. *Q J Exp Physiol* 73:33-45, 1988.

53. Kushner I, Somerville JA: Permeability of human synovial membrane to plasma proteins. Relationship to molecular size and inflammation. *Arthritis Rheum* 14:560-70, 1971.

54. Lawrence RC, Felson DT, Helmick CG, Arnold LM, Choi H, Deyo RA, Gabriel S, Hirsch R, Hochberg MC, Hunder GG, Jordan JM, Katz JN, Kremers HM, Wolfe F: Estimates of the prevalence of arthritis and other rheumatic conditions in the United States. Part II. *Arthritis Rheum* 58:26-35, 2008.

55. Le Graverand M-PH, Eggerer J, Sciore P, Reno C, Vignon E, Otterness I, Hart DA: Matrix metalloproteinase-13 expression in rabbit knee joint connective tissues: influence of maturation and response to injury. *Matrix Biol* 19:431-41, 2000.

56. Le Graverand MP, Eggerer J, Vignon E, Otterness IG, Barclay L, Hart DA: Assessment of specific mRNA levels in cartilage regions in a lapine model of osteoarthritis. *J Orthop Res* 20:535-44, 2002.

57. Lee HG, Cowman MK: An agarose gel electrophoretic method for analysis of hyaluronan molecular weight distribution. *Anal Biochem* 219:278-87, 1994.

58. Lee SY, Niikura T, Reddi AH: Superficial zone protein (lubricin) in the different tissue compartments of the knee joint: modulation by transforming growth factor beta 1 and interleukin-1 beta. *Tissue Eng Part A* 14:1799-807, 2008.

59. Levick JR: Contributions of the lymphatic and microvascular systems to fluid absorption from the synovial cavity of the rabbit knee. *J Physiol* 306:445-61, 1980.

60. Levick JR: Permeability of rheumatoid and normal human synovium to specific plasma proteins. *Arthritis Rheum* 24:1550-60, 1981.

61. Levick JR: Blood flow and mass transport in synovial joints. In: *Handbook of Physiology, Section 2, The Cardiovascular System, Volume IV, The Microcirculation,* ed. by M Renkin, Michel C, The American Physiological Society, 1984, 917-47.

62. Levick JR: Synovial fluid and trans-synovial flow in stationary and moving normal joints. In: *Joint loading: biology and health of articular structures* ed. by HJ Helminen, Kiviranta I, Säämänen AM, Tammi M, Paukkonen K, Wright & Sons, Bristol, 1987, 149-86.

63. Levick JR: A two-dimensional morphometry-based model of interstitial and transcapillary flow in rabbit synovium. *Exp Physiol* 76:905-21, 1991.

64. Levick JR: Synovial Fluid. Determinants of volume turnover and material concentration. In: *Articular cartilage and osteoarthritis,* ed. by KE Kuettner, Schleyerbach R, Peyron JG, Hascall VC, Raven Press, New York, 1992, 529-41.

65. Levick JR: An analysis of the interaction between interstitial plasma protein, interstitial flow, and fenestral filtration and its application to synovium. *Microvasc Res* 47:90-125, 1994.

66. Levick JR: Microvascular architecture and exchange in synovial joints. *Microcirculation* 2:217-33, 1995.

67. Levick JR, Knight AD: Interaction of plasma colloid osmotic pressure and joint fluid pressure across the endothelium-synovium layer: significance of extravascular resistance. *Microvasc Res* 35:109-21, 1988.

68. Levick JR, McDonald JN: Ultrastructure of transport pathways in stressed synovium of the knee in anaesthetized rabbits. *J Physiol* 419:493-508, 1989.

69. Levick JR, McDonald JN: Viscous and osmotically mediated changes in fluid movement across synovium in response to intraarticular albumin. *Microvasc Res* 47:68-89, 1994.

70. Levick JR, McDonald JN: Fluid movement across synovium in healthy joints: role of synovial fluid macromolecules. *Ann Rheum Dis* 54:417-23, 1995.

71. Lotz MK, Kraus VB: New developments in osteoarthritis. Posttraumatic osteoarthritis: pathogenesis and pharmacological treatment options. *Arthritis Res Ther* 12:211, 2010.

72. Lu Y, Levick JR, Wang W: Concentration polarization of hyaluronan on the surface of the synovial lining of infused joints. *J Physiol* 561:559-73, 2004.

73. Maroudas A: Physicochemical Properties of Articular Cartilage. In: *Adult Articular Cartilage,* ed. by MAR Freeman, Pitman Medical, Tunbridge Wells, England, 1979, 215-90.

74. Mazzucco D, Scott R, Spector M: Composition of joint fluid in patients undergoing total knee replacement and revision arthroplasty: correlation with flow properties. *Biomaterials* 25:4433-45, 2004.

75. McCarty WJ, Cheng JC, Hansen BC, Yamaguchi T, Masuda K, Sah RL: The biophysical mechanisms of altered hyaluronan concentration in synovial fluid after anterior cruciate ligament transection. *Arthritis Rheum* 64:3993-4003, 2012.

76. McCarty WJ, Nguyen QT, Hui AY, Chen AC, Sah RL: Cartilage Tissue Engineering. In: *Comprehensive Biomaterials,* ed. by P Ducheyne, Healy KE, Hutmacher DE, Grainger DE, Kirkpatrick CJ, 2011, 199-212.

77. McDonald JN, Levick JR: Effect of extravascular plasma protein on pressure-flow relations across synovium in anaesthetized rabbits. *J Physiol* 465:539-59, 1993.

78. McInnes IB, Schett G: The pathogenesis of rheumatoid arthritis. *New England Journal of Medicine* 365:2205-19, 2011.

79. Momberger TS, Levick JR, Mason RM: Hyaluronan secretion by synoviocytes is mechanosensitive. *Matrix Biol* 24:510-9, 2005.

80. Momberger TS, Levick JR, Mason RM: Mechanosensitive synoviocytes: a Ca2+ - PKCalpha-MAP kinase pathway contributes to stretch-induced hyaluronan synthesis in vitro. *Matrix Biol* 25:306-16, 2006.

81. Mow VC, Ratcliffe A: Structure and function of articular cartilage and meniscus. In: *Basic Orthopaedic Biomechanics,* ed. by VC Mow, Hayes WC, Raven Press, New York, 1997, 113-78.

82. Nugent GE, Aneloski NM, Schmidt TA, Schumacher BL, Voegtline MS, Sah RL: Dynamic shear stimulation of bovine cartilage biosynthesis of proteoglycan 4 (PRG4). *Arthritis Rheum* 54:1888-96, 2006.

83. Nugent GE, Schmidt TA, Schumacher BL, Voegtline MS, Bae WC, Jadin KD, Sah RL: Static and dynamic compression regulate cartilage metabolism of proteoglycan 4 (PRG4). *Biorheology* 43:191-200, 2006.

84. Nugent-Derfus GE, Takara T, O'Neill JK, Cahill SB, Gortz S, Pong T, Inoue H, Aneloski NM, Wang WW, Vega KI, Klein TJ, Hsieh-Bonassera ND, Bae WC, Burke JD, Bugbee WD, Sah RL: Continuous passive motion applied to whole joints stimulates chondrocyte biosynthesis of PRG4. *Osteoarthritis Cartilage* 15:566-74, 2007.

85. Ogston AG, Stanier JE: The physiological function of hyaluronic acid in synovial fluid: viscous, elastic and lubricant properties. *J Phys* 119:244-52, 1953.

86. Ohno S, Tanimoto K, Fujimoto C, Ijuin K, Honda K, Tanaka N, Doi T, Nakahara M, Tanne K: Molecular cloning of rabbit hyaluronic acid synthases and their expression patterns in synovial membrane and articular cartilage. *Biochim Biophys Acta* 1520:71-8, 2001.

87. Pappenheimer JR: Passage of molecules through capillary walls. *Physiol Rev* 33:387-423, 1951.

88. Patlak CS, Goldstein DA, Hoffman JF: The flow of solute and solvent across a two-membrane system. *J Theor Biol* 5:426-42, 1963.

89. Pennock AT, Robertson CM, Emmerson BC, Harwood FL, Amiel D: Role of apoptotic and matrix-degrading genes in articular cartilage and meniscus of mature and aged rabbits during development of osteoarthritis. *Arthritis Rheum* 56:1529-36, 2007.

90. Price FM, Levick JR, Mason RM: Changes in glycosaminoglycan concentration and synovial permeability at raised intra-articular pressure in rabbit knees. *J Physiol* 495 (Pt 3):821-33, 1996.

91. Price FM, Levick JR, Mason RM: Glycosaminoglycan concentration in synovium and other tissues of rabbit knee in relation to synovial hydraulic resistance. *J Physiol (Lond)* 495:803-20, 1996.

92. Price FM, Mason RM, Levick JR: Radial organization of interstitial exchange pathway and influence of collagen in synovium. *Biophys J* 69:1429-39, 1995.

93. Raleigh AR, McCarty WJ, Chen AC, Meinert C, Klein TJ, Sah RL: Synovial joints: Mechanobiology and tissue engineering of articular cartilage and synovial fluid. In: *Comprehensive Biomaterials,* ed. by P Ducheyne, Healey KE, Hutmacher DE, Grainger DE, Kirkpatrick CJ, Elsevier, 2017, 107-34.

94. Raleigh AR, Sun Y, Qian D, Temple-Wong MM, Kato K, Murata K, Firestein GS, Masuda K, Sah RL: Synovial fluid hyaluronan fluctuation in post-traumatic osteoarthritis: Dependence on the dynamic balance between biosynthesis, loss, and fluid flux *Trans Orthop Res Soc* 42:1506, 2017.

95. Recklies AD, White C, Melching L, Roughley PJ: Differential regulation and expression of hyaluronan synthases in human articular chondrocytes, synovial cells and osteosarcoma cells. *Biochem J* 354:17-24, 2001.

96. Reesink HL, Watts AE, Mohammed HO, Jay GD, Nixon AJ: Lubricin/proteoglycan 4 increases in both experimental and naturally occurring equine osteoarthritis. *Osteoarthritis Cartilage* 25:128-37, 2017.

97. Rhee DK, Marcelino J, Baker M, Gong Y, Smits P, Lefebvre V, Jay GD, Stewart M, Wang H, Warman ML, Carpten JD: The secreted glycoprotein lubricin protects cartilage surfaces and inhibits synovial cell overgrowth. *J Clin Invest* 115:622-31, 2005.

98. Ropes MW, Rossmeisl EC, Bauer W: The origin and nature of normal human synovial fluid. *J Clin Invest* 19:795-9, 1940.

99. Sabaratnam S, Arunan V, Coleman PJ, Mason RM, Levick JR: Size selectivity of hyaluronan molecular sieving by extracellular matrix in rabbit synovial joints. *J Physiol* 567:569-81, 2005.

100. Sabaratnam S, Coleman PJ, Mason RM, Levick JR: Interstitial matrix proteins determine hyaluronan reflection and fluid retention in rabbit joints: effect of protease. *J Physiol* 578:291-9, 2007.

101. Schmid K, Macnair MB: Characterization of the proteins of human synovial fluid in certain disease states. *J Clin Invest* 35:814-24, 1956.

102. Schmid K, Macnair MB: Characterization of the proteins of certain postmortem human synovial fluids. *J Clin Invest* 37:708-18, 1958.

103. Schmid T, Lindley K, Su J, Soloveychik V, Block J, Kuettner K, Schumacher B: Superficial zone protein (SZP) is an abundant glycoprotein in human synovial fluid and serum. *Trans Orthop Res Soc* 26:82, 2001.

104. Schmid TM, Su J-L, Lindley KM, Soloveychik V, Madsen L, Block JA, Kuettner KE, Schumacher BL: Superficial zone protein (SZP) is an abundant glycoprotein in human synovial fluid with lubricating properties. In: *The Many Faces of Osteoarthritis,* ed. by KE Kuettner, Hascall VC, Raven Press, New York, 2002, 159-61.

105. Schmidt TA, Gastelum NS, Han EH, Nugent-Derfus GE, Schumacher BL, Sah RL: Differential regulation of proteoglycan 4 metabolism in cartilage by IL-1alpha, IGF-I, and TGF-beta1. *Osteoarthritis Cartilage* 16:90-7, 2008.

106. Schmidt TA, Gastelum NS, Nguyen QT, Schumacher BL, Sah RL: Boundary lubrication of articular cartilage: role of synovial fluid constituents. *Arthritis Rheum* 56:882-91, 2007.

107. Schmidt TA, Sah RL: Effect of synovial fluid on boundary lubrication of articular cartilage. *Osteoarthritis Cartilage* 15:35-47, 2007.

108. Schmidt TA, Schumacher BL, Han EH, Klein TJ, Voegtline MS, Sah RL: Chemomechanical coupling in articular cartilage: IL-1a and TGF-ß1 regulate chondrocyte synthesis and secretion of proteoglycan 4. In: *Physical Regulation of Skeletal Repair,* ed. by RK Aaron, Bolander ME, American Academy of Orthopaedic Surgeons, Chicago, 2005, 151-61.

109. Schumacher BL, Block JA, Schmid TM, Aydelotte MB, Kuettner KE: A novel proteoglycan synthesized and secreted by chondrocytes of the superficial zone of articular cartilage. *Arch Biochem Biophys* 311:144-52, 1994.

110. Schumacher BL, Hughes CE, Kuettner KE, Caterson B, Aydelotte MB: Immunodetection and partial cDNA sequence of the proteoglycan, superficial zone protein, synthesized by cells lining synovial joints. *J Orthop Res* 17:110-20, 1999.

111. Schumacher BL, Schmidt TA, Voegtline MS, Chen AC, Sah RL: Proteoglycan 4 (PRG4) synthesis and immunolocalization in bovine meniscus. *J Orthop Res* 23:562-8, 2005.

112. Scott D, Coleman PJ, Abiona A, Ashhurst DE, Mason RM, Levick JR: Effect of depletion of glycosaminoglycans and non-collagenous proteins on interstitial hydraulic permeability in rabbit synovium. *J Physiol* 511 (Pt 2):629-43, 1998.

113. Scott D, Coleman PJ, Mason RM, Levick JR: Glycosaminoglycan depletion greatly raises the hydraulic permeability of rabbit joint synovial lining. *Exp Physiol* 82:603-6, 1997.

114. Scott D, Coleman PJ, Mason RM, Levick JR: Concentration dependence of interstitial flow buffering by hyaluronan in synovial joints. *Microvasc Res* 59:345-53, 2000.

115. Scott D, Coleman PJ, Mason RM, Levick JR: Interaction of intraarticular hyaluronan and albumin in the attenuation of fluid drainage from joints. *Arthritis Rheum* 43:1175-82, 2000.

116. Scott D, Levick JR, Miserocchi G: Non-linear dependence of interstitial fluid pressure on joint cavity pressure and implications for interstitial resistance in rabbit knee. *Acta Physiol Scand* 179:93-101, 2003.

117. Sellam J, Berenbaum F: The role of synovitis in pathophysiology and clinical symptoms of osteoarthritis. *Nat Rev Rheumatol* 6:625-35, 2010.

118. Smith MD, Triantafillou S, Parker A, Youssef PP, Coleman M: Synovial membrane inflammation and cytokine production in patients with early osteoarthritis. *J Rheumatol* 24:365-71, 1997.

119. Spicer AP, McDonald JA: Characterization and molecular evolution of a vertebrate hyaluronan synthase gene family. *J Biol Chem* 273:1923-32, 1998.

120. Starling EH: On the absorption of fluids from the connective tissue spaces. *J Physiol* 19:312-26, 1896.

121. Staverman AJ: The theory of measurement of osmotic pressure. *Rec Trav Chim* 70:344-52, 1951.

122. Stockwell RA: Chondrocytes. *J Clin Pathol Suppl (R Coll Pathol)* 12:7-13, 1978.

123. Stuhlmeier KM, Pollaschek C: Differential effect of transforming growth factor beta (TGF-beta) on the genes encoding hyaluronan synthases and utilization of the p38 MAPK pathway in TGF-beta-induced hyaluronan synthase 1 activation. *J Biol Chem* 279:8753-60, 2004.

124. Swann DA, Slayter HS, Silver FH: The molecular structure of lubricating glycoprotein-I, the boundary lubricant for articular cartilage. *J Biol Chem* 256:5921-5, 1981.

125. Swann DA, Sotman S, Dixon M, Brooks C: The isolation and partial characterization of the major glycoprotein (LGP-I) from the articular lubricating fraction from bovine synovial fluid. *Biochem J* 161:473-85, 1977.

126. Sweeney SE, Firestein GS: Rheumatoid arthritis: regulation of synovial inflammation. *The international journal of biochemistry & cell biology* 36:372-8, 2004.

127. Temple-Wong MM, Ren S, Quach P, Hansen BC, Chen AC, Hasegawa A, D'Lima DD, Koziol J, Masuda K, Lotz MK, Sah RL: Hyaluronan concentration and size distribution in

human knee synovial fluid: variations with age and cartilage degeneration. *Arthritis Res Ther* 18:18, 2016.

128. Wilder FV, Hall BJ, Barrett JP, Jr., Lemrow NB: History of acute knee injury and osteoarthritis of the knee: a prospective epidemiological assessment. The Clearwater Osteoarthritis Study. *Osteoarthritis Cartilage* 10:611-6, 2002.

129. Zhang D, Cheriyan T, Martin SD, Gomoll AH, Schmid TM, Spector M: Lubricin distribution in the torn human anterior cruciate ligament and meniscus. *J Orthop Res* 29:1916-22, 2011.

CHAPTER 2

SYNOVIAL FLUID MODEL INCORPORATING BIOSYNTHESIS, LOSS, AND DILUTION ELUCIDATES HYALURONAN DYNAMICS IN EXPERIMENTAL OSTEOARTHRITIS

2.1 Abstract

The lubricant function of synovial fluid (SF) is diminished after injury, often because of a decrease in the concentration of hyaluronan (c^{SF}_{HA}). Here, a theoretical model describing the biophysical mechanisms governing c^{SF}_{HA} was extended to include the substantial shifts in SF volume (V^{SF}) in post-traumatic osteoarthritis (PTOA). This allowed analysis of the relative contributions to decreased c^{SF}_{HA} of altered V^{SF} and HA generation (G^{SF}_{HA}), loss (L^{SF}_{HA}), and clearance (CL^{SF}_{HA}). At 1-42 days post-injury, the effect of ACL transection (ACLT) in the rabbit model of PTOA was evaluated in the context of the model. The combined theoretical-experimental findings resolved the apparent paradox between the ACLT-induced decrease in c^{SF}_{HA} (-49% to -80% vs. CTRL) and increased G^{SF}_{HA} (+71-593%) and m^{SF}_{HA} (+24-187%), with both joint swelling (increased V^{SF}, +61-449%) and increased L^{SF}_{HA} (+68-591%) causing decreases in c^{SF}_{HA}. Thus, a biophysically-based, quantitative synovial joint model for the dynamics of HA

can be evaluated in health or disease, and help to elucidate multiple biophysical phenomena governing c^{SF}_{HA}.

2.2 Introduction

Traumatic joint injury increases the likelihood of developing OA through mechanisms that may include diminished lubrication [16, 53]. One synovial fluid (SF) lubricant component is hyaluronan (HA, abbreviations and symbols are summarized in **Tables 1** and **2**, respectively) [20, 45]. The normal concentration of HA in SF (c^{SF}_{HA}) is 1-4 mg/mL [3, 12, 36, 51]. In healthy joints, most (>70%) HA exists at high molecular mass (M_r) of 2-7 million [12, 29, 51]. The value of c^{SF}_{HA} is functionally important, as HA lowers the friction coefficient and mechanical interaction of articulating cartilage surfaces in a concentration-dependent manner [1, 48]. Following trauma, as well as during aging and OA progression, c^{SF}_{HA} decreases [20, 36, 51]. The lubricating function of HA-deficient SF is restored *in vitro* by the addition of high-concentration and high-M_r HA [1, 48].

In synovial joints such as the knee, SF is encapsulated by synovium and articular cartilage (AC). The synovium consists of a thin synovial lining (SL) and thicker synovial subintima (SS) [4, 45]. The SL acts as a membrane, allowing selective passage of molecules between the SF joint space and SS microvasculature and lymphatics via a combination of diffusive and advective fluxes [32]. The SL contains 1-3 layers of fibroblast- and macrophage-like synoviocytes (FLS and MLS), with FLS producing lubricant components of the SF [6, 23]. SF has been analyzed traditionally for regulatory molecules and biomarkers, and recently as a reservoir of lubricant molecules [20]. Lubricant synthesis by joint lining cells, as well as net fluxes of solutes and fluid, influence the biochemical composition of SF [20, 45].

HA is produced by HA synthases (HAS), which exist as three different isoforms, HAS1, HAS2, and HAS3 [46, 50]. These synthases span the FLS plasma membrane, where they produce and secrete HA. In cells transfected with mammalian HAS genes, HAS2 produced high

(> 2.0 Md) M_r forms of HA, which constitutes >70% of SF HA [29]; in contrast, HAS1 and HAS3 produced a lower M_r HA (0.1-2.0 Md) [22]. In rabbit FLS, HA production was associated with *HAS2* gene expression, but not *HAS1* or *HAS3* expression [41, 43]. While the SL, with its relatively large surface area and high FLS cell density [21], is the primary source of SF HA, a quantitative relationship between *HAS* gene expression and HA production by FLS is unknown.

The biophysical mechanism by which c^{SF}_{HA} is diminished after acute injury appears multifactorial. While c^{SF}_{HA} is predicted to depend on HA synthesis, HA loss, and SF volume [7], the pathophysiological roles of these processes in HA dynamics in PTOA is unclear [5]. Animal models of PTOA allow analysis of SF composition and cellular metabolism over defined post-injury time periods [8, 28]. Following ACLT destabilization of rabbit knees, HA concentration and residence time are decreased [9, 37], and accompanied by SF effusion and SL hyperplasia [34, 37]. In renal physiology, a tangible descriptor of the rate of loss of a solute is the clearance rate, the equivalent volume of solute-containing fluid (plasma) that is cleared per unit time [18]. Analogously, CL^{SF}_{HA} can provide a practical metric of the rate of SF volume (containing HA) that is cleared from the knee joint.

Here, we sought to elucidate the biophysical basis for decreased c^{SF}_{HA} following joint injury, specifically the time-dependent variation in HA lubricant generation and loss, and SF volume change. Our aims were to (1) extend a previous theoretical compartmental model for c^{SF}_{HA}, incorporating SF volume, HA secretion, HA loss, and HA clearance, and (2) in the rabbit ACLT model of PTOA, evaluate the relative contributions of these biophysical factors to decreased c^{SF}_{HA} by integrating theoretical and experimental analyses.

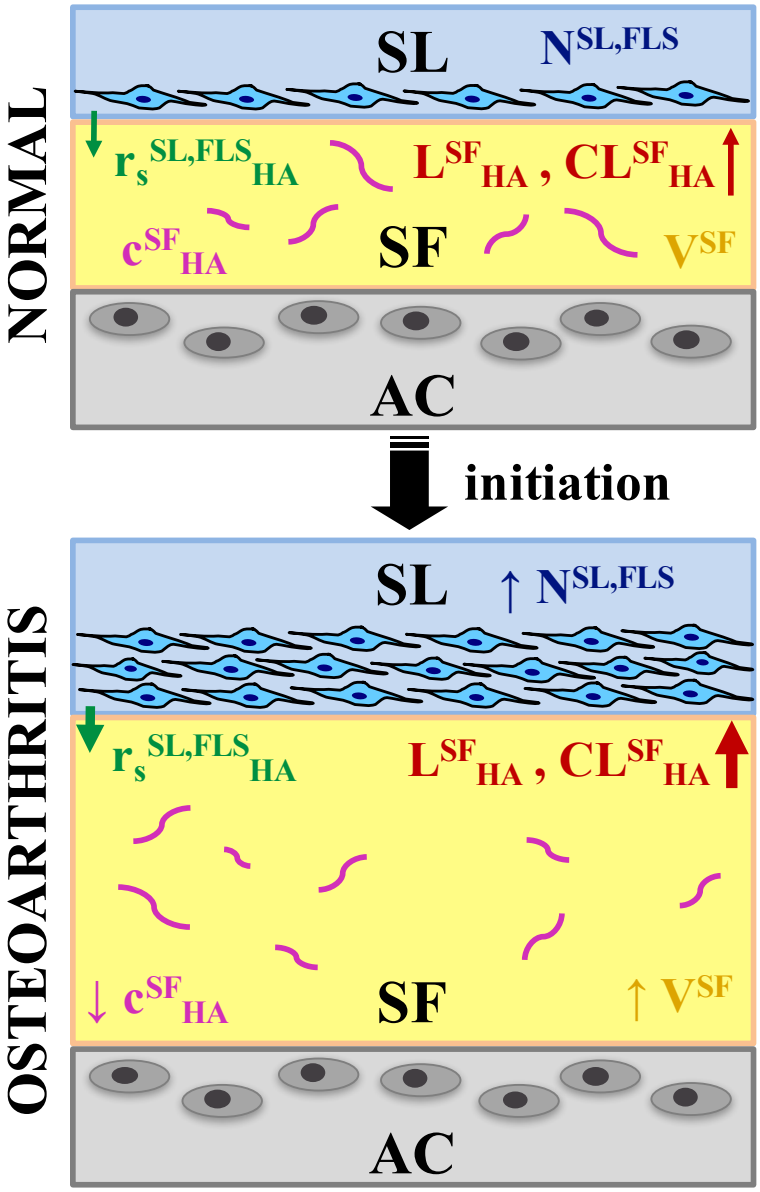

Figure 2.1: Schematic of specific aims for modeling synovial joint HA dynamics. Data from *in vivo* experiments were used to develop a synovial joint compartmental model using variables and parameters that were measured directly or fit. Variations in the variables and parameters (**Table 2**) reflect biophysical mechanisms that underlie the progression from a normal to PTOA state following an initiation event (such as ACLT). Constituent compartments and cell types include synovial fluid (SF) and synovial lining (SL) containing fibroblast-like synoviocytes (FLS). Articular cartilage (AC) is considered a barrier to HA.

2.3 Volume-Varying Compartmental Model for Hyaluronan in Synovial Fluid

Previously described compartmental mass balance models [7, 45] of c^{SF}_{HA} dynamics were extended here, accounting for variations in SF volume, V^{SF}. Model variables and parameters are summarized in **Table 2**.

The overall mass of HA in the SF of a synovial joint, m^{SF}_{HA}, is accounted for by a conservation law. Changes in m^{SF}_{HA} with time depend on the balance between the rates of HA generation (secretion into SF), G^{SF}_{HA}, and HA loss from SF, L^{SF}_{HA}, according to:

$$\frac{dm^{SF}_{HA}(t)}{dt} = G^{SF}_{HA}(t) - L^{SF}_{HA}(t) \quad . \tag{1}$$

Equation (1) can be rewritten as:

$$\frac{dm^{SF}_{HA}(t)}{dt} = \gamma(t) \cdot G^{SF}_{HA,0} \quad , \tag{2}$$

where γ is a dimensionless parameter that describes net HA generation (or loss) rate, relative to $G^{SF}_{HA,0}$, the normal generation rate at time 0:

$$\gamma(t) = \frac{G^{SF}_{HA}(t) - L^{SF}_{HA}(t)}{G^{SF}_{HA,0}} \quad . \tag{3}$$

The mass balance can be related to biochemical and physiological quantities. Assuming a well-mixed SF compartment, m^{SF}_{HA} is the product of concentration, c^{SF}_{HA}, and volume, V^{SF}:

$$m^{SF}_{HA}(t) = c^{SF}_{HA}(t) \cdot V^{SF}(t) \quad . \tag{4}$$

G^{SF}_{HA} can be described as the product of the HA synthesis rate per million FLS cells in the SL, $r_s{}^{SL,FLS}_{HA}$, and the total number of FLS cells, $N^{SL,FLS}$:

$$G^{SF}_{HA}(t) = r_s{}^{SL,FLS}_{HA}(t) \cdot N^{SL,FLS}(t) \quad . \tag{5}$$

L^{SF}_{HA} can be described as the product of the SF clearance rate, CL^{SF}_{HA}, and c^{SF}_{HA} [7, 18]:

$$L^{SF}_{HA}(t) = CL^{SF}_{HA}(t) \cdot c^{SF}_{HA}(t) . \tag{6}$$

Then, **equation (1)** can be rewritten as follows:

$$\frac{d\left[V^{SF}(t) \cdot c^{SF}_{HA}(t)\right]}{dt} = G^{SF}_{HA}(t) - c^{SF}_{HA}(t) \cdot CL^{SF}_{HA}(t) . \tag{7}$$

Applying the product rule to the left hand side of **equation (7)** and rearranging to solve for the time-rate of concentration change yields:

$$\frac{dc^{SF}_{HA}(t)}{dt} = \frac{G^{SF}_{HA}(t) - c^{SF}_{HA}(t) \cdot \left[CL^{SF}_{HA}(t) + \dfrac{dV^{SF}(t)}{dt}\right]}{V^{SF}(t)} . \tag{8}$$

In **equation (8)**, the dV^{SF}/dt term effectively adds to the clearance effect, causing c^{SF}_{HA} to diminish (dc^{SF}_{HA}/dt to become more negative). Multiplying the numerator and denominator of the right hand side of **equation (8)** by $1/CL^{SF}_{HA}$ yields

$$\frac{dc^{SF}_{HA}(t)}{dt} = \frac{c^{SF}_{HA,SS}(t) - c^{SF}_{HA}(t) \cdot \left(1 + \alpha(t)\right)}{\tau(t)} , \tag{9}$$

where the characteristic time, τ, is

$$\tau(t) = \frac{V^{SF}(t)}{CL^{SF}_{HA}(t)} , \tag{10}$$

the pseudo-steady-state c^{SF}_{HA}, $c^{SF}_{HA,SS}$, is

$$c^{SF}_{HA,SS}(t) = \frac{G^{SF}_{HA}(t)}{CL^{SF}_{HA}(t)} , \tag{11}$$

and the dimensionless parameter α is

$$\alpha(t) = \frac{dV^{SF}(t)/dt}{CL^{SF}_{HA}(t)} . \tag{12}$$

Thus, **equation (3, 10-12)** describe how the four parameters, τ, $c^{SF}_{HA,SS}$, γ, and α, are influenced by G^{SF}_{HA}, L^{SF}_{HA}, CL^{SF}_{HA}, V^{SF}, and dV^{SF}/dt, and **equation (9)** describes how dc^{SF}_{HA}/dt is related to c^{SF}_{HA} through these parameters.

Equation (7) can also be re-arranged to describe how c^{SF}_{HA} depends on $c^{SF}_{HA,SS}$ and the dimensionless parameters, α and β:

$$c^{SF}_{HA}(t) = \frac{\left(1-\beta(t)\right)}{\left(1+\alpha(t)\right)} \cdot c^{SF}_{HA,SS}(t), \tag{13}$$

where β describes the relative rates of mass turnover, between concentration-driven mass change in SF and synthesis, G^{SF}_{HA}:

$$\beta(t) = \frac{V^{SF}(t) \cdot dc^{SF}_{HA}(t)/dt}{G^{SF}_{HA}(t)}. \tag{14}$$

Multiplying both numerator and denominator of **equation (13)** by (1+α(*t*)) and assuming small values of α and β results in:

$$c^{SF}_{HA}(t) \sim \left(1-\left(\alpha(t)+\beta(t)\right)\right) \cdot c^{SF}_{HA,SS}(t). \tag{15}$$

Thus, c^{SF}_{HA} is approximately proportional to $c^{SF}_{HA,SS}$, as reduced by the sum of the dimensionless parameters, α and β.

Table 2.1: Abbreviations of terms used in the model setup of the synovial joint to study HA dynamics.

Abbreviation	Term
AC	articular cartilage
ACLT	anterior cruciate ligament transection
FLS	fibroblast-like synoviocytes
HA	hyaluronan
HAS	hyaluronan synthase
MLS	macrophage-like synoviocytes
M_r	molecular mass
PTOA	post-traumatic osteoarthritis
SF	synovial fluid
SL	synovial lining
SS	synovial subintima

Table 2.2: Symbol, description, units, and method of estimation for variables and parameters used in compartmental model of HA dynamics in the synovial joint.

Symbol	Description	Units	Estimation
α	ratio of rate of SF volume change to clearance rate	-	calculated
β	ratio of rate of buildup of HA in SF to rate of HA secretion	-	calculated
c^{SF}_{HA}	HA concentration in SF	mg/mL	*in vivo*
$c^{SF}_{HA,SS}$	HA concentration in SF at steady state	mg/mL	calculated
CL^{SF}_{HA}	rate of SF HA clearance	μL/day	estimated
γ	relative HA turnover (difference between rates of generation and loss), normalized to initial CTRL values	-	calculated
G^{SF}_{HA}	rate of HA generation (secretion) into SF	μg/day	calculated
L^{SF}_{HA}	rate of HA loss from SF	μg/day	estimated
m^{SF}_{HA}	HA mass in SF	μg	calculated
$N^{SL,FLS}$	number of FLS in SL	cells	measured [21, 30, 34]
$r_s{}^{SL,FLS}_{HA}$	rate of HA synthesis by FLS in SL	μg/(million cells • day)	*in vitro* / *in vivo*
t	time	days	prescribed
τ	characteristic time, ratio of SF volume to rate of SF HA clearance	days	calculated
V^{SF}	SF volume	μL	*in vivo*

2.4 Materials and Methods

Study design. The study is summarized here and in **Fig. 1**. Adult female New Zealand White (NZW) rabbits were subjected to unilateral ACLT, and knee joints were harvested at 1, 4, 7, 14, 28, and 42 days post-injury (n=6-7 per group). At harvest, SF, lavage fluids, and SL were collected from ACLT and Non-OP knees. In addition, fluids and tissue were harvested from other rabbits, both healthy (n=37) as controls (CTRL) or ACLT (n=26) for additional $N^{SL,FLS}$ measures (see supplemental methods). Data from *in vivo* CTRL, Non-OP, and ACLT SF and lavage fluids were analyzed for c^{SF}_{HA} and V^{SF}, while SL was analyzed for the rate of HA synthesis by FLS ($r_s{}^{SL,FLS}_{HA}$) estimated from qPCR data, calibrated to secretion rates *in vitro*.

Data are reported as mean±SE. Each measure was analyzed for normality and homogeneity of variance. For measures that did not satisfy these assumptions, data were log-transformed or analyzed using the nonparametric Kruskall-Wallis or related-samples Wilcoxon signed rank tests. All statistical analyses were performed using SPSS (IBM). Results were considered significant if $P<0.05$.

The effects of ACLT vs. Non-OP and time after surgery on c^{SF}_{HA}, V^{SF}, m^{SF}_{HA}, and $r_s{}^{SL,FLS}_{HA}$ were analyzed by two-way repeated measures ANOVA with Sidak post-hoc testing. m^{SF}_{HA} was calculated from **equation (4)** for each sample. At each time point, ACLT and Non-OP SF were compared by paired two-tailed *t*-test, and also compared to CTRL by two-tailed ANOVA and Dunnett's test. Separately, for ACLT and Non-OP, variation with time was assessed, both by one-way two-tailed ANOVA with Sidak post-hoc testing and by curve fitting.

The variables V^{SF}, c^{SF}_{HA}, and $r_s{}^{SL,FLS}_{HA}$, for each treatment group, were curve fit to the critically-damped 2nd order system solution in order to capture time-dependent behavior:

$$Y(t) = (P - C) \cdot \left(1 - F \cdot (1 - t/T)\right) \cdot e^{F \cdot (1 - t/T)} + C \quad . \tag{16}$$

Y(t) in **equation (16)** is the critically-damped system solution to a second order differential equation, allowing a transient response, followed by return to a steady-state value, where *t* is the time (days post-injury), Y(0) is the initial value, C is the steady-state value, T and P are the time and Y(T) values, respectively, at the transient peak, and F is a dimensionless number (0<F<1), weighting the differences in the initial value, Y(0)-C, to the final value from C:

$$\frac{Y(0) - C}{P - C} = (1 - F) \cdot e^{F} \quad . \tag{17}$$

For ACLT or Non-OP groups, experimental variables and each data point post-injury (1, 4, 7, 14, 28, and 42 days) were fit to **equation (16)** by minimizing least squares estimates for each parameter (C, P, T, and F) using a Trust-Region algorithm in MATLAB's Curve Fitting Toolbox.

Y(t) starts (*t*=0) at $(P\text{-}C)\cdot(1\text{-}F)\cdot e^{F}+C$ (**equation (17)**), peaks (*t*=T) at *P*, and asymptotes ($t \rightarrow \infty$) to *C*. For fits of ACLT V^{SF} and $r_s^{SL,FLS}{}_{HA}$ where data indicated a peak and then tendency to return to the Non-OP steady-state value, the Non-OP value for C was used in order to constrain the curve fits to be physiologically reasonable. The goodness of fit was assessed as the coefficient of determination (R^2). Whether each curve fit parameter was a positive value was assessed by one-sided *t*-test.

From these fits, model variables and parameters were calculated and estimated. HA generation ($G^{SF}{}_{HA}$) was calculated from **equation (5)** using continuous fits of $r_s^{SL,FLS}{}_{HA}$ and $N^{SL,FLS}$ (**Fig. 5**), the latter estimated from DNA in discs harvested from ACLT and Non-OP SL at 1, 2, 4, and 28 days post-ACLT (n=6-8/grp), modeled to increase exponentially to a plateau post-injury [52], and converted to total SL FLS based on estimates for SL surface area [25, 30]. HA loss rate

(L^{SF}_{HA}, **equation (1)**) and clearance rate (CL^{SF}_{HA}, **equation (6)**) were unknowns and fit from the model and continuous-time curve fits of G^{SF}_{HA}, V^{SF}, and c^{SF}_{HA}. Then, the characteristic variables $c^{SF}_{HA,SS}$ and τ, and dimensionless parameters γ, α, and β, were calculated by inserting continuous fits for G^{SF}_{HA}, L^{SF}_{HA}, CL^{SF}_{HA}, V^{SF}, dV^{SF}/dt, and dc^{SF}_{HA}/dt into **equation (3, 10-12, 14)**. Finally, the time-associated dependence of c^{SF}_{HA} on $c^{SF}_{HA,SS}$, α, and β was determined from **equation (13, 15)**, while that of dc^{SF}_{HA}/dt was determined from **equation (9)**. In CTRL knees, V^{SF}, c^{SF}_{HA}, and G^{SF}_{HA} were not all measured within the same knee, so mean±SE for loss terms, characteristic variables, and dimensionless parameters were calculated from products and quotients error propagation.

Detailed methods. A total of 95 adult female NZW rabbits were used in this study. All animal protocols were approved by UCSD IACUC.

To examine the time course of acute injury, 37 rabbits (9-18 mos) underwent surgery for ACLT [37] in the right knee. A drawer test was used to confirm knee destabilization. The left knee of rabbits was not operated upon (Non-OP). Following surgery, rabbits were allowed to move freely in cages and received a standard diet and water *ad libitum*. At 1-42 days after ACLT, animals were euthanized via intravenous injection of pentobarbital sodium for analysis. Additionally, healthy rabbits (n=32 total, 6-18 mos) were euthanized and used as a CTRL.

SL tissue, SF, and lavage fluids were harvested. After the knee joint was opened, the cut ends of the ACL, and the intact PCL, were visualized to confirm the surgical model. SL was dissected from medial and lateral gutters and was immediately submerged and stored in RNAlater (Qiagen). SF was aspirated from the parapatellar region of the knee joint using a 50 μL 27G micro syringe (BD). Then, lavage fluid was collected by injecting 1 mL sterile saline (23G syringe), flexing and extending the knee joint 10 times, and aspirating. Synovial and lavage fluids were weighed to estimate neat volume, centrifuged for clarification of cells and debris

prior to storage.

The concentration of HA was assessed in neat SF and conditioned medium samples. SF samples were first digested with Proteinase K (0.5 mg/mL in 100 mM sodium phosphate, 5 mM Na_2-EDTA, pH 7.1, overnight at 37°C) (Roche) and then boiled for 10 minutes to inactivate the enzyme. Digested SF and conditioned medium were then assayed for HA using an ELISA-like assay (R&D Systems) [51].

SF volume (V^{SF}) was estimated from neat and lavage fluids. Protein concentration was assayed using bicinchoninic acid (Thermo) [51] within neat and lavage fluids [11]. The volume of residual SF was estimated, assuming that lavage and SF contained the protein that was diluted from neat SF concentrations. Residual and neat SF volumes were summed to obtain V^{SF}. To test for efficiency of total joint protein ($m^{Joint}_{protein}$) to calculate V^{SF} as compared to the total joint HA (m^{Joint}_{HA}), the two V^{SF} were compared for matched samples. The range of V^{SF} calculated from $m^{Joint}_{protein}$ was 33-643 μL; that from m^{Joint}_{HA} was 18-966 μL. The V^{SF} values were correlated (r^2=0.70, P<0.001, n=18 comparisons). The slope of the equation of best fit $V^{SF}_{\text{by HA}}$=1.10*($V^{SF}_{\text{by protein}}$)+18.44) was not different from 1 (P=0.61).

HAS gene expression was analyzed in SL from ACLT, Non-OP, and CTRL knees using qPCR. SL was submerged in liquid nitrogen and pulverized. RNA was isolated from SL using QIAzol reagent (Qiagen) and the RNeasy Mini Kit with a DNAse I incubation step (Qiagen). RNA was quantified using a NanoDrop 1000 spectrophotometer (Thermo Scientific). RNA (40 ng) was reverse transcribed, and resultant cDNA was ligated and amplified using the Whole Transcriptome Amplification Kit (Qiagen). Real-time qPCR was carried out on a Rotor-Gene Q platform with SYBR green reporter (Qiagen) using rabbit-specific primers for HA synthase 1, 2, and 3 (*HAS1*, *HAS2*, *HAS3*), glyceraldehyde 3-phosphate dehydrogenase (*GAPDH*), and

ribosomal protein S18 (*RPS18*) from Qiagen (**Table 3)**. Amplification curves were converted to absolute copy numbers (CN) of gene transcripts using standard curves. The expected PCR product size was confirmed by electrophoresis. Data are reported as CN ratio of gene of interest to the geometric mean of *GAPDH* and *RPS18*. FLS expression of *HAS2* were used for $r_s^{SL,FLS}{}_{HA}$ (**Fig. 6**), as FLS *HAS1* and *HAS3* expression were below the limits of detection.

Table 2.3: Qiagen primers used for qPCR of rabbit FLS and SL. *The reference position is the position of the amplicon in the RefSeq sequence (via Qiagen).

Target Gene	Product Size [bp]	RefSeq Accession No.	Reference Position*	Catalog No.
RPS18	146	XM_002714532	204	PPN10659A
GAPDH	109	NM_001082253	1117	PPN00377A
HAS1	119	XM_008249800	206	PPN14578A
HAS2	132	NM_001082010	511	PPN00030A
HAS3	150	NM_001082709	1610	PPN00712A

Effect of ACLT on $N^{SL,FLS}$ and estimation of A^{SL}. To examine the effect of ACLT on $N^{SL,FLS}$, SL was harvested from an additional 26 rabbits (9-18 mos) following surgery for ACLT (with the left knee as a contralateral control) at 1, 2, 4, and 28 days post-surgery (n=6-8 rabbits per time point).

SL was analyzed for $N^{SL,FLS}$. After dissection as described above, discs (3 mm diameter) were harvested and lyophilized. Following overnight digestion in a solution of proteinase K (Roche, 0.5 mg/mL) at 60°C in PBE (100 mM sodium phosphate, 5 mM Na2EDTA, pH 7.1), samples were assayed using PicoGreen reagent (Invitrogen) [40]. Fluorescence was measured with an excitation wavelength of 480 nm and emission wavelength of 520 nm in a spectrofluorimetric plate reader (SpectraMax Gemini, Molecular Devices). Fluorescence values were converted to ng DNA using standards of calf thymus DNA (Sigma) in the same buffer solution as samples. DNA content was normalized to determine cell number (7.8 pg DNA/cell) [24, 42]. Cells per SL disc were scaled to cells per joint SL ($N^{SL,FLS}$) using calculations of SL area based on the expected ratio of V^{SF} to tissue (cartilage and SL) area in CTRL joints (0.1 mm) [7, 25, 30]. The area of the SL (A^{SL}=6.7 cm^2) was estimated from simplified joint geometry and prior studies [25, 30].

Calibration of HA secretion to HAS1, HAS2, HAS3 gene expression. The relationship between *HAS* gene expression and HA secretion for adult female NZW rabbit FLS was assessed *in vitro*. FLS were cultured in basal medium (0.5% FBS) or with stimulating cytokines (0.1, 1.0 ng/mL TGF-β1 and IL-1β) [6, 10, 19]. In parallel, replicate SL samples from knees of CTRL rabbits were harvested and either immediately processed for PCR or cultured for 24 hours in basal medium supplemented with 1% FBS to obtain a daily secretion value. FLS and SL were analyzed for expression of *HAS1, HAS2,* and *HAS3* by qPCR, as described above. HA in

conditioned medium was assessed, as described above. The relationship between *in vitro* FLS *HAS2* expression and HA secretion data was assessed by linear regression, and the slope of the fit was used to scale *in vivo* expression values, accounting for differences between cell (FLS) and tissue (SL) synthesis rates. The effect of culture condition on *in vitro* FLS HA secretion rates and gene expression was analyzed using one-way repeated measures ANOVA with Sidak post-hoc testing.

Data availability. The data that supports the findings of this study are available from the corresponding author upon reasonable request.

2.5 Results

ACLT causes time-varying changes in c^{SF}_{HA}, V^{SF}, and $r_s^{SL,FLS}{}_{HA}$

c^{SF}_{HA} was lower in ACLT compared to Non-OP knees (P<0.001) and affected by time (P<0.05), with an interaction effect (P<0.05, **Fig. 2a**). Compared to Non-OP, ACLT c^{SF}_{HA} was substantially lower at both early (-51% to -64%, d4 and d7, P<0.05, and -51% trend at d1, P=0.14) and late (-47% and -33% at d28 and d42, P<0.05) time points post-injury. Both Non-OP and ACLT c^{SF}_{HA} were affected by time (P<0.05 by ANOVA and curve fits). Compared to c^{SF}_{HA} in CTRL (2.68±0.27 mg/mL), ACLT c^{SF}_{HA} was lower at all time points (-49% to –80%, P<0.01), while Non-OP c^{SF}_{HA} was lower only at d7 and d14 post-injury (-50% and -44%, P<0.01).

V^{SF} was higher in ACLT compared to Non-OP knees (P<0.001) and affected by time (P<0.001), with an interaction effect (P<0.05, **Fig. 2b**). Compared to Non-OP, ACLT V^{SF} trended higher by d1, d4, and d14 post-injury (+85-210%, P=0.06-0.09), and was markedly higher at d7, d28, and d42 following injury (+140-345%, P<0.05). ACLT V^{SF} was affected by time (P<0.001), and, compared to CTRL V^{SF} (102±8 μL), became higher by d7, and remained elevated through d42 (+268% to +449%, P<0.05). Non-OP V^{SF} varied with time, increasing (P<0.05 by curve fit) to a peak of P=176 μL (+74%) at T=12 days (**Fig. 2b**, inset).

$r_s^{SL,FLS}{}_{HA}$ was higher in ACLT compared to Non-OP knees (P<0.001) and affected by time (P<0.05), with an interaction tendency (P=0.17, **Fig. 2c**). Compared to Non-OP, ACLT $r_s^{SL,FLS}{}_{HA}$ was higher at d14 and d28 (+190% to +210%, P<0.05). Compared to CTRL (4.09±1.02 μg HA/(million cells · day), ACLT, but not Non-OP, $r_s^{SL,FLS}{}_{HA}$, was higher at d14 and d28 post-injury (+228 and +220%, P<0.05). $r_s^{SL,FLS}{}_{HA}$ varied with time for ACLT (P<0.05), increasing to a peak of 13.8 μg HA/(million cells · day) at T=19.1 days (**Fig. 2c**, inset). $r_s^{SL,FLS}{}_{HA}$ for Non-OP knees did not vary detectably with time.

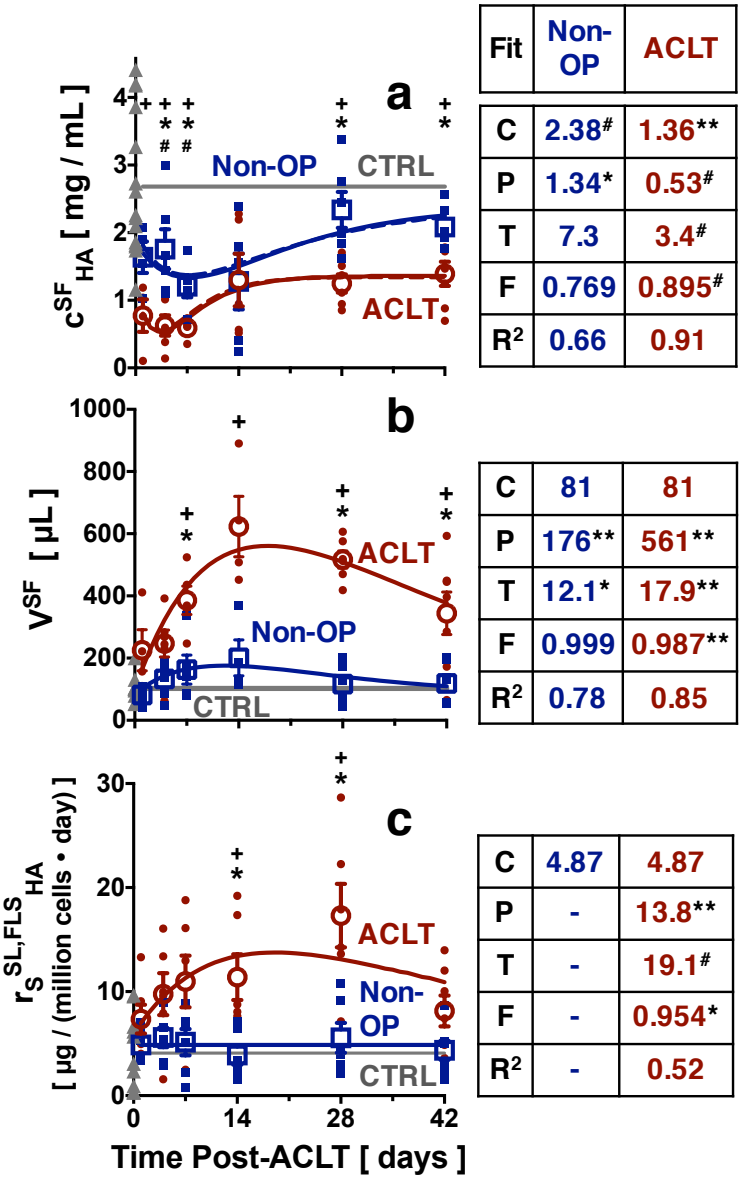

Fit	Non-OP	ACLT
C	2.38#	1.36**
P	1.34*	0.53#
T	7.3	3.4#
F	0.769	0.895#
R^2	0.66	0.91

C	81	81
P	176**	561**
T	12.1*	17.9**
F	0.999	0.987**
R^2	0.78	0.85

C	4.87	4.87
P	-	13.8**
T	-	19.1#
F	-	0.954*
R^2	-	0.52

Figure 2.2: Effect of ACLT on experimentally assessed variables and mathematical fits of the mass balance model of HA in the rabbit knee. (a) c^{SF}_{HA}, **(b)** V^{SF} and **(c)** $r_s^{SL,FLS}{}_{HA}$ from *in vivo* SF and SL. Data are shown as individual values for **Non-OP** (■) and **ACLT** (●) or as mean±SE (○, □), n=4-7; **CTRL** data are plotted as individual values at t=0 (▲) or as mean (— , n=15, 10, 11). **P*<0.05 for ACLT vs. Non-OP, +*P*<0.05 for ACLT vs. CTRL, #*P*<0.05 for Non-OP vs. CTRL. Tabulated values correspond to parameters in **equation (16)** for curve fits (— in **A-C**), with units of C, P, and T as shown on the axes, and the significance of each parameter (C, P, T, F) indicated as ***P*<0.01, **P*<0.05, #*P*<0.10, with R^2 as shown. Approximated c^{SF}_{HA} from **equation (15)** are also shown (- - -) in (**A**).

ACLT causes time-varying changes in m^{SF}_{HA}, L^{SF}_{HA}, and CL^{SF}_{HA}

m^{SF}_{HA} tended to be higher for ACLT compared to Non-OP knees (P=0.10), and was affected by time (P<0.05), with an interaction effect (P<0.05, **Fig. 3a**). m^{SF}_{HA} was higher in ACLT than Non-OP knees at d28 post-injury (+351 μg, +123%, P<0.05), and trended towards a sustained elevation at d42 (+219 μg, +89%, P=0.13). m^{SF}_{HA} varied with time for ACLT (P<0.001), but not Non-OP. Compared to CTRL (253±48 μg), ACLT, but not Non-OP, m^{SF}_{HA} was higher at d28 post-injury (+171%, P<0.05).

The computed dm^{SF}_{HA}/dt, from curve fits for c^{SF}_{HA} and V^{SF} (**equation (4)**, **Fig. 3b**), was altered following ACLT. Non-OP dm^{SF}_{HA}/dt was near zero (-3 to +15 μg/day, **Fig. 3b**), while ACLT dm^{SF}_{HA}/dt was elevated at early time points (+29 to +56 μg/day, d4-14 post-injury), driven by large increases in V^{SF} (**Fig. 2b**) relative to substantial decreases in c^{SF}_{HA} (**Fig. 2a**). ACLT dm^{SF}_{HA}/dt was slightly negative at later time points (-10 to -13 μg/day, d28-42, **Fig. 3b**), as V^{SF} moderately decreased toward CTRL values while c^{SF}_{HA} increased slightly toward CTRL values.

Consequently, L^{SF}_{HA}, estimated from G^{SF}_{HA} and dm^{SF}_{HA}/dt (**equation (1)**, **Fig. 3b**), was altered in ACLT but not Non-OP knees. Compared to CTRL L^{SF}_{HA} (197±58 μg HA/day), ACLT L^{SF}_{HA} was markedly higher for all time points (+68-591%), increasing to ~1,300 μg HA/day by d14, and remaining elevated throughout (~1,100 μg HA/day at d42 post-injury, **Fig. 3b**).

The estimated CL^{SF}_{HA} (**equation (6)**) was much higher in ACLT than Non-OP knees, and persisted throughout the 42-day time course (**Fig. 3c**). Compared to CTRL (74±23 μL/day) and Non-OP knees (107-175 μL/day), ACLT CL^{SF}_{HA} was higher by an order of magnitude at both acute (~420-1575 μL/day, d1-7) and more chronic (~810-1120 μL/day, d14-42) time points, driven by increased L^{SF}_{HA} (**Fig. 3b**) and decreased c^{SF}_{HA} (**Fig. 2a**).

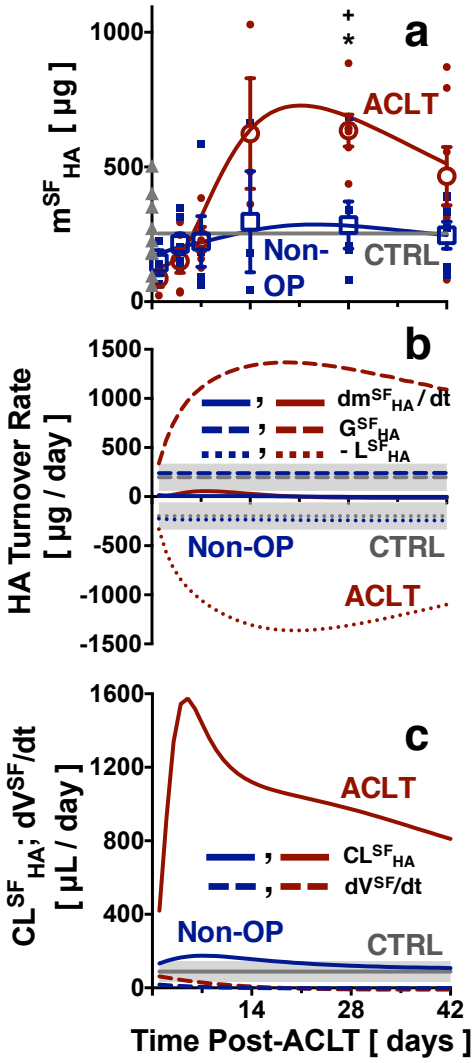

ACLT causes changes in c^{SF}_{HA} by affecting the dynamic balance between biosynthesis, loss, and

Figure 2.3: Effect of ACLT on fit variables and parameters in the mass balance model of HA in the rabbit knee. (a) m^{SF}_{HA} data and curve fits (—), **(b)** variation in m^{SF}_{HA} post-injury (—) due to synthesis (G^{SF}_{HA},- - -) and loss ($-L^{SF}_{HA}$, ···) (**equation (1)**), and **(c)** CL^{SF}_{HA} (—) and dV^{SF}/dt (- - -), all as calculated or estimated from measured variables in **Fig. 2**. Data for m^{SF}_{HA} are shown as individual values for **Non-OP** (■) and **ACLT** (●), as mean±SE (○, □), n=4-7; **CTRL** data are plotted as individual values at t=0 (▲) or as mean (— , n=9). **P*<0.05 for ACLT vs. Non-OP, +*P*<0.05 for ACLT vs. CTRL. **CTRL** values for G^{SF}_{HA}, L^{SF}_{HA}, and CL^{SF}_{HA} are mean±95% CI as calculated from products and quotients error propagation (■, n=9-27).

dilution indicated by γ, τ, $c^{SF}_{HA,SS}$, α, and β

γ (**Fig. 4a**), the normalized net difference between generation and loss rates (**equation (3)**), was affected by ACLT, being transiently elevated and then chronically diminished. In ACLT knees, γ was initially markedly elevated (0.15-0.28, +415-823% vs. Non-OP, d4-14), and then later was negative (-0.05 to -0.07, -379% to -501%, d28-42), due to an increasingly large ACLT L^{SF}_{HA} term relative to G^{SF}_{HA} (**Fig. 3b**). In Non-OP knees, γ was close to zero (-0.01 to 0.06, d4-42, **Fig. 3b**).

τ, the characteristic time for HA-containing V^{SF} clearance (**equation (10)**), was lower after ACLT (0.21 to 0.53 days, -49% to -85%, **Fig. 4b**) than both CTRL and Non-OP τ (1.4±0.5 and 0.8-1.2 days, respectively). This was due to the ACLT-induced increase in CL^{SF}_{HA} (denominator) being more than the relative increase in V^{SF} (numerator).

$c^{SF}_{HA,SS}$ (**equation (11), Fig. 4c**, the ratio of G^{SF}_{HA} to CL^{SF}_{HA}) was affected by ACLT and was substantially decreased in ACLT knees for all time points (to 0.6-1.3 mg/mL, -50% to -80% vs. CTRL, **Fig. 4c**). This decrease was due to the relatively large increase in CL^{SF}_{HA} (denominator, **Fig. 3c**) relative to the increase in G^{SF}_{HA} (numerator, **Fig. 3b**). Non-OP $c^{SF}_{HA,SS}$ values (1.4-2.2 mg/mL) were decreased (-17% to -49% vs. CTRL), but trended higher towards CTRL values by d42 (**Fig. 4c**).

α (**equation (12)**, **Fig. 4d**, the dimensionless ratio of dV^{SF}/dt to CL^{SF}_{HA}, reflecting relative volume turnover) was altered bi-directionally in both ACLT and Non-OP knees (**Fig. 4d**). At early time, α was markedly positive in both ACLT and Non-OP knees (0.03-0.13, d1-7), due to increased V^{SF}. At later time, Non-OP α was slightly negative (-0.01 to -0.02, d14-42, **Fig. 4d**), while ACLT α was near zero (+25-62% vs. Non-OP, d28-42), as dV^{SF}/dt was much less than CL^{SF}_{HA}.

β (**equation (14)**, **Fig. 4e**, the dimensionless rate ratio of HA buildup to secretion) was also altered bi-directionally in both ACLT and Non-OP knees. Non-OP β was negative at early time points (-0.002 to -0.061, d1-7) due to a negative dc^{SF}_{HA}/dt, but became positive as c^{SF}_{HA} increased (0.005-0.029, d7-42, **Fig. 4e**). Comparatively, ACLT β was lower at later time points (-45% to -99%, d14-42, **Fig. 4e**), due to a greater G^{SF}_{HA} term.

The net of α+β, reducing c^{SF}_{HA} relative to $c^{SF}_{HA,SS}$ (**equation (15)**) was close to zero over all time (**Fig. 4f**). Thus, the modeled $c^{SF}_{HA,SS}$ (**Fig. 4c**) was close to c^{SF}_{HA} (**Fig. 2a**).

dc^{SF}_{HA}/dt also exhibited a bi-directional response, initially markedly negative. It was driven by the difference between $c^{SF}_{HA,SS}$ and the current value of c^{SF}_{HA} (numerator, since α was near zero), and also τ (denominator, **equation (9)**, **Fig. 4g**). At early time, ACLT dc^{SF}_{HA}/dt was greater in magnitude than Non-OP (to 0.04-0.08 mg/(mL·day), +21-895%, d7-14) due to a smaller τ, but then diminished and was close to zero for d21-42. Non-OP dc^{SF}_{HA}/dt was negative at early time points (-0.01 to -0.14 mg/(mL·day), d1-7, **Fig. 4g**) due to a positive α term (**Fig. 4d**, **equation (9)**), but then quickly became positive and was close to zero for the remaining time (0.00 to 0.04 mg/(mL·day), d7-42).

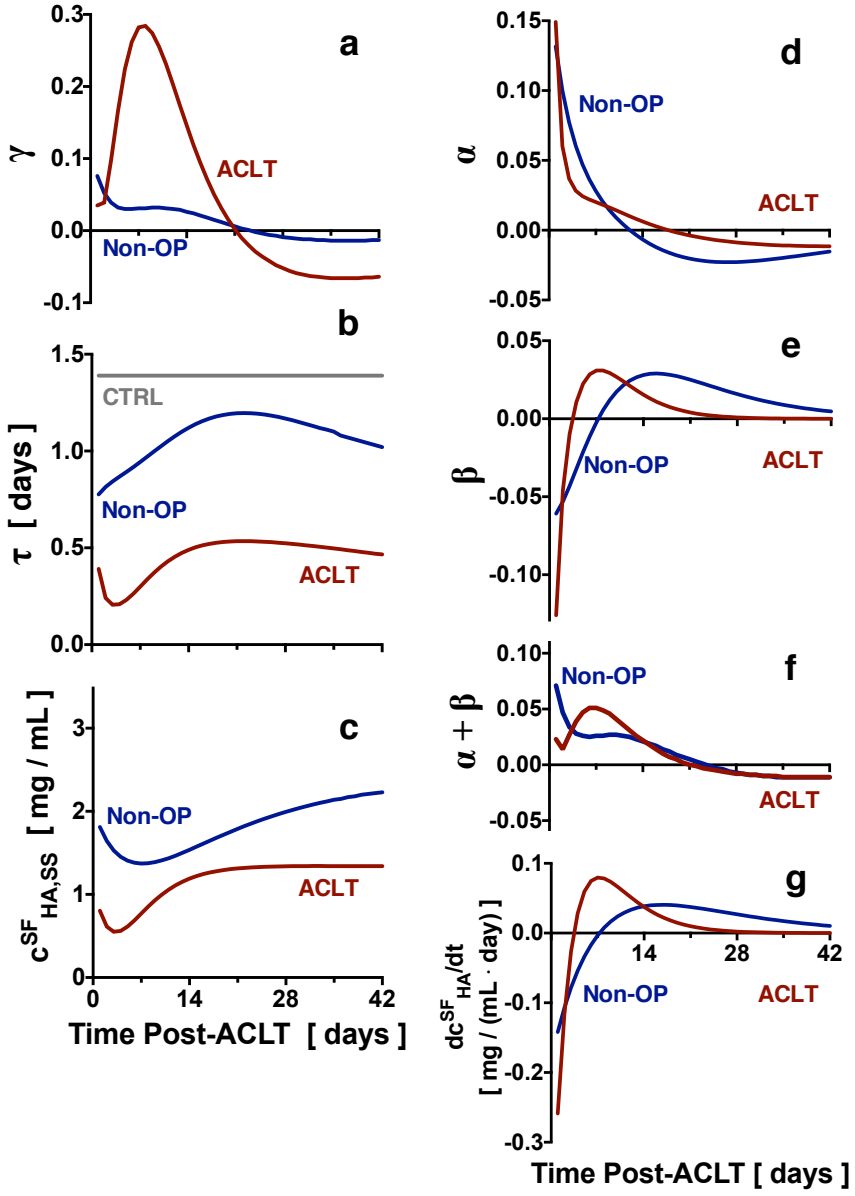

Figure 2.4: Effect of characteristic and dimensionless parameters on c^{SF}_{HA} and dc^{SF}_{HA}/dt. The characteristic variables and dimensionless parameters **(a)** γ (**equation (3)**), **(b)** τ (**equation (10)**), **(c)** $c^{SF}_{HA,SS}$ (**equation (11)**), **(d)** α (**equation (12)**), **(e)** β (**equation (14)**), **(f)** α+β (**equation (15)**), and **(g)** dc^{SF}_{HA}/dt post-injury due to variations in τ, α, and $c^{SF}_{HA,SS}$ (**equation (9)**). Modeled variables and parameters for Non-OP (blue), ACLT (red), with CTRL (grey) mean value as calculated from products and quotients error propagation (n=9-27).

ACLT causes increased $N^{SL,FLS}$

ACLT $N^{SL,FLS}$ was higher vs. Non-OP (P<0.01) and was not affected by time (P=0.39), with a trend towards an interaction effect (P=0.12). Non-OP $N^{SL,FLS}$ was not affected by time (P=0.95), although there was a trend towards an effect for ACLT (P=0.05). Compared to Non-OP ($8.80x10^7$ $\pm 1.12x10^7$ cells/SL), ACLT $N^{SL,FLS}$ was higher at d4 (+110%) and 28 (+102%) post-injury (P<0.05, **Fig. 5**).

In vitro relationship between HAS1, HAS2, HAS3 gene expression and HA secretion

In vitro, HA secretion by FLS was correlated with *HAS2* gene expression and was affected by culture condition (P<0.01). Secretion was higher with both low (+249%, P<0.05) and high (+316%, P<0.05) cytokine stimulation compared to the basal condition (**Fig. 6**).

While *in vitro* FLS *HAS2* expression was not affected significantly by culture conditions (P=0.19), HA secretion increased with *HAS2* gene expression (r^2=0.44, P<0.05, **Fig. 6**). *HAS2* expression resulting from low or high cytokine concentration was elevated +44% and +103%, respectively, relative to basal conditions (**Fig. 6**). Similar to *in vivo* SL, expression of *HAS1* and *HAS3* by FLS *in vitro* were below the limits of detection.

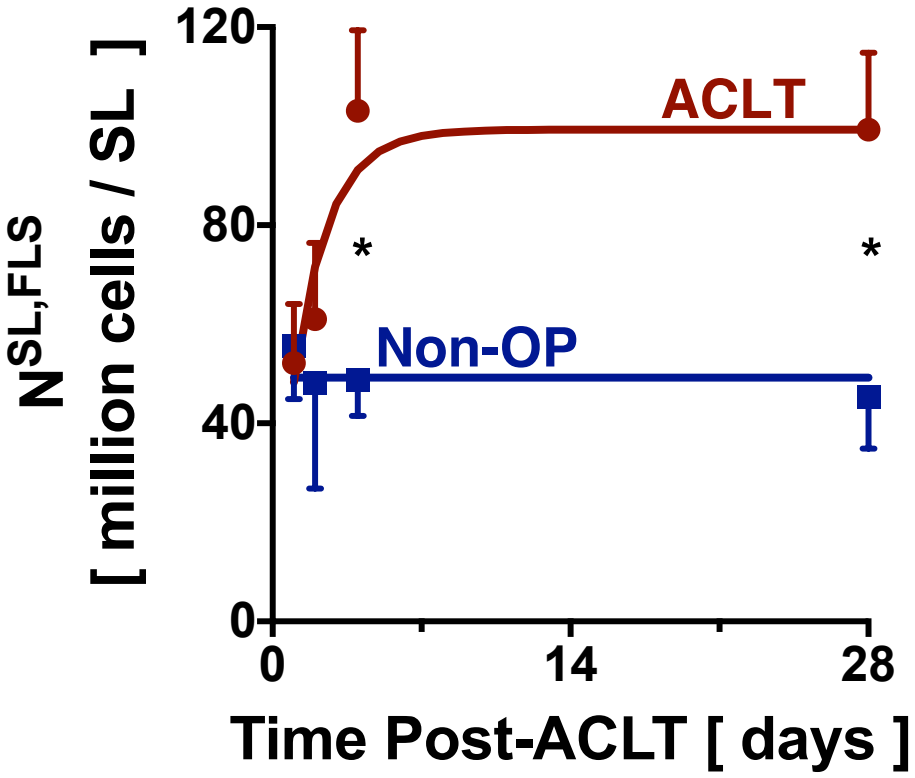

Figure 2.5: Variation in $N^{SL,FLS}$ following ACLT in the rabbit knee. Data for Non-OP (■) and ACLT (●) are mean±SE, n=6-8. *P<0.05 for ACLT vs. Non-OP. Curve fit for ACLT (—) was exponential, with a 2X increase from Non-OP (—) $N^{SL,FLS}$.

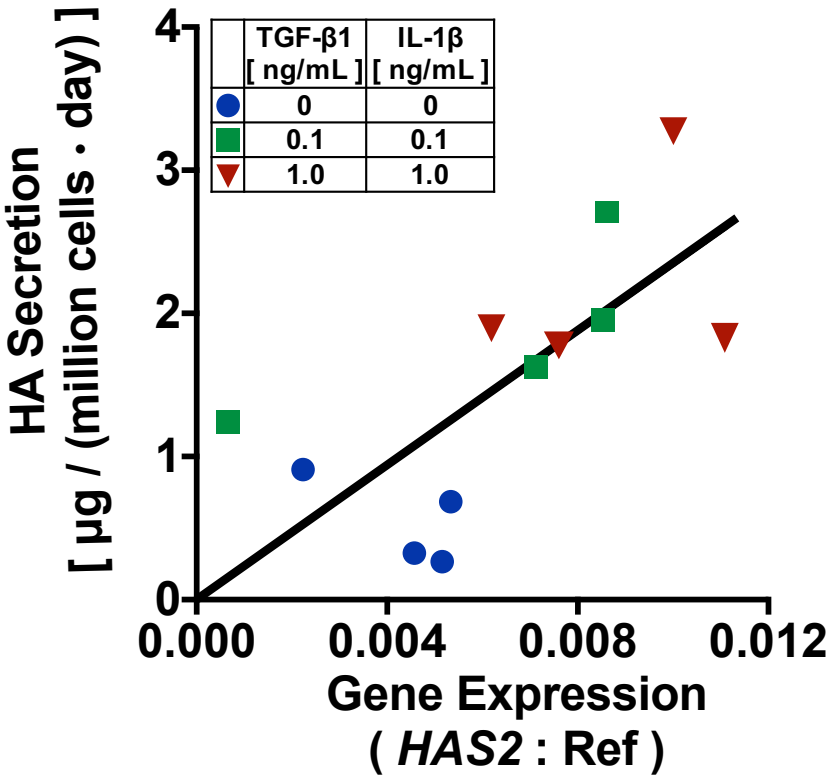

Figure 2.6: *HAS2* expression and HA synthesis by FLS. *In vitro* relationship between *HAS2* expression and HA secretion for FLS cultures, n=12. Regression line is for *HAS2* expression versus HA secretion ($y=235X$, $r^2=0.44$, $P<0.05$).

2.6 Discussion

In this study, a quantitative compartmental mass balance model of HA in SF was extended to account for SF volume changes, and then used to assess factors affecting c^{SF}_{HA} following acute injury in a rabbit model of PTOA (**Fig. 1**). Experimental data (c^{SF}_{HA}, V^{SF}, and $r_s^{SL,FLS}{}_{HA}$) were compared and fit to estimate model parameters that are difficult to measure directly *in vivo*. Compared to CTRL knees, at early time points (d1-7) following ACLT, c^{SF}_{HA} decreased quickly (-71% to –80%). V^{SF} and $r_s^{SL,FLS}{}_{HA}$ increased gradually but substantially (+61-321%, +70-176%, respectively) relative to CTRL joints. At later time points (d14-42) post-injury, the early decrease in c^{SF}_{HA} was maintained (-49% to -57% vs. CTRL), as were increases in V^{SF} (+268-449%) and $r_s^{SL,FLS}{}_{HA}$ (+168-237%). Although these quantities plateaued and then trended towards CTRL values (**Figs. 2, 3**), c^{SF}_{HA} and V^{SF} remained substantially different from CTRL values even at d42. The measured alterations led to marked changes in the modeled loss terms (L^{SF}_{HA}, CL^{SF}_{HA}, **equation (1, 6)**), characteristic variables (τ, **equation (10)**, and $c^{SF}_{HA,SS}$, **equation (11)**), and dimensionless parameters (γ, **equation (3)**, α, **equation (12)**, and β, **equation (14)**). The mass transport model fit well and thus indicate the biophysical mechanisms of altered SF lubricant composition at acute and chronic times post-injury.

The experimental assessment of SF dynamics compared ACLT, Non-OP, and CTRL knees. Contralateral ACLT vs. Non-OP limbs were compared, as c^{SF}_{HA} varies much less between knees than between subjects [51]. Both ACLT and Non-OP knees showed transient changes, so comparisons were also to CTRL rabbits. Due to limited SF volumes from the latter groups, sample size for certain assays was less than the total number of joints per group. V^{SF} was calculated from biochemical analysis of neat and lavage fluids, as V^{SF} is underestimated by the volume aspirated due to residual SF [11]. $N^{SL,FLS}$ (**Fig. 5**) was estimated from a portion of SL,

scaled up to the entire joint [7, 25, 30]. Thus, experimental measures of the rabbit PTOA model allowed analysis of the *in vivo* joint environment.

The measures after ACLT of c^{SF}_{HA} (decreased, **Fig. 2a**) [2, 37, 44], V^{SF} (increased, **Fig. 2b**), and $r_s^{SL,FLS}_{HA}$ (increased, **Fig. 2c**) extended prior analyses of injured humans and rabbits. A large increase in V^{SF} was also noted in previous studies (+70-2600%) of rabbit knees following acute injury or induced arthritis [35, 37]. The range of $r_s^{SL,FLS}_{HA}$ rates in the present study (4-18 μg/(million cells · day)) is consistent with previous reports for human FLS cultured *in vitro* [6, 19], as well as rabbit FLS *in vivo* [11]. The calibrated relationship between $r_s^{SL,FLS}_{HA}$ and *HAS* gene expression was assessed [14], and likely depends on the complex local microenvironment *in vivo* [21, 41]. The increase in $r_s^{SL,FLS}_{HA}$ following injury may be due to biochemical (cytokine) and mechanical (stretch) factors. In acute inflammation, cytokines are released and include IL-1β and TNF-α [17], both of which induce *HAS* expression and HA secretion in FLS [6, 46]. Additionally, FLS are mechano-sensitive, and large increases in V^{SF} due to joint swelling cause stretch [38], and may induce FLS to increase HA secretion [11, 41]. The *in vivo* measures of c^{SF}_{HA}, V^{SF}, and $r_s^{SL,FLS}_{HA}$ allowed biophysical analysis in the context of the mass balance model.

The model-based study approach provides an explanation for the apparent paradox between the ACLT-induced decrease in c^{SF}_{HA} (**Fig. 2a**) and increased G^{SF}_{HA} (**Fig. 3b**) and m^{SF}_{HA} (**Fig. 3a**), as both joint swelling (increased V^{SF}, **Fig. 2a**) and increased L^{SF}_{HA} and CL^{SF}_{HA} (**Fig. 3c**) caused c^{SF}_{HA} to decrease. In previous studies, L^{SF}_{HA} was assessed by injecting exogenous or radiolabeled HA and monitoring c^{SF}_{HA} or HA residence over time [9, 21]. Based on reported values for injected m^{SF}_{HA} and HA half-life, L^{SF}_{HA} in healthy joints was estimated [9, 21] to be 150-450 μg HA/day, encompassing values of L^{SF}_{HA} for CTRL and Non-OP knees in the present study (**Fig. 3b**). Estimates of L^{SF}_{HA} based on injection of exogenous HA depend on injection volume

and HA M_r, as increases in V^{SF} (and thus joint hydrostatic pressure) drive advective transport and loss of HA from the joint, while lower M_r HA also reduce HA retention [11, 47]. The present estimates of L^{SF}_{HA} reflect overall (mostly high-M_r [37]) HA, without exogenous HA injection.

The increased mass loss rate L^{SF}_{HA} (+68-591% vs. CTRL, **equation (6)**, **Fig. 3b**), volume turnover CL^{SF}_{HA} (+471-2041% vs. CTRL, **equation (6)**, **Fig. 3c**), and decreased characteristic time τ (-61 to -85% vs. CTRL, **equation (10)**, **Fig. 4b**) provide metrics that clarify the extent of HA loss normally, and induced by ACLT. Increased L^{SF}_{HA} and CL^{SF}_{HA}, as well as decreased τ, following injury (**Fig. 3b**, **c**, **Fig. 4b**) are likely due to both biophysical and catabolic mechanisms. Loss rates due to transport (efflux) or degradation can be proportionate to c^{SF}_{HA}, similar in form to L^{SF}_{HA} in **equation (6)**. Following injury, L^{SF}_{HA} may be increased due to higher HA efflux, mediated by altered SL properties (increased permeability [31], decreased reflection coefficient [49], and increased surface area [33]), in conjunction with increases in fluid flux, driven by gradients in hydrostatic and oncotic pressures [26, 30]. Increased L^{SF}_{HA} may also be due to degradation of HA to lower M_r forms by hyaluronidases or reactive oxygen species, which then are rapidly lost from the joint space [27, 39]. Increased catabolism of HA by resident joint cells (analyzed by injection of radiolabeled HA and monitoring the location of HA metabolites) [27] has been estimated to be ~30% of the total HA lost. Previous reports of HA residence time in knee joints (1.1-1.6 days in healthy joints and 0.3-0.7 days following injury or arthritis induction in rabbit or sheep models) [9, 11, 15, 37] were similar to estimates of τ (1.4±0.5 days for CTRL, 0.8-1.2 days for Non-OP, 0.2-0.5 days for ACLT) in the present study.

The estimates of L^{SF}_{HA} and CL^{SF}_{HA} reflect rate processes occurring over a time period between two measurements of V^{SF} and c^{SF}_{HA}, as well as $r_s^{SL,FLS}{}_{HA}$ (**equation (1, 4-6)**). Such measurements could be soon after injury (e.g. prior to administration of a therapeutic), and at a

follow-up time (e.g. to test for efficacy of the therapeutic). Since CL^{SF}_{HA} (**Fig. 3c**) is estimated from L^{SF}_{HA} and c^{SF}_{HA}, it depends similarly on sampling times. For such measurements, fluid (SF, lavage) and tissue (SL) sampling are needed for biochemical analysis. V^{SF} might be assessed, alternatively, using imaging methods.

The characteristic variables τ (**equation (10)**, **Fig. 4b**) and $c^{SF}_{HA,SS}$ (**equation (11)**, **Fig. 4c**), and the dimensionless parameters γ (**equation (3)**, **Fig. 4a**), α (**equation (12)**, **Fig. 4d**), and β (**equation (14)**, **Fig. 4e**) help to explain the joint-scale transport causing the decreased c^{SF}_{HA} in ACLT joints (**equation (13)**, **Fig. 2a**). The large increases in the loss terms L^{SF}_{HA} and CL^{SF}_{HA} (**Fig. 3b**, **c**) drove acute (d1-7) and pronounced decreases in ACLT τ (**Fig. 4b**, to 0.21 days) and $c^{SF}_{HA,SS}$ (**Fig. 4c**, to 0.55 mg/mL), as well as a slight increase in α (**Fig. 4d**, to 0.15). The losses were not compensated for by the large increase in ACLT G^{SF}_{HA} at early time (**Fig. 3b**), with an immediate increase in γ (**Fig. 4a**, to 0.28) and decrease in β (**Fig. 4e**, to -0.13). At later times (d7-42), the persistent increases in L^{SF}_{HA} and CL^{SF}_{HA} maintained the reduction in ACLT τ (0.30-0.53 days) and $c^{SF}_{HA,SS}$ (0.55-1.34 mg/mL). The increase in L^{SF}_{HA} outpaced that in G^{SF}_{HA} at later time and γ became negative (-0.01 to -0.07, **Fig. 4a**). These calculated variables and parameters provide insights into relationships between biophysical variables in health and disease progression.

These results provide a foundation for using a biophysically-based, quantitative synovial joint model to elucidate the dynamics of HA, and potentially other molecules, in SF in healthy or diseased states. Because SF HA lubricant function depends on concentration [13, 45, 48], a detailed understanding of, and ability to quantify, the underlying basis for changes during joint injury and arthritis would be useful to target pathogenesis and evaluate putative therapies. The inverse relationship between dG^{SF}_{HA}/dt and dc^{SF}_{HA}/dt following ACLT (and thus the substantial

and long-lasting L^{SF}_{HA}) suggests that metrics and markers of synovial joint health need to include not only biological indices at the levels of cells (biosynthesis) and molecules (solute flux), but also physical properties of tissues (membrane transport) and organs (effusion).

2.7 Acknowledgments

This chapter, in full, will be submitted to *Nature Biomedical Engineering*. The dissertation author was the primary author and thanks co-authors Michele M. Temple-Wong, Yang Sun, Dongfang Qian, Kenji Kato, Koichiro Murata, Gary S. Firestein, Koichi Masuda, and Robert L. Sah. This work was supported by research grants from the National Institutes of Health (R01 AR055637, T32 AR060712), the Department of Defense (DOD OR13085), the UC San Diego Frontiers of Innovation Scholarship Program, and the San Diego Fellowship.

The authors thank Dr. Samuel Ward and Dr. Gregory Heldt for use of CTRL rabbit tissue.

2.8 References

1. Antonacci JM, Schmidt TA, Serventi LA, Cai MZ, Shu YL, Schumacher BL, McIlwraith CW, Sah RL: Effects of equine joint injury on boundary lubrication of articular cartilage by synovial fluid: role of hyaluronan. *Arthritis Rheum* 64:2917-26, 2012.

2. Asari A, Miyauchi S, Sekiguchi T, Machida A, Kuriyama S, Miyazaki K, Namiki O: Hyaluronan, cartilage destruction and hydrarthrosis in traumatic arthritis. *Osteoarthritis Cartilage* 2:79-89, 1994.

3. Balazs EA: The physical properties of synovial fluid and the special role of hyaluronic acid. In: *Disorders of the Knee,* ed. by AJ Helfet, Lippincott Co., Philadelphia, 1974, 63-75.

4. Bartok B, Firestein GS: Fibroblast-like synoviocytes: key effector cells in rheumatoid arthritis. *Immunol Rev* 233:233-55, 2010.

5. Barton KI, Shekarforoush M, Heard BJ, Sevick JL, Vakil P, Atarod M, Martin R, Achari Y, Hart DA, Frank CB, Shrive NG: Use of pre-clinical surgically induced models to understand biomechanical and biological consequences of PTOA development. *J Orthop Res* 35:454-65, 2017.

6. Blewis ME, Lao BJ, Schumacher BL, Bugbee WD, Sah RL, Firestein GS: Interactive cytokine regulation of synoviocyte lubricant secretion. *Tissue Eng Part A* 16:1329-37, 2010.

7. Blewis ME, Nugent-Derfus GE, Schmidt TA, Schumacher BL, Sah RL: A model of synovial fluid lubricant composition in normal and injured joints. *Eur Cell Mater* 13:26-39, 2007.

8. Bluteau G, Gouttenoire J, Conrozier T, Mathieu P, Vignon E, Richard M, Herbage D, Mallein-Gerin F: Differential gene expression analysis in a rabbit model of osteoarthritis induced by anterior cruciate ligament (ACL) section. *Biorheology* 39:247-58, 2002.

9. Brown TJ, Laurent UB, Fraser JR: Turnover of hyaluronan in synovial joints: elimination of labelled hyaluronan from the knee joint of the rabbit. *Exp Physiol* 76:125-34, 1991.

10. Chenevier-Gobeaux C, Morin-Robinet S, Lemarechal H, Poiraudeau S, Ekindjian JC, Borderie D: Effects of pro- and anti-inflammatory cytokines and nitric oxide donors on

hyaluronic acid synthesis by synovial cells from patients with rheumatoid arthritis. *Clin Sci (Lond)* 107:291-6, 2004.

11. Coleman PJ, Scott D, Ray J, Mason RM, Levick JR: Hyaluronan secretion into the synovial cavity of rabbit knees and comparison with albumin turnover. *J Physiol* 503 (Pt 3):645-56, 1997.

12. Dahl LB, Dahl IM, Engstrom-Laurent A, Granath K: Concentration and molecular weight of sodium hyaluronate in synovial fluid from patients with rheumatoid arthritis and other arthropathies. *Ann Rheum Dis* 44:817-22, 1985.

13. Elsaid KA, Jay GD, Warman ML, Rhee DK, Chichester CO: Association of articular cartilage degradation and loss of boundary-lubricating ability of synovial fluid following injury and inflammatory arthritis. *Arthritis Rheum* 52:1746-55, 2005.

14. Feder ME, Walser JC: The biological limitations of transcriptomics in elucidating stress and stress responses. *J Evol Bio* 18:901-10, 2005.

15. Fraser JR, Kimpton WG, Pierscionek BK, Cahill RN: The kinetics of hyaluronan in normal and acutely inflamed synovial joints: observations with experimental arthritis in sheep. *Semin Arthritis Rheum* 22:9-17, 1993.

16. Gelber AC, Hochberg MC, Mead LA, Wang NY, Wigley FM, Klag MJ: Joint injury in young adults and risk for subsequent knee and hip osteoarthritis. *Ann Intern Med* 133:321-8, 2000.

17. Goldring MB: Osteoarthritis and cartilage: the role of cytokines. *Curr Rheumatol Rep* 2:459-65, 2000.

18. Guyton AC, Hall JE. Textbook of Medical Physiology. 11th ed. Philadelphia: Elsevier Saunders; 2006.

19. Haubeck HD, Kock R, Fischer DC, Van de Leur E, Hoffmeister K, Greiling H: Transforming growth factor beta 1, a major stimulator of hyaluronan synthesis in human synovial lining cells. *Arthritis Rheum* 38:669-77, 1995.

20. Hui AY, McCarty WJ, Masuda K, Firestein GS, Sah RL: A systems bIology approach to synovial joint lubrication in health, injury, and disease. *Wiley Interdiscip Rev Syst Biol Med* 4:15-37, 2012.

21. Ingram KR, Wann AK, Angel CK, Coleman PJ, Levick JR: Cyclic movement stimulates hyaluronan secretion into the synovial cavity of rabbit joints. *J Physiol* 586:1715-29, 2008.

22. Itano N, Sawai T, Yoshida M, Lenas P, Yamada Y, Imagawa M, Shinomura T, Hamaguchi M, Yoshida Y, Ohnuki Y, Miyauchi S, Spicer AP, McDonald JA, Kimata K: Three isoforms of mammalian hyaluronan synthases have distinct enzymatic properties. *J Biol Chem* 274:25085-92, 1999.

23. Kiener HP, Watts GF, Cui Y, Wright J, Thornhill TS, Skold M, Behar SM, Niederreiter B, Lu J, Cernadas M, Coyle AJ, Sims GP, Smolen J, Warman ML, Brenner MB, Lee DM: Synovial fibroblasts self-direct multicellular lining architecture and synthetic function in three-dimensional organ culture. *Arthritis Rheum* 62:742-52, 2010.

24. Kim YJ, Sah RLY, Doong JYH, Grodzinsky AJ: Fluorometric assay of DNA in cartilage explants using Hoechst 33258. *Anal Biochem* 174:168-76, 1988.

25. Knight AD, Levick JR: The density and distribution of capillaries around a synovial cavity. . *Q J Exp Physiol* 68:629-44, 1983.

26. Knight AD, Levick JR, McDonald JN: Relation between trans-synovial flow and plasma osmotic pressure, with an estimation of the albumin reflection coefficient in the rabbit knee. *Q J Exp Physiol* 73:47-65, 1988.

27. Laurent UB, Fraser JR, Engstrom-Laurent A, Reed RK, Dahl LB, Laurent TC: Catabolism of hyaluronan in the knee joint of the rabbit. *Matrix* 12:130-6, 1992.

28. Le Graverand MP, Eggerer J, Vignon E, Otterness IG, Barclay L, Hart DA: Assessment of specific mRNA levels in cartilage regions in a lapine model of osteoarthritis. *J Orthop Res* 20:535-44, 2002.

29. Lee HG, Cowman MK: An agarose gel electrophoretic method for analysis of hyaluronan molecular weight distribution. *Anal Biochem* 219:278-87, 1994.

30. Levick JR: The influence of hydrostatic pressure on trans-synovial fluid movement and on capsular expansion in the rabbit knee. *J Physiol* 289:69-82, 1979.

31. Levick JR: Permeability of rheumatoid and normal human synovium to specific plasma proteins. *Arthritis Rheum* 24:1550-60, 1981.

32. Levick JR: Synovial fluid and trans-synovial flow in stationary and moving normal joints. In: *Joint loading: biology and health of articular structures* ed. by HJ Helminen, Kiviranta I, Säämänen AM, Tammi M, Paukkonen K, Wright & Sons, Bristol, 1987, 149-86.

33. Levick JR: An analysis of the interaction between interstitial plasma protein, interstitial flow, and fenestral filtration and its application to synovium. *Microvasc Res* 47:90-125, 1994.

34. Lukoschek M, Schaffler MB, Burr DB, Boyd RD, Radin EL: Synovial membrane and cartilage changes in experimental osteoarthrosis. *J Orthop Res* 6:475-92, 1988.

35. Matsuzaka S, Sato S, Miyauchi S: Estimation of joint fluid volume in the knee joint of rabbits by measuring the endogenous calcium concentration. *Clin Exp Rheumatol* 20:531-4, 2002.

36. Mazzucco D, Scott R, Spector M: Composition of joint fluid in patients undergoing total knee replacement and revision arthroplasty: correlation with flow properties. *Biomaterials* 25:4433-45, 2004.

37. McCarty WJ, Cheng JC, Hansen BC, Yamaguchi T, Masuda K, Sah RL: The biophysical mechanisms of altered hyaluronan concentration in synovial fluid after anterior cruciate ligament transection. *Arthritis Rheum* 64:3993-4003, 2012.

38. McCarty WJ, Masuda K, Sah RL: Fluid movement and joint capsule strains due to flexion in rabbit knees. *J Biomech* 44:2761-7, 2011.

39. McCord JM: Free radicals and inflammation: Protection of synovial fluid by superoxide dismutase. *Science* 185:529-31, 1974.

40. McGowan KB, Kurtis MS, Lottman LM, Watson D, Sah RL: Biochemical quantification of DNA in human articular and septal cartilage using PicoGreen and Hoechst 33258. *Osteoarthritis Cartilage* 10:580-7, 2002.

41. Momberger TS, Levick JR, Mason RM: Hyaluronan secretion by synoviocytes is mechanosensitive. *Matrix Biol* 24:510-9, 2005.

42. Neuman MK, Briggs KK, Masuda K, Sah RL, Watson D: A compositional analysis of cadaveric human nasal septal cartilage. *Laryngoscope* 123:2120-4, 2013.

43. Ohno S, Tanimoto K, Fujimoto C, Ijuin K, Honda K, Tanaka N, Doi T, Nakahara M, Tanne K: Molecular cloning of rabbit hyaluronic acid synthases and their expression patterns in synovial membrane and articular cartilage. *Biochim Biophys Acta* 1520:71-8, 2001.

44. Praest BM, Greiling H, Kock R: Assay of synovial fluid parameters: hyaluronan concentration as a potential marker for joint diseases. *Clin Chim Acta* 266:117-28, 1997.

45. Raleigh AR, McCarty WJ, Chen AC, Meinert C, Klein TJ, Sah RL: Synovial joints: Mechanobiology and tissue engineering of articular cartilage and synovial fluid. In: *Comprehensive Biomaterials,* ed. by P Ducheyne, Healey KE, Hutmacher DE, Grainger DE, Kirkpatrick CJ, Elsevier, 2017, 107-34.

46. Recklies AD, White C, Melching L, Roughley PJ: Differential regulation and expression of hyaluronan synthases in human articular chondrocytes, synovial cells and osteosarcoma cells. *Biochem J* 354:17-24, 2001.

47. Sabaratnam S, Arunan V, Coleman PJ, Mason RM, Levick JR: Size selectivity of hyaluronan molecular sieving by extracellular matrix in rabbit synovial joints. *J Physiol* 567:569-81, 2005.

48. Schmidt TA, Gastelum NS, Nguyen QT, Schumacher BL, Sah RL: Boundary lubrication of articular cartilage: role of synovial fluid constituents. *Arthritis Rheum* 56:882-91, 2007.

49. Scott D, Coleman PJ, Mason RM, Levick JR: Direct evidence for the partial reflection of hyaluronan molecules by the lining of rabbit knee joints during trans-synovial flow. *J Physiol* 508 (Pt 2):619-23, 1998.

50. Spicer AP, McDonald JA: Characterization and molecular evolution of a vertebrate hyaluronan synthase gene family. *J Biol Chem* 273:1923-32, 1998.

51. Temple-Wong MM, Ren S, Quach P, Hansen BC, Chen AC, Hasegawa A, D'Lima DD, Koziol J, Masuda K, Lotz MK, Sah RL: Hyaluronan concentration and size distribution in human knee synovial fluid: variations with age and cartilage degeneration. *Arthritis Res Ther* 18:18, 2016.

52. Walker ER, Boyd RD, Wu DD, Lukoschek M, Burr DB, Radin EL: Morphologic and morphometric changes in synovial membrane associated with mechanically induced osteoarthrosis. *Arthritis Rheum* 34:515-24, 1991.

53. Wilder FV, Hall BJ, Barrett JP, Jr., Lemrow NB: History of acute knee injury and osteoarthritis of the knee: a prospective epidemiological assessment. The Clearwater Osteoarthritis Study. *Osteoarthritis Cartilage* 10:611-6, 2002.

CHAPTER 3

DECREASED SYNOVIAL FLUID PROTEOGLYCAN-4 CONCENTRATION IN ACL-TRANSECTED KNEE JOINTS IS DUE TO A DYNAMIC IMBALANCE IN BIOSYNTHESIS, CLEARANCE, AND EFFUSION

3.1 Abstract

The lubricating function of synovial fluid (SF) is decreased following injury or during arthritis progression, and often due to a diminished concentration of proteoglycan-4 (c^{SF}_{PRG4}). A theoretical model describing the biophysical mechanisms governing c^{SF}_{PRG4} was extended to include synthesis by chondrocytes ($r_s^{AC,ACH}{}_{PRG4}$) and synoviocytes ($r_s^{SL,FLS}{}_{PRG4}$), and shifts in SF volume (V^{SF}) that occur in post-traumatic osteoarthritis (PTOA). This allowed analysis of the relative contributions to normal and decreased c^{SF}_{PRG4} (-56% to -75% vs. CTRL) at 1-42 days post-injury in the rabbit ACL transection (ACLT) model of PTOA. In both CTRL and ACLT knees, SL was estimated to be the primary producer of PRG4 in SF (~90-93% of total 90-140 μg PRG4 secreted per day) due to its large surface area and high cell density. Decreased ACLT c^{SF}_{PRG4} was attributed to increased V^{SF} (+61-449%), decreased PRG4 generation (G^{SF}_{PRG4}) by both chondrocytes and synoviocytes (-3% to -35%), and increased clearance (CL^{SF}_{PRG4}, +6-114%). Though ACLT CL^{SF}_{PRG4} was initially similar to CTRL values (~870 μL/day), by d42 it had increased to ~1,900 μL/day, reducing the PRG4 SF residence time τ (from a peak of 0.50 to 0.20

days). Thus, a biophysically-based, quantitative synovial joint model for PRG4 dynamics can be evaluated in healthy and PTOA joints, and helps to delineate the biological and biophysical phenomena governing c^{SF}_{PRG4}, and to inform the timing and dosing for lubricant-restoring therapeutics following injury.

3.2 Introduction

Osteoarthritis (OA) is a debilitating joint disease that costs >$100 billion a year in lost economic output in the US alone [8]. Following acute joint injury, the likelihood of post-traumatic osteoarthritis (PTOA) is increased, through mechanisms that may include diminished lubrication mediated by synovial fluid (SF) [15, 18, 28, 51, 54]. In synovial joints such as the knee, SF is bounded by a thin synovial lining (SL) and articular cartilage (AC). The SL is backed by thicker synovial subintima (SS) and a fibrous joint capsule, and serves as a membrane to allow selective passage of molecules both into and out of the SF joint space [5, 17, 40]. Fibroblast-like synoviocytes (FLS) within the SL and articular chondrocytes (ACH) within the AC produce lubricant components of the SF [6, 30]. The metabolism of cells in the joint, as well as volume fluxes, influence the biochemical composition and concentrations in SF.

The concentration of proteoglycan-4 (PRG4, c^{SF}_{PRG4}) in SF, is often altered following injury or during arthritis progression [2-4, 13, 15]. PRG4, also known as superficial zone protein (SZP), lubricin, and megakaryocyte stimulating factor (MSF) [23], is a 345 kDa mucinous glycoprotein produced by chondrocytes within the superficial zone of cartilage and by FLS in the SL [26, 27, 29, 43, 47, 48, 50]. As a lubricant, PRG4 reduces the interaction of articulating cartilage surfaces, especially when these surfaces are in close contact [25, 45]. In human SF, PRG4 concentrations (c^{SF}_{PRG4}) range from 130-450 μg/mL [15, 34, 44] and are variably affected by acute injury [4, 13] or osteoarthritis [34].

Animal models may help to elucidate mechanisms of PTOA. Following naturally-occurring injury [2, 9, 13] or in experimental models of joint injury [14, 51], c^{SF}_{PRG4} is variably increased or decreased depending on the time point and model system. Following anterior cruciate ligament transection (ACLT) in rabbit knees, synovial hyperplasia and

neovascularization, SF effusions, and cartilage degradation are drastically increased [35, 36], but c^{SF}_{PRG4} varies based on time point post-injury [15], as does *PRG4* gene expression in both SL [14] and AC [55].

A mass balance model [7] was introduced previously to account for c^{SF}_{PRG4}, and its dependence on synthesis and loss rates. Literature data was used for PRG4 secretion by resident cells and loss by efflux or degradation in healthy human joints. However, the relative contribution of the two putative sources, AC and SL, to the overall mass and maintenance of SF PRG4 in healthy and arthritic joints is unclear. In addition, there is little data to describe injury-induced alterations to c^{SF}_{PRG4} in terms of time-varying biological and biophysical variables, particularly *in vivo*. While c^{SF}_{PRG4} depends on the extent of PRG4 synthesis, loss, and altered SF volume, the role of these variables in PTOA progression remains to be established.

Here, we tested the hypothesis that the altered c^{SF}_{PRG4} following joint injury reflects time-dependent variation in the extents of PRG4 lubricant generation and loss, in addition to SF volume changes. Our aims were to (1) extend a previous compartmental model for c^{SF}_{PRG4}, incorporating SF volume, PRG4 secretion, PRG4 loss, and PRG4 clearance, and to integrate these theoretical results with experimental analysis to evaluate the contributions of biological and biophysical variables, (2) including AC vs. SL to c^{SF}_{PRG4} in the normal adult rabbit knee, and (3) to decreased c^{SF}_{PRG4} in the rabbit ACLT model of PTOA.

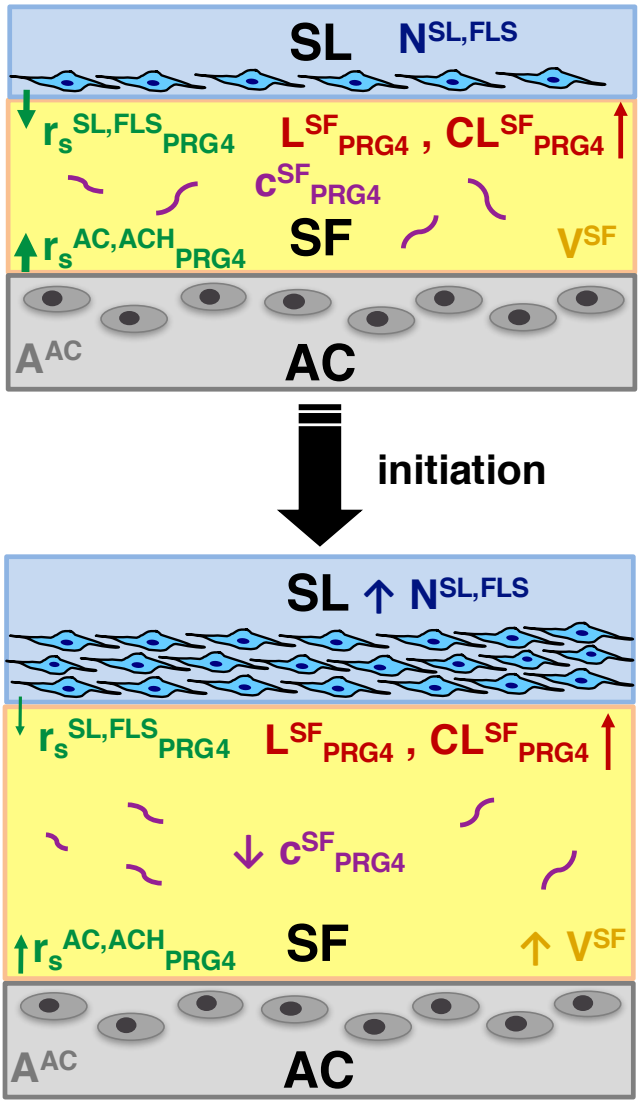

Figure 3.1: Schematic of specific aims for modeling synovial joint PRG4 dynamics. Data from *in vivo* experiments were used to develop a synovial joint compartmental model using variables and parameters that were measured directly or fit. Variations in the variables and parameters (**Table 2**) reflect biophysical mechanisms that underlie the progression from a normal to PTOA state following an initiation event (such as ACLT). Constituent compartments and cell types include synovial fluid (SF), articular cartilage (AC) containing articular chondrocytes (ACH), and synovial lining (SL) containing fibroblast-like synoviocytes (FLS).

3.3 Volume-Varying Compartmental Model for Proteoglycan-4 in Synovial Fluid

The dynamics of c^{SF}_{PRG4} depend on interacting fluid and tissue components of the synovial joint, and were analyzed here by extending previously described compartmental mass balance models [7, 40] to account for variations in SF volume, V^{SF}. Model variables and parameters are summarized in **Table 2**.

The overall mass of PRG4 in the SF of a synovial joint, m^{SF}_{PRG4}, can be accounted for by a conservation law. Changes in m^{SF}_{PRG4} with time depend on the balance between the rates of PRG4 generation (secretion into SF), G^{SF}_{PRG4}, and PRG4 loss from SF, L^{SF}_{PRG4}, according to:

$$\frac{dm^{SF}_{PRG4}(t)}{dt} = G^{SF}_{PRG4}(t) - L^{SF}_{PRG4}(t) \quad . \tag{1}$$

Eqn. 1 can be rewritten as:

$$\frac{dm^{SF}_{PRG4}(t)}{dt} = \gamma(t) \cdot G^{SF}_{PRG4,0} \quad , \tag{2}$$

where γ is a dimensionless parameter that describes net PRG4 generation (or loss) rate, relative to $G^{SF}_{PRG4,0}$, the normal generation rate at time 0:

$$\gamma(t) = \frac{G^{SF}_{PRG4}(t) - L^{SF}_{PRG4}(t)}{G^{SF}_{PRG4,0}} \quad . \tag{3}$$

This mass balance can be related to biochemical and physiological quantities. Assuming a well-mixed SF compartment, m^{SF}_{PRG4} is the product of concentration, c^{SF}_{PRG4}, and V^{SF}:

$$m^{SF}_{PRG4}(t) = c^{SF}_{PRG4}(t) \cdot V^{SF}(t) \quad . \tag{4}$$

G^{SF}_{PRG4} can be described as the sum of active synthesis in AC (the product of the PRG4 synthesis rate per cm^2 in AC, $r_s{}^{AC,ACH}_{PRG4}$, and the AC area, A^{AC}) and SL (the product of the PRG4

synthesis rate per cell in SL, $r_s^{SL,FLS}{}_{PRG4}$, and the total number of FLS cells, $N^{SL,FLS}$):

$$G_{PRG4}^{SF}(t) = \left(r_{s\,PRG4}^{SL,FLS}(t) \cdot N^{SL,FLS}(t)\right) + \left(r_{s\,PRG4}^{AC,ACH}(t) \cdot A^{AC}\right). \tag{5}$$

$L^{SF}{}_{PRG4}$ can be described as the product of the SF clearance rate, $CL^{SF}{}_{PRG4}$, and $c^{SF}{}_{PRG4}$ [7, 20]:

$$L_{PRG4}^{SF}(t) = CL_{PRG4}^{SF}(t) \cdot c_{PRG4}^{SF}(t). \tag{6}$$

Then, **eqn. 1** can be rewritten as follows:

$$\frac{d\left[V^{SF}(t) \cdot c_{PRG4}^{SF}(t)\right]}{dt} = G_{PRG4}^{SF}(t) - c_{PRG4}^{SF}(t) \cdot CL_{PRG4}^{SF}(t). \tag{7}$$

Applying the product rule to the left hand side of **eqn. 2** and rearranging to solve for the time-rate of concentration change yields:

$$\frac{dc_{PRG4}^{SF}(t)}{dt} = \frac{G_{PRG4}^{SF}(t) - c_{PRG4}^{SF}(t) \cdot \left[CL_{PRG4}^{SF}(t) \cdot \frac{dV^{SF}(t)}{dt}\right]}{V^{SF}(t)}. \tag{8}$$

In **eqn. 8**, the dV^{SF}/dt term effectively adds to the clearance effect, causing $c^{SF}{}_{PRG4}$ to diminish ($dc^{SF}{}_{PRG4}/dt$ to become more negative). Multiplying the numerator and denominator of the right hand side of **eqn. 8** by $1/CL^{SF}{}_{PRG4}$ yields

$$\frac{d\left[c_{PRG4}^{SF}(t)\right]}{dt} = \frac{c_{PRG4,SS}^{SF}(t) - c_{PRG4}^{SF}(t) \cdot \left(1 + \alpha(t)\right)}{\tau(t)}, \tag{9}$$

where the characteristic time, τ, is

$$\tau(t) = \frac{V^{SF}(t)}{CL_{PRG4}^{SF}(t)}. \tag{10}$$

The pseudo-steady-state $c^{SF}{}_{PRG4}$, $c^{SF}{}_{PRG4,SS}$, is

$$c^{SF}_{PRG4,SS}(t) = \frac{G^{SF}_{PRG4}(t)}{CL^{SF}_{PRG4}(t)}, \tag{11}$$

and the dimensionless variable α is

$$\alpha(t) = \frac{dV^{SF}(t)/dt}{CL^{SF}_{PRG4}(t)}. \tag{12}$$

Thus, **eqns. 3**, **10-12** describe how the four parameters, τ, $c^{SF}_{PRG4,SS}$, γ, and α, are influenced by G^{SF}_{PRG4}, L^{SF}_{PRG4}, CL^{SF}_{PRG4}, V^{SF}, and dV^{SF}/dt. **Eqn. 9** describes how dc^{SF}_{PRG4}/dt is related to c^{SF}_{PRG4} through these parameters.

Eqn. 7 can also be re-arranged to describe how c^{SF}_{PRG4} depends on $c^{SF}_{PRG4,SS}$ and the dimensionless parameters, α and β:

$$c^{SF}_{PRG4}(t) = \frac{\left(1-\beta(t)\right)}{\left(1+\alpha(t)\right)} \cdot c^{SF}_{PRG4,SS}(t), \tag{13}$$

where β describes the relative rates of mass turnover, between concentration-driven mass change in SF and synthesis, G^{SF}_{PRG4}:

$$\beta(t) = \frac{V^{SF}(t) \cdot dc^{SF}_{PRG4}(t)/dt}{G^{SF}_{PRG4}(t)}. \tag{14}$$

Multiplying both numerator and denominator of **eqn. 13** by (1+α(*t*)) and assuming small values of α and β results in:

$$c^{SF}_{PRG4}(t) \sim \left(1-\left(\alpha(t)+\beta(t)\right)\right) \cdot c^{SF}_{PRG4,SS}(t). \tag{15}$$

Thus, c^{SF}_{PRG4} is approximately proportional to $c^{SF}_{PRG4,SS}$, as reduced by the sum of the dimensionless parameters, α and β.

Table 3.1: Abbreviations of terms used in the model setup of PRG4 dynamics in the synovial joint.

Term	Description
AC	articular cartilage
ACH	articular chondrocytes
FLS	fibroblast-like synoviocytes
PRG4	proteoglycan 4
SF	synovial fluid
SL	synovial lining

Table 3.2: Symbol, description, units, and method of estimation for variables and parameters used in compartmental model of PRG4 dynamics in the synovial joint.

Symbol	Description	Units	Estimation Method
α	ratio of rate of SF volume change to clearance rate	-	calculated
A^{AC}	area of AC	cm^2	measured
β	ratio of rate of buildup of PRG4 in SF to rate of PRG4 secretion	-	calculated
c^{SF}_{PRG4}	PRG4 concentration in SF	mg/mL	*in vivo*
$c^{SF}_{PRG4,SS}$	PRG4 concentration in SF at steady state	mg/mL	calculated
CL^{SF}_{PRG4}	rate of SF PRG4 clearance	µL/day	estimated
γ	relative PRG4 turnover (difference between rates of generation and loss), normalized to initial CTRL values	-	calculated
G^{SF}_{PRG4}	rate of PRG4 generation (secretion) into SF	µg/day	calculated
L^{SF}_{PRG4}	rate of PRG4 loss from SF	µg/day	estimated
m^{SF}_{PRG4}	PRG4 mass in SF	µg	calculated
$N^{SL,FLS}$	number of FLS in SL	cells	measured
$r_s^{AC,ACH}{}_{PRG4}$	rate of PRG4 synthesis by ACH in AC	µg/(cm^2 · day)	*in vitro* / *in vivo*
$r_s^{SL,FLS}{}_{PRG4}$	rate of PRG4 synthesis by FLS in SL	µg/(million cells · day)	*in vitro* / *in vivo*
t	time	days	prescribed
τ	characteristic time	days	calculated
V^{SF}	SF volume	µL	*in vivo*

3.4 Materials and Methods

Study Design. The study is summarized here and in **Fig. 1**. Adult female New Zealand White (NZW) rabbits were subjected to unilateral ACLT, and knee joints were harvested at 1, 4, 7, 14, 28, and 42 days post-injury (n=6-7 per group). At harvest, SF, lavage fluids, AC, and SL were collected from ACLT and Non-OP knees. In addition, fluids and tissue were harvested from other rabbits, both healthy (n=37) as controls (CTRL) or ACLT (n=26) for additional $N^{SL,FLS}$ measures. Data from *in vivo* CTRL, Non-OP, and ACLT SF and lavage fluids were analyzed for $c^{SF}{}_{PRG4}$ and V^{SF}, while AC and SL were analyzed for the rate of PRG4 synthesis by ACH ($r_s{}^{AC,ACH}{}_{PRG4}$) or FLS ($r_s{}^{SL,FLS}{}_{PRG4}$) estimated from qPCR data, calibrated to secretion rates *in vitro*.

Data are reported as mean±SE. Each measure was analyzed for normality and homogeneity of variance. For measures that did not satisfy these assumptions, data were log-transformed or analyzed using the nonparametric Kruskall-Wallis test. All statistical analyses were performed using SPSS (IBM). Results were considered significant if $P<0.05$.

The effects of ACLT vs. Non-OP and time after surgery on $c^{SF}{}_{PRG4}$, V^{SF}, $r_s{}^{AC,ACH}{}_{PRG4}$, and $r_s{}^{SL,FLS}{}_{PRG4}$ were analyzed using two-way repeated measures ANOVA with Sidak post-hoc testing. $m^{SF}{}_{PRG4}$ was calculated from **eqn. 4** for each sample. At each time point, ACLT and Non-OP SF were compared by paired *t*-test, and also compared to CTRL by ANOVA and Dunnett's test. For ACLT or Non-OP, variation with time was analyzed by one-way ANOVA with Sidak post-hoc testing. Each ACLT and Non-OP time point was also compared to CTRL by ANOVA and Dunnett's test. Separately, for ACLT and Non-OP, variation with time was assessed, both by one-way ANOVA with Sidak post-hoc testing and by curve fitting.

The variables V^{SF}, $c^{SF}{}_{PRG4}$, $r_s{}^{AC,ACH}{}_{PRG4}$ and $r_s{}^{SL,FLS}{}_{PRG4}$ for each treatment group were curve fit to capture time-dependent behavior, where appropriate:

$$Y(t) = (P - C) \cdot \left(1 - F \cdot (1 - t/T)\right) \cdot e^{F \cdot (1 - t/T)} + C \quad . \tag{16}$$

Y(t) starts (*t*=0) at *(P-C)·(1-F)·e^F+C* (**eqn. S4**), peaks (*t*=T) at *P*, and asymptotes (*t*→∞) to *C*. The goodness of fit was assessed as the coefficient of determination (R^2). Whether each curve fit parameter was a positive value was assessed by one-sided *t*-test.

Y(t) in **eqn. 16** is the general solution to a second-order, linear, nonhomogeneous differential equation, allowing a transient response, followed by return to a steady-state value, where *t* is the time (days post-injury), Y(0) is the initial value, C is the steady-state value, T and P are the time and Y(T) values, respectively, at the transient peak, and F is a dimensionless number (0<F<1), weighting the differences in the initial value, Y(0)-C, to the final value from C:

$$\frac{Y(0) - C}{P - C} = (1 - F) \cdot e^F \quad . \tag{17}$$

For ACLT or Non-OP groups, experimental variables and each data point post-injury (1, 4, 7, 14, 28, and 42 days) were fit to **eqn. 16** by minimizing least squares estimates for each parameter (C, P, T, and F) using a Trust-Region algorithm in MATLAB's Curve Fitting Toolbox.

From these fits, model variables and parameters were calculated and estimated. PRG4 generation (G^{SF}_{PRG4}) was calculated from **eqn. 5** using continuous fits of $r_s^{AC,ACH}{}_{PRG4}$, $r_s^{SL,FLS}{}_{PRG4}$ and $N^{SL,FLS}$, the latter estimated from DNA in discs harvested from ACLT and Non-OP SL at 1, 2, 4, and 28 days post-ACLT (n=6-8/grp), modeled to increase exponentially to a plateau post-injury [53], and converted to total SL FLS based on estimates for SL surface area [31, 33], as described previously [41]. A^{AC} was estimated from digital quantification (ImageJ) of *en face* cartilage surface images in a cohort of CTRL rabbits, and was 4.07±0.04 cm^2/joint. PRG4 loss rate (L^{SF}_{PRG4}, **eqn. 1**) and clearance rate (CL^{SF}_{PRG4}, **eqn. 6**) were unknowns and fit from the model

and continuous-time curve fits of G^{SF}_{PRG4}, V^{SF}, and c^{SF}_{PRG4}. Then, the characteristic variables $c^{SF}_{PRG4,SS}$ and τ, and dimensionless parameters γ, α, and β, were calculated by inserting continuous fits for G^{SF}_{PRG4}, L^{SF}_{PRG4}, CL^{SF}_{PRG4}, V^{SF}, dV^{SF}/dt, and dc^{SF}_{PRG4}/dt into **eqns. 3, 10-12,** and **14**. Finally, the time-associated dependence of c^{SF}_{PRG4} on $c^{SF}_{PRG4,SS}$, α, and β was determined from **eqns. 13** and **15**, while that of dc^{SF}_{PRG4}/dt was determined from **eqn. 9**. In CTRL knees, V^{SF}, c^{SF}_{PRG4}, and G^{SF}_{PRG4} were not all measured within the same knee, so mean±SE for loss terms, characteristic variables, and dimensionless parameters were calculated from products and quotients error propagation.

Detailed methods. A total of 115 adult female NZW rabbits were used in this study. All animal protocols were approved by UCSD IACUC.

To examine the time course of acute injury, 37 rabbits (9-18 mos) underwent surgery for ACLT [36] in the right knee. A drawer test was used to confirm knee destabilization. The left knee of rabbits was not operated upon (Non-OP). Following surgery, rabbits were allowed to move freely in cages and received a standard diet and water *ad libitum*. At 1-42 days after ACLT, animals were euthanized via intravenous injection of pentobarbital sodium for analysis. Additionally, healthy rabbits (n=78 total, 6-18 mos) were euthanized and used as a CTRL.

SL tissue, SF, and lavage fluids were harvested. After the knee joint was opened, the cut ends of the ACL, and the intact PCL, were visualized to confirm the surgical model. SL was dissected from medial and lateral gutters and AC was scraped from the femoral condyles. Both SL and AC were immediately submerged and stored in RNAlater (Qiagen). SF was aspirated from the parapatellar region of the knee joint using a 50 μL 27G micro syringe. Then, lavage fluid was collected by injecting 1 mL sterile saline (23G syringe), flexing and extending the knee joint 10 times, and aspirating. Synovial and lavage fluids were centrifuged for clarification of

cells and debris prior to storage.

Portions of SF samples were digested with *Streptomyces hyaluronidase* (s. hy'ase) (Santa Cruz Biotech) at 10.0 U/mL in buffer (0.2M NaAc, 0.15M NaCl, 0.05M EDTA, pH 4.65) overnight at 37°C. PRG4 in digested SF and in conditioned media was analyzed using a (1) western blot-like assay using peanut agglutinin conjugated to horseradish peroxidase (PNA-HRP, EY Laboratories) to detect O-linked β(1-3)Gal-GalNAc regions of PRG4, or, alternatively, using a (2) western blot assay with mouse monoclonal antibody 9G3 (anti-PRG4, Millipore) [1] to detect a glycosylated epitope within the mucin domain of PRG4. Portions of digested SF equivalent to 0.10-0.30 μL of SF were added to sample buffer (0.5X TAE, 0.05% SDS, 4.9% glycerol, 0.05% bromophenol blue), applied to 2% agarose gels (Lonza, Rockland, ME), separated by horizontal electrophoresis (42 mAmps for 30 min, followed by 84 mAmps for 60 min) on 2% agarose gels (3 mm thick) in TAE buffer (0.4M Tris-acetate and 0.01 M ethylenediaminetetraacetic acid, pH 8.3) with 0.1% SDS. Proteins were transferred to membranes overnight (100 mAmps) in transfer buffer (6.25mM tris, 0.048M glycine, 0.025% SDS, pH 8.3), blocked with (1) 1% PBS-Tween or (2) 5% milk and 0.1% PBS-Tween, and probed with (1) PNA-HRP (0.66 μg/mL) for 1 hr at room temperature or (2) either a nonspecific IgG or 9G3 (0.002 μg/mL) overnight at 4C. Membranes probed with nonspecific IgG or 9G3 were rinsed extensively (0.1% PBS-Tween) and incubated with goat anti-mouse conjugated to horseradish peroxidase (0.007 μg/mL) for 1 hr at room temperature. Following the addition of ECL-Plus (Thermo Fisher Scientific), membranes were imaged for blue fluorescence (STORM imager, GMI). Intensity of staining was quantified in a custom MATLAB program. The PRG4 in SF was quantified with the use of standards of PRG4 from human SF.

SF volume (V^{SF}) was estimated from neat and lavage fluids. Protein concentration was

assayed using bicinchoninic acid (Thermo Fisher Scientific) [52] within neat and lavage fluids [11]. The volume of residual SF was estimated, assuming that lavage and SF contained the protein that was diluted from neat SF concentrations. Residual and neat SF volumes were summed to obtain V^{SF}, as described previously [41].

PRG4 gene expression was analyzed in AC and SL from ACLT, Non-OP, and CTRL knees using qPCR. Tissues were submerged in liquid nitrogen and pulverized. RNA was isolated from SL and AC using QIAzol reagent (Qiagen) and the RNeasy Mini Kit with a DNAse I incubation step (Qiagen). RNA was quantified using a NanoDrop 1000 spectrophotometer (Thermo Scientific). RNA (40 ng) was reverse transcribed, and resultant cDNA was ligated and amplified using the Whole Transcriptome Amplification Kit (Qiagen). Real-time qPCR was carried out on a Rotor-Gene Q platform with SYBR green reporter (Qiagen) using rabbit-specific primers for proteoglycan 4 (*PRG4*), glyceraldehyde 3-phosphate dehydrogenase (*GAPDH*), and ribosomal protein S18 (*RPS18*) from Qiagen (**Table 3**). Amplification curves were converted to absolute copy numbers (CN) of gene transcripts using standard curves. The expected PCR product size was confirmed by electrophoresis. Data are reported as CN ratio of gene of interest to *GAPDH* and *RPS18*.

The relationship between *PRG4* gene expression and PRG4 secretion for adult female NZW rabbit SL and AC was assessed *in vitro*. AC and SL explants, or FLS in monolayer, were cultured in basal medium (0.5-10% FBS) with or without stimulating cytokines (0.1-10.0 ng/mL TGF-β1 ± IL-1β) [6, 10, 21]. Cultured AC, SL, and FLS were analyzed for expression of *PRG4* by qPCR, as described above. PRG4 in conditioned medium was assessed, as described above.

Table 3.3: Qiagen primers used for qPCR of rabbit FLS and SL. *The reference position is the position of the amplicon in the RefSeq sequence (via Qiagen).

Target Gene	Product Size [bp]	RefSeq Accession No.	Reference Position*	Catalog No.
RPS18	146	XM_002714532	204	PPN10659A
GAPDH	109	NM_001082253	1117	PPN00377A
PRG4	79	XM_008268756.1	2238	PPN09434A

3.5 Results

ACLT causes time-varying changes in c^{SF}_{PRG4}, V^{SF}, $r_s^{SL,FLS}{}_{PRG4}$, and $r_s^{AC,ACH}{}_{PRG4}$

c^{SF}_{PRG4} was lower in ACLT compared to Non-OP knees (P<0.05), and affected interactively (P<0.05), but was not independently (P=0.55) by time (**Fig. 2A**). Compared to Non-OP, ACLT c^{SF}_{PRG4} was substantially lower at later time points post-injury (-69% and -50% at d28 and 42, P<0.05). Both Non-OP and ACLT c^{SF}_{PRG4} were affected by time (P<0.05 by curve fit). ACLT c^{SF}_{PRG4} decreased to 69 μg/mL at T=39.9 days (**Fig. 2A**, inset). Compared to CTRL (160±14 μg/mL), ACLT c^{SF}_{PRG4} was lower at d28 and 42 post-injury (-53% to –65%, P<0.01). Non-OP c^{SF}_{PRG4} also decreased (to 94 μg/mL), but this decrease was transient (T=7.8 days).

V^{SF} was higher in ACLT compared to Non-OP knees (P<0.001) and affected by time (P<0.001), with an interaction effect (P<0.05, **Fig. 2B**). Compared to Non-OP, ACLT V^{SF} trended higher by d1, d4, and d14 post-injury (+85-210%, P=0.06-0.09), and was markedly higher at d7, d28, and d42 following injury (+140-345%, P<0.05). ACLT V^{SF} was affected by time (P<0.001), and, compared to CTRL V^{SF} (102±8 μL), became higher by d7, and remained elevated through d42 (+268% to +449%, P<0.05). Non-OP V^{SF} varied with time, increasing (P<0.05 by curve fit) to a peak of P=176 μL (+74%) at T=12 days (**Fig. 2B**, inset).

$r_s^{AC,ACH}{}_{PRG4}$ was lower in ACLT compared to Non-OP knees (P<0.001), with a tendency for interactive (P=0.05), but not independent (P=0.58), effects of time (**Fig. 2C**). Compared to Non-OP, ACLT $r_s^{AC,ACH}{}_{PRG4}$ was lower at d4, 28 and 42 post-injury (-59% to -79%, P<0.05). $r_s^{AC,ACH}{}_{PRG4}$ did not vary with time for Non-OP knees (P=0.23), though there was a trend for ACLT (P=0.18). Compared to CTRL (2.54±0.37 μg PRG4/(cm^2 · day), Non-OP $r_s^{AC,ACH}{}_{PRG4}$ was higher at d28 and 42 post-injury (+204-222%, P<0.05), but there was no difference for ACLT $r_s^{AC,ACH}{}_{PRG4}$ (P=0.21).

$r_s^{SL,FLS}{}_{PRG4}$ was lower in ACLT compared to Non-OP knees (P<0.001), but was not affected by time (P=0.22), without an interaction effect (P=0.92, **Fig. 2D**). Compared to Non-OP, ACLT $r_s^{SL,FLS}{}_{PRG4}$ was lower at all time points (-42% to -68%, P<0.05). ACLT $r_s^{SL,FLS}{}_{PRG4}$ was affected by time (P<0.001), and, compared to CTRL (2.65±0.38 μg PRG4/(million cells · day)), was lower at d4-42 post-injury (-56% to -65%, P<0.001). Non-OP $r_s^{SL,FLS}{}_{PRG4}$ varied with time, decreasing (P<0.05 by curve fit) to a peak of P=2.9 μg PRG4/(million cells · day) at T=22.3 days (**Fig. 2D**, inset).

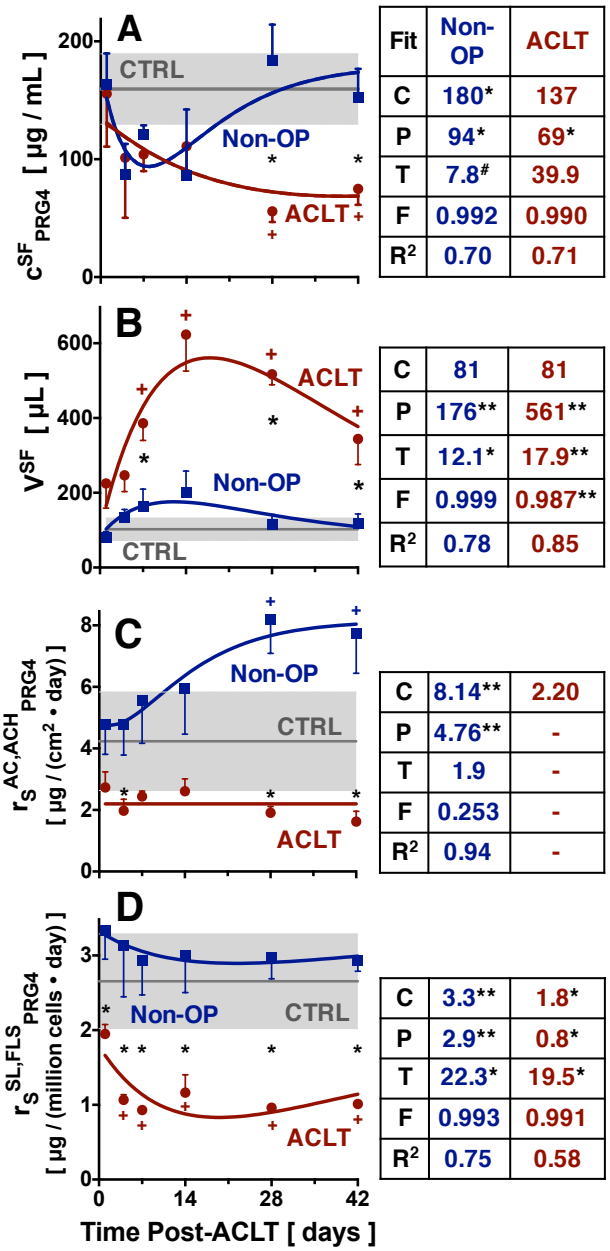

Fit	Non-OP	ACLT
C	180*	137
P	94*	69*
T	7.8#	39.9
F	0.992	0.990
R^2	0.70	0.71

C	81	81
P	176**	561**
T	12.1*	17.9**
F	0.999	0.987**
R^2	0.78	0.85

C	8.14**	2.20
P	4.76**	-
T	1.9	-
F	0.253	-
R^2	0.94	-

C	3.3**	1.8*
P	2.9**	0.8*
T	22.3*	19.5*
F	0.993	0.991
R^2	0.75	0.58

Figure 3.2: Effect of ACLT on experimentally assessed variables and mathematical fits of the mass balance model of PRG4 in the rabbit knee. **(A)** c^{SF}_{PRG4}, **(B)** V^{SF}, **(C)** $r_s^{AC,ACH}{}_{PRG4}$, and **(D)** $r_s^{SL,FLS}{}_{PRG4}$ from *in vivo* SF, AC, and SL. Data for **Non-OP** (■) and **ACLT** (●) are mean±SE, n=4-7; CTRL data are mean±95% CI (■, n=6-21). **P*<0.05 for ACLT vs. Non-OP, $^{+,+}$*P*<0.05 for ACLT vs. CTRL. Tabulated values correspond to parameters in **eqn. 16** for curve fits (— in **A-C**), with units of C, P, and T as shown on the axes, and the significance of each parameter (C, P, T, F) indicated as ***P*<0.01, **P*<0.05, $^{\#}$*P*<0.10, with R^2 as shown. Approximated c^{SF}_{PRG4} from **eqn. 15** are also shown (- - -) in (**A**).

ACLT causes time-varying changes in m^{SF}_{PRG4}, L^{SF}_{PRG4}, and CL^{SF}_{PRG4}

m^{SF}_{PRG4} was affected by ACLT (P<0.001), but not significantly by time (P=0.13) with no interaction effect (P=0.48, **Fig. 3A**). While Sidak statistics did not show ACLT or Non-OP m^{SF}_{PRG4} varying with time (P=0.30-0.89), Dunnett comparisons to CTRL showed that ACLT, but not Non-OP, m^{SF}_{PRG4} was higher (+34-86%, P<0.05) at d14 and 28 post-injury.

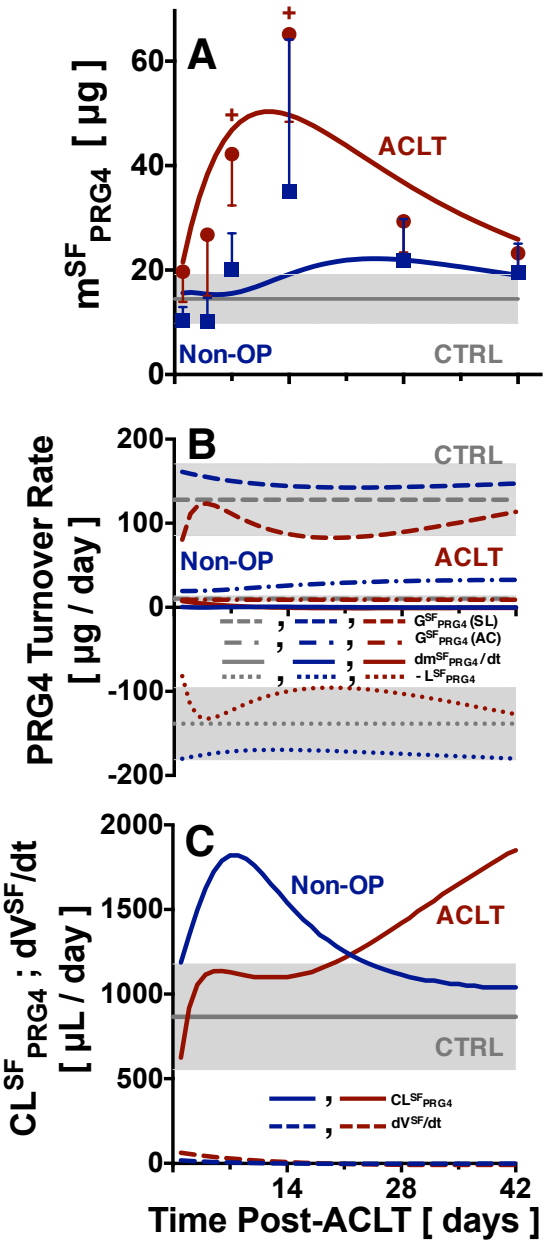

Figure 3.3: Effect of ACLT on fit variables and parameters in the mass balance model of PRG4 in the rabbit knee. (A) m^{SF}_{PRG4}, **(B)** variation in m^{SF}_{PRG4} post-injury (—) due to synthesis (G^{SF}_{PRG4},- - -) and loss ($-L^{SF}_{PRG4}$, ···) (**eqn. 1**), and **(C)** CL^{SF}_{PRG4} (—) and dV^{SF}/dt (- - -), all as calculated or estimated from measured variables in **Fig. 2**. Data for **Non-OP** (■) and **ACLT** (●) are mean±SE, n=4-7. **P*<0.05 for ACLT vs. Non-OP, ^{+}P<0.05 for ACLT vs. CTRL. CTRL values are mean±95% CI (■, n=9-21).

ACLT causes changes in c^{SF}_{PRG4} by affecting the dynamic balance between biosynthesis, loss, and dilution

γ (**Fig. 4A**), the normalized net difference between generation and loss rates (**eqn. 3**), was affected by ACLT, being transiently elevated and then chronically diminished. In ACLT knees, γ was initially markedly elevated (0.01-0.05, d1-7), and then later was slightly negative (-0.004 to -0.007, d14-42), due to an increasingly large ACLT L^{SF}_{PRG4} term relative to G^{SF}_{PRG4} (**Fig. 3B**). In Non-OP knees, γ was close to zero (-0.002 to 0.004, d1-42, **Fig. 3B**).

τ, the characteristic time for PRG4-containing V^{SF} clearance (**eqn. 10**), was higher after ACLT (0.20 to 0.50 days, +72-358%, **Fig. 4B**) compared to both CTRL and Non-OP τ (0.12±0.05 and 0.09-0.13 days, respectively). This was due to the ACLT-induced increase in V^{SF} (numerator, **Fig. 2B**, **eqn. 10**) in addition to the substantial decrease in CL^{SF}_{PRG4} (denominator, **Fig. 2C**).

$c^{SF}_{PRG4,SS}$ (**eqn. 11, Fig. 4C**, the ratio of G^{SF}_{PRG4} to CL^{SF}_{PRG4}) was affected by ACLT and was substantially decreased in ACLT knees for later time (to 68-72 μg/mL, -55% to -57% vs. CTRL, d28-42, **Fig. 4C**). This decrease was due to the relatively large decrease in G^{SF}_{PRG4} (numerator, **Fig. 3B**) relative to the decrease in CL^{SF}_{PRG4} (denominator, **Fig. 3B**). Non-OP $c^{SF}_{PRG4,SS}$ values (93-174 μg/mL) were decreased (-2% to -41% vs. CTRL, d1-28), but returned to CTRL values by d42 (**Fig. 4C**).

α (**eqn. 12**, **Fig. 4D**, the dimensionless ratio of dV^{SF}/dt to CL^{SF}_{PRG4}, reflecting relative volume turnover) was altered bi-directionally in ACLT knees (**Fig. 4D**). At early time, α was markedly positive ACLT knees (0.03-0.10, d1-7), due to increased V^{SF}. ACLT α was slightly less than zero at later time (-0.005 to -0.006, d28-42), as dV^{SF}/dt was negative. Non-OP α was close to zero for all time (-0.002 to 0.015, d1-42, **Fig. 4D**).

β (**eqn. 14**, **Fig. 4E**, the dimensionless rate ratio of PRG4 buildup to secretion) was altered bi-directionally in both ACLT and Non-OP knees. Non-OP β was slightly negative at early time points (-0.001 to -0.013, d1-7) due to a negative dc^{SF}_{PRG4}/dt, but became slightly positive as c^{SF}_{PRG4} increased (to 0.004, d14-42, **Fig. 4E**). ACLT was lower for nearly all time (-0.003 to -0.012, d4-28, **Fig. 4E**), and was ~zero from d28-42, due to a persistently negative dc^{SF}_{PRG4} term. The net of α+β, reducing c^{SF}_{PRG4} relative to $c^{SF}_{PRG4,SS}$ (**eqn. 15**) was slightly above zero (0.01-0.09) from d1-7, and near zero (±0.02) from d7-42 (**Fig. 4F**). Thus, the modeled $c^{SF}_{PRG4,SS}$ (**Fig. 4C**) was close to that of c^{SF}_{PRG4} (**Fig. 2A**) for both ACLT and Non-OP knees.

dc^{SF}_{PRG4}/dt (**eqn. 9, Fig. 4G**) also exhibited a bi-directional response in ACLT and Non-OP knees, and was initially markedly negative in both. This decrease was driven by the difference between $c^{SF}_{PRG4,SS}$ and the current value of c^{SF}_{PRG4} (numerator, since α was near zero), and also τ (denominator). At early time, ACLT dc^{SF}_{PRG4}/dt was lower in magnitude than Non-OP (to -3.7 to -4.3 μg/(mL·day), -57 to -81%, d1-4) due to a larger τ, but then diminished and was close to zero (-2.08 to 0.08, d14-42). Non-OP dc^{SF}_{HA}/dt was negative at early time points (-8.5 to -22.3 μg/(mL·day), d1-4, **Fig. 4G**) due to a slightly positive α term (**Fig. 4D**, **eqn. 9**), but then was close to zero for the remaining time (-1.2 to 4.0 μg/(mL·day), d7-42).

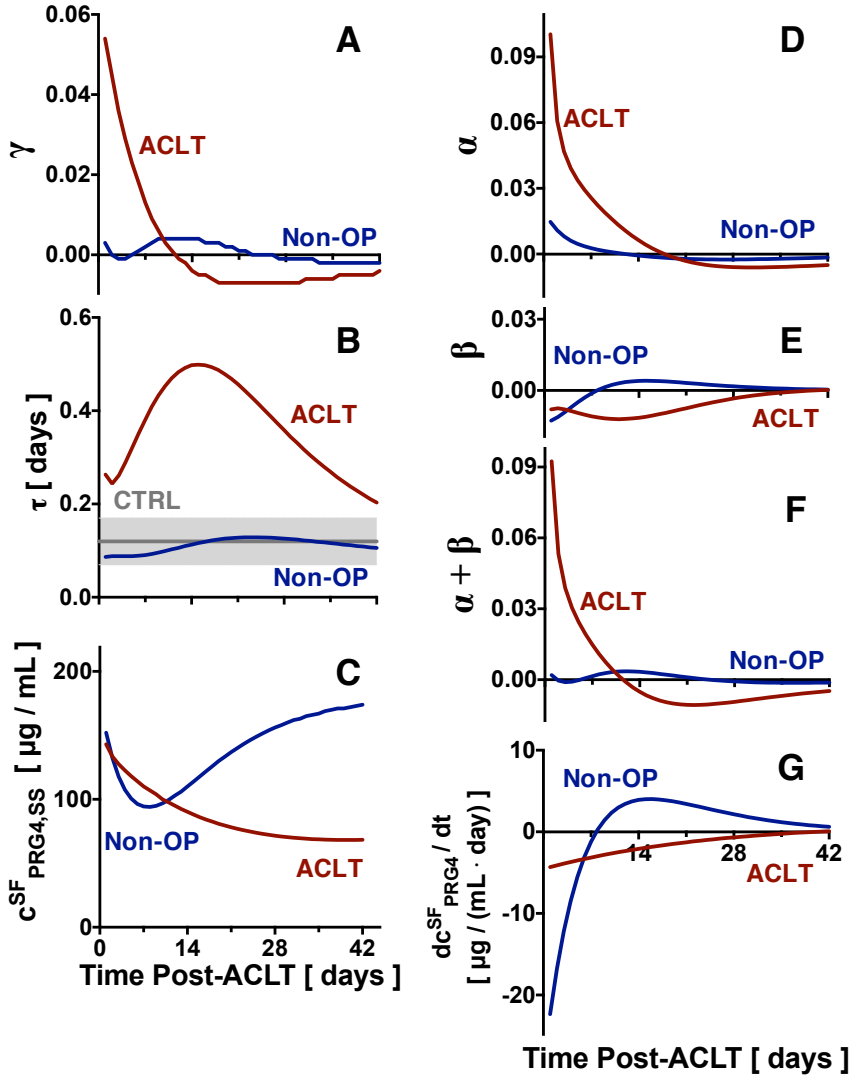

Figure 3.4: Effect of characteristic and dimensionless parameters on c^{SF}_{PRG4} and dc^{SF}_{PRG4}/dt. The characteristic parameters **(A)** γ (**eqn. 3**), **(B)** τ (**eqn. 10**), **(C)** modeled $c^{SF}_{PRG4,SS}$ (**eqn. 11**), **(D)** α (**eqn. 12**), **(E)** β (**eqn. 14**), **(F)** α+β (**eqn. 15**), and **(G)** dc^{SF}_{PRG4}/dt post-injury due to variations in τ, α, and $c^{SF}_{PRG4,SS}$ (**eqn. 9**). Modeled variables and parameters for Non-OP (blue), ACLT (red). CTRL values are mean±95% CI (■, n=9-21).

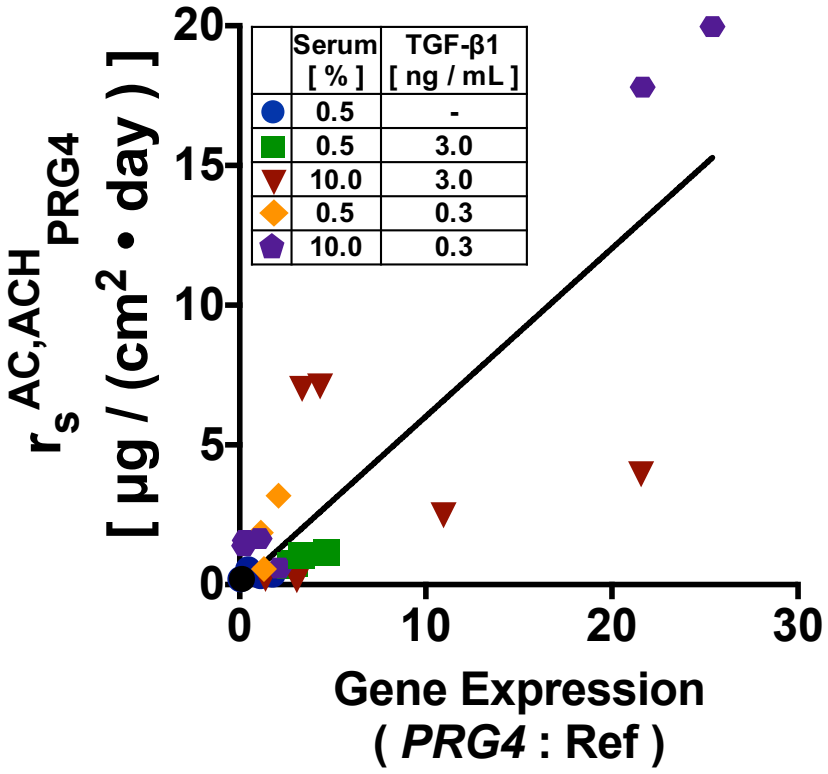

Figure 3.5: *PRG4* expression and PRG4 synthesis by ACH. *In vitro* relationship between *PRG4* expression and PRG4 secretion for AC cultures, n=24. Regression line is for *PRG4* expression versus PRG4 secretion ($y=0.602X$, $r^2=0.67$, $P<0.001$).

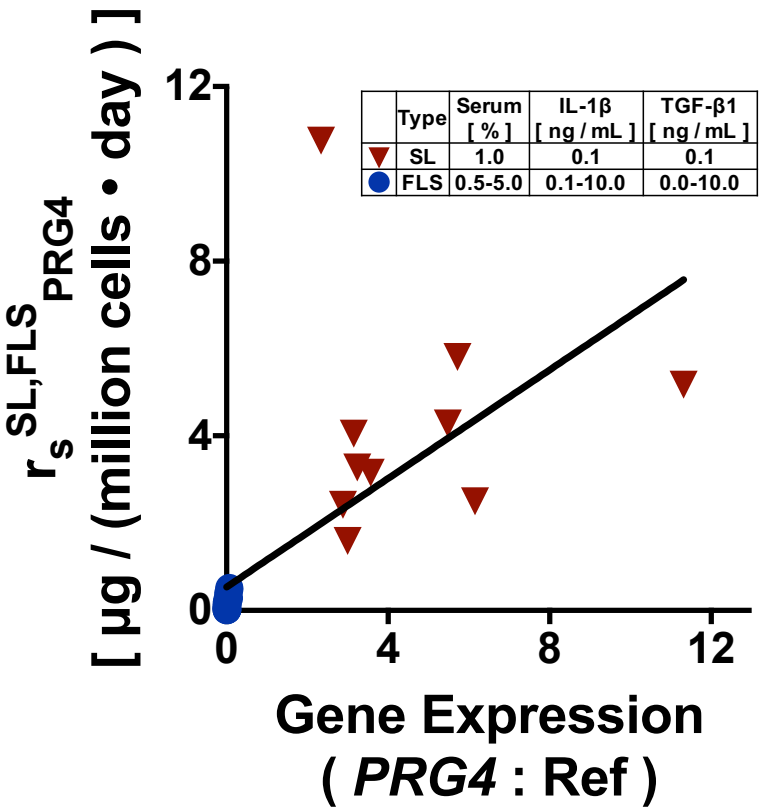

Figure 3.6: *PRG4* expression and PRG4 synthesis by FLS. *In vitro* relationship between *PRG4* expression and PRG4 secretion for FLS and SL cultures, n=55. Regression line is for *PRG4* expression versus PRG4 secretion (y=0.622X+0.536, r^2=0.46, P<0.001).

3.6 Discussion

In this study, a quantitative compartmental mass balance model of PRG4 in SF was extended to identify characteristic variables and dimensionless parameters so that their effect on c^{SF}_{PRG4} following acute injury in a rabbit model of PTOA could be evaluated (**Fig. 1**). Experimental data (c^{SF}_{PRG4}, V^{SF}, $r_s^{AC,ACH}{}_{PRG4}$, and $r_s^{SL,FLS}{}_{PRG4}$) were compared for ACLT, Non-OP, and CTRL knees, and were fit to estimate model parameters that are difficult to measure directly *in vivo*. Compared to CTRL knees, at early time points (d1-7) following ACLT, c^{SF}_{PRG4} was initially maintained and then decreased, to 97 μg/mL (-40% vs. CTRL). During this time period V^{SF} increased gradually but substantially (+61-321%) and $r_s^{SL,FLS}{}_{PRG4}$, but not $r_s^{AC,ACH}{}_{PRG4}$, decreased immediately (-33% to -81%). At later time points (d28-42) post-injury, the decrease in ACLT c^{SF}_{PRG4} persisted over time and was substantial (56-75 μg/mL, -53% to -65% vs. CTRL). Increases in V^{SF} were maintained (+268-449%), as were decreases in $r_s^{SL,FLS}{}_{PRG4}$ (-77% to -80%). These ACLT quantities trended towards, but were still substantially different from, CTRL values at d42.

The experimental design compared SF dynamics between ACLT, Non-OP, and CTRL knees. Here, a paired, contralateral limb study design was employed to take advantage of intra-subject consistency. However, an internal contralateral unoperated control has limitations, including potential systemic effects of local injury, so a healthy CTRL cohort of rabbits is included for comparison. Due to limited SF volumes from the latter groups, sample size for certain assays was less than the total number of joints per group. Additionally, the variables V^{SF} and $N^{SL,FLS}$ were calculated with some extrapolation. V^{SF} was calculated from biochemical analysis of neat and lavage fluids, as V^{SF} is underestimated by the volume aspirated due to residual SF [11, 41]. $N^{SL,FLS}$ was estimated from a portion of SL [41], scaled up to the entire joint

[7, 31, 33]. These experimental measures of the rabbit PTOA model allowed analysis of the *in vivo* joint environment.

ACLT-induced changes in c^{SF}_{PRG4} (chronically decreased, **Fig. 2A**) and V^{SF} (increased, **Fig. 2B**) were consistent with, and extended, prior analyses in different model systems at limited time points. The sampling of tissues at both acute (d1-7) and extended (d14-42) time post-injury allowed for the development of a fit of variable quantities during PTOA progression. In humans, c^{SF}_{PRG4} in healthy joints is 130-450 μg/mL [44], with c^{SF}_{PRG4} being increased [4] or decreased [13] following acute injury. Reported c^{SF}_{PRG4} ranges in rabbits are slightly lower (~20-270 μg/mL) [15], and decreases in c^{SF}_{PRG4} following injury were observed in PTOA models in rabbits [15] and guinea pigs [51]. A large increase in V^{SF} was also noted in previous studies (+70-1100%) of rabbit knees following acute injury [34, 36].

The assessment of both CTRL and ACLT-induced $r_s^{AC,ACH}{}_{PRG4}$ and $r_s^{SL,FLS}{}_{PRG4}$ (both decreased, **Fig. 2C, D**) have several novel implications. First, SL appears to be the dominant contributor of PRG4 in the synovial joint (**Fig. 2 C,D, Fig. 3B**). In CTRL knees, AC contributed to 7.5% of the estimated G^{SF}_{PRG4}, while SL contributed 92.5% of the total (**Fig. 3B**). This is due to the high number of FLS in SL (~50-100 million FLS) [41] and large area (~6.7 cm^2, estimated from simplified joint geometry and prior studies [31, 33]) relative to that of cartilage (~2 million PRG4-secreting ACH in the superficial zone of AC assuming secreting cell depth of ~40 μm [12] over a surface area of 4.1 cm^2). This conclusion depends in part on the calibrated relationship between $r_s^{AC,ACH}{}_{PRG4}$, $r_s^{SL,FLS}{}_{PRG4}$, and AC and SL *PRG4* gene expression, which likely depends on the complex local microenvironment *in vivo* [24, 37].

Second, ACLT induced an inhibition of $r_s^{AC,ACH}{}_{PRG4}$ and $r_s^{SL,FLS}{}_{PRG4}$ in the rabbit ACLT model. The range for CTRL, Non-OP, and ACLT $r_s^{AC,ACH}{}_{PRG4}$ (2-8 μg/(cm^2·day) and for $r_s^{SL,FLS}{}_{PRG4}$

(1-3 μg/(million cells·day) in the present study are consistent with previous reports for human *in vitro* FLS and AC cultures under varying cytokine stimulation [6, 46]. The decreases in $r_s^{AC,ACH}{}_{PRG4}$ and $r_s^{SL,FLS}{}_{PRG4}$ following ACLT may be due to mechanical (altered loading) or biochemical (altered cytokine environment) factors. Static and dynamic loading can increase $r_s^{AC,ACH}{}_{PRG4}$ by bovine cartilage [38, 39], so shifting of weight-bearing to Non-OP knees could result in ACLT $r_s^{AC,ACH}{}_{PRG4}$ being decreased and Non-OP being increased, consistent with the present study (**Fig. 2C**). Additionally, injury-induced cartilage degeneration has been associated with decreased *PRG4* expression (and therefore calculated $r_s^{AC,ACH}{}_{PRG4}$) in a sheep load-altering meniscectomy model [55]. Decreased SL *PRG4* expression may be due to increased IL-1β and TNF-α during acute inflammation [14, 19, 32]. While AC and SL contributions to $G^{SF}{}_{PRG4}$ were evaluated here, PRG4 has more recently been identified in other joint tissues such as the meniscus [49, 56] and ligaments [32], suggesting that cell types within these tissues may also secrete PRG4 into SF. However, pilot studies indicated that such tissues contributed minimally to $c^{SF}{}_{PRG4}$.

The model-based approach allowed attributing the ACLT-induced decrease in $c^{SF}{}_{PRG4}$ (**Fig. 2A**) at later time to decreased $G^{SF}{}_{PRG4}$ (**Fig. 3B**) and increased V^{SF} (**Fig. 2B**). Initially (d1-14), the lower mass loss rate $L^{SF}{}_{PRG4}$ (-4 to -41% vs. CTRL, **eqn. 6**, **Fig. 3B**), relatively unchanged volume turnover $CL^{SF}{}_{PRG4}$ (-27% to +31%, **eqn. 6**, **Fig. 3C**), and increased characteristic time τ (+106-321%, **eqn. 10**, **Fig. 4B**) resulted in a maintenance of $c^{SF}{}_{PRG4}$ (**Fig. 2A**) despite joint effusions (**Fig. 2B**). At later times (d28-42), increasing $CL^{SF}{}_{PRG4}$ (+64-114% vs. CTRL) relative to a decreased $G^{SF}{}_{PRG4}$ (-8 to -26%) resulted in a decreased $c^{SF}{}_{PRG4}$ (-55% to -57%). Changes to $L^{SF}{}_{PRG4}$, $CL^{SF}{}_{PRG4}$, and τ are likely due to a combination of biological, biophysical, and catabolic mechanisms. In normal joints, $c^{SF}{}_{PRG4}$ is expected to reach steady-state

concentration 10-40X faster than HA following a perturbation [7], so τ is expected to be lower for PRG4 than for HA (~1.5 days in CTRL joints) [41]. CTRL (0.12±0.05 days) and Non-OP τ (0.09-0.13 days) are low, as expected [11], while the increase in ACLT τ (to 0.5 days), especially at early time (**Fig. 4B**), may reflect increased PRG4 release from tissue matrices (not accounted for by G^{SF}_{PRG4}) [16, 42], or increased retention within the joint due to complexing with other joint molecules such as surface-active phospholipids [22], which have been shown to increase in concentration following joint injury [4].

Following ACLT, the large effusions (increased V^{SF}) dilute m^{SF}_{PRG4} in the joint and contributed to a progressive decrease in c^{SF}_{PRG4}. The decrease in c^{SF}_{PRG4} worsened as PTOA progressed, due to chronically decreased G^{SF}_{PRG4} by resident cells. The characteristic variables τ (**eqn. 10**, **Fig. 4B**) and $c^{SF}_{PRG4,SS}$ (**eqn. 11**, **Fig. 4C**), and dimensionless parameters γ (**eqn. 3**, **Fig. 4A**), α (**eqn. 12**, **Fig. 4D**), and β (**eqn. 14**, **Fig. 4E**), help to explain the biological and biophysical basis for early and sustained decrease in c^{SF}_{PRG4} in ACLT joints (**eqn. 13**, **Fig. 2A**). ACLT G^{SF}_{PRG4} was initially decreased (reduced $r_s^{SL,FLS}{}_{PRG4}$) but increased transiently as FLS proliferated [41] (**Fig. 3B**), increasing γ immediately post-injury (**Fig. 4A**, to 0.05). The decreased loss term CL^{SF}_{PRG4} at early time (d1-7) drove increased ACLT τ (**Fig. 4B**, to 0.38 days) and α (**Fig. 4D**, to 0.10), but the increased PRG4 residence time was not enough to counteract increased SF effusions driving c^{SF}_{PRG4} lower. At later times (d14-42), ACLT L^{SF}_{PRG4} and CL^{SF}_{PRG4} gradually increased, with CL^{SF}_{PRG4} being higher than CTRL values by d42 (to 1850 μL/day, +115%). This increase in PRG4 loss caused further decreases in ACLT c^{SF}_{PRG4}, with $c^{SF}_{PRG4,SS}$ reaching levels much lower than those of CTRL by d42 (68 μg/mL, -57%), and τ (decreasing to CTRL levels of ~0.20 days). At these later times the increase in L^{SF}_{PRG4} outpaced that in G^{SF}_{PRG4} (γ became slightly negative, -0.004 to -0.007, **Fig. 4A**), and c^{SF}_{PRG4} reached a quasi-plateau,

suggesting that the ACLT joints would continue to lose lubricant content with time.

These results provide a foundation for developing and calibrating a continuous-time synovial joint model for SF PRG4 dynamics in health and PTOA to provide insights into relationships between key joint biophysical variables and to better inform the timing of putative therapeutics. Because SF PRG4 lubricant function depends on concentration [15, 40, 45], a detailed understanding of, and ability to quantify, the underlying basis for changes during joint injury and arthritis would be useful to target pathogenesis and evaluate potential therapies.

3.7 Acknowledgments

This chapter, in full, will be submitted to *European Cells and Materials*. The dissertation author was the primary author and thanks co-authors Julian J. Garcia, Maegen J. Cravotta, Barbara L. Schumacher, Kenjo Kato, Gary S. Firestein, Koichi Masuda, and Robert L. Sah. This work was supported by research grants from the National Institutes of Health (R01 AR055637, T32 AR060712), the Department of Defense (DOD OR13085), the UC San Diego Frontiers of Innovation Scholarship Program, and the San Diego Fellowship.

The authors thank Dr. Samuel Ward and Dr. Gregory Heldt for use of CTRL rabbit tissue.

3.8 References

1. Ai M, Cui Y, Sy MS, Lee DM, Zhang LX, Larson KM, Kurek KC, Jay GD, Warman ML: Anti-lubricin monoclonal antibodies created using lubricin-knockout mice immunodetect lubricin in several species and in patients with healthy and diseased joints. *PLoS One* 10:e0116237, 2015.

2. Antonacci JM, Schmidt TA, Serventi LA, Cai MZ, Shu YL, Schumacher BL, McIlwraith CW, Sah RL: Effects of equine joint injury on boundary lubrication of articular cartilage by synovial fluid: role of hyaluronan. *Arthritis Rheum* 64:2917-26, 2012.

3. Atarod M, Ludwig TE, Frank CB, Schmidt TA, Shrive NG: Cartilage boundary lubrication of ovine synovial fluid following anterior cruciate ligament transection: a longitudinal study. *Osteoarthritis Cartilage* 23:640-7, 2015.

4. Ballard BL, Antonacci JM, Temple-Wong MM, Hui AY, Schumacher BL, Bugbee WD, Schwartz AK, Girard PJ, Sah RL: Effect of tibial plateau fracture on lubrication function and composition of synovial fluid. *J Bone Joint Surg Am* 94:e64(1-9), 2012.

5. Bartok B, Firestein GS: Fibroblast-like synoviocytes: key effector cells in rheumatoid arthritis. *Immunol Rev* 233:233-55, 2010.

6. Blewis ME, Lao BJ, Schumacher BL, Bugbee WD, Sah RL, Firestein GS: Interactive cytokine regulation of synoviocyte lubricant secretion. *Tissue Eng Part A* 16:1329-37, 2010.

7. Blewis ME, Nugent-Derfus GE, Schmidt TA, Schumacher BL, Sah RL: A model of synovial fluid lubricant composition in normal and injured joints. *Eur Cell Mater* 13:26-39, 2007.

8. Buckwalter JA, Saltzman C, Brown T: The impact of osteoarthritis: implications for research. *Clin Orthop Relat Res*:S6-15, 2004.

9. Catterall JB, Stabler TV, Flannery CR, Kraus VB: Changes in serum and synovial fluid biomarkers after acute injury (NCT00332254). *Arthritis Res Ther* 12:R229, 2010.

10. Chenevier-Gobeaux C, Morin-Robinet S, Lemarechal H, Poiraudeau S, Ekindjian JC, Borderie D: Effects of pro- and anti-inflammatory cytokines and nitric oxide donors on

hyaluronic acid synthesis by synovial cells from patients with rheumatoid arthritis. *Clin Sci (Lond)* 107:291-6, 2004.

11. Coleman PJ, Scott D, Ray J, Mason RM, Levick JR: Hyaluronan secretion into the synovial cavity of rabbit knees and comparison with albumin turnover. *J Physiol* 503 (Pt 3):645-56, 1997.

12. Eggli PS, Hunziker EB, Schenk RK: Quantitation of structural features characterizing weight- and less-weight-bearing regions in articular cartilage: a stereological analysis of medial femoral condyles in young adult rabbits. *Anat Rec* 222:217-27, 1988.

13. Elsaid KA, Fleming BC, Oksendahl HL, Machan JT, Fadale PD, Hulstyn MJ, Shalvoy R, Jay GD: Decreased lubricin concentrations and markers of joint inflammation in the synovial fluid of patients with anterior cruciate ligament injury. *Arthritis Rheum* 58:1707-15, 2008.

14. Elsaid KA, Jay GD, Chichester CO: Reduced expression and proteolytic susceptibility of lubricin/superficial zone protein may explain early elevation in the coefficient of friction in the joints of rats with antigen-induced arthritis. *Arthritis Rheum* 56:108-16, 2007.

15. Elsaid KA, Jay GD, Warman ML, Rhee DK, Chichester CO: Association of articular cartilage degradation and loss of boundary-lubricating ability of synovial fluid following injury and inflammatory arthritis. *Arthritis Rheum* 52:1746-55, 2005.

16. Elsaid KA, Machan JT, Waller K, Fleming BC, Jay GD: The impact of anterior cruciate ligament injury on lubricin metabolism and the effect of inhibiting tumor necrosis factor alpha on chondroprotection in an animal model. *Arthritis Rheum* 60:2997-3006, 2009.

17. Firestein GS: Etiology and pathogenesis of rheumatoid arthritis. In: *Kelley's Textbook of Rheumatology,* ed. by GS Firestein, Saunders/Elsevier, Philadelphia, PA, 2009, 1035-86.

18. Gelber AC, Hochberg MC, Mead LA, Wang NY, Wigley FM, Klag MJ: Joint injury in young adults and risk for subsequent knee and hip osteoarthritis. *Ann Intern Med* 133:321-8, 2000.

19. Goldring MB: Osteoarthritis and cartilage: the role of cytokines. *Curr Rheumatol Rep* 2:459-65, 2000.

20. Guyton AC, Hall JE. Textbook of Medical Physiology. 11th ed. Philadelphia: Elsevier Saunders; 2006.

21. Haubeck H-D, Kock R, Fischer D-C, van de Leur E, Hoffmeister K, Greiling H: Transforming growth factor ß1, a major stimulator of hyaluronan synthesis in human synovial lining cells. *Arthritis Rheum* 38:669-77, 1995.

22. Hills BA: Boundary lubrication in vivo. *Proc Inst Mech Eng H* 214:83-94, 2000.

23. Ikegawa S, Sano M, Koshizuka Y, Nakamura Y: Isolation, characterization and mapping of the mouse and human PRG4 (proteoglycan 4) genes. *Cytogenet Cell Genet* 90:291-7, 2000.

24. Ingram KR, Wann AK, Angel CK, Coleman PJ, Levick JR: Cyclic movement stimulates hyaluronan secretion into the synovial cavity of rabbit joints. *J Physiol* 586:1715-29, 2008.

25. Jay GD: Characterization of a bovine synovial fluid lubricating factor. I. Chemical, surface activity and lubricating properties. *Connect Tissue Res* 28:71-88, 1992.

26. Jay GD, Britt DE, Cha CJ: Lubricin is a product of megakaryocyte stimulating factor gene expression by human synovial fibroblasts. *J Rheumatol* 27:594-600, 2000.

27. Jay GD, Tantravahi U, Britt DE, Barrach HJ, Cha CJ: Homology of lubricin and superficial zone protein (SZP): products of megakaryocyte stimulating factor (MSF) gene expression by human synovial fibroblasts and articular chondrocytes localized to chromosome 1q25. *J Orthop Res* 19:677-87, 2001.

28. Jay GD, Torres JR, Rhee DK, Helminen HJ, Hytinnen MM, Cha CJ, Elsaid K, Kim KS, Cui Y, Warman ML: Association between friction and wear in diarthrodial joints lacking lubricin. *Arthritis Rheum* 56:3662-9, 2007.

29. Jones AR, Flannery CR: Bioregulation of lubricin expression by growth factors and cytokines. *Eur Cell Mater* 13:40-5; discussion 5, 2007.

30. Kiener HP, Watts GF, Cui Y, Wright J, Thornhill TS, Skold M, Behar SM, Niederreiter B, Lu J, Cernadas M, Coyle AJ, Sims GP, Smolen J, Warman ML, Brenner MB, Lee DM: Synovial fibroblasts self-direct multicellular lining architecture and synthetic function in three-dimensional organ culture. *Arthritis Rheum* 62:742-52, 2010.

31. Knight AD, Levick JR: The density and distribution of capillaries around a synovial cavity. . *Q J Exp Physiol* 68:629-44, 1983.

32. Lee SY, Niikura T, Reddi AH: Superficial zone protein (lubricin) in the different tissue compartments of the knee joint: modulation by transforming growth factor beta 1 and interleukin-1 beta. *Tissue Eng Part A* 14:1799-807, 2008.

33. Levick JR: The influence of hydrostatic pressure on trans-synovial fluid movement and on capsular expansion in the rabbit knee. *J Physiol* 289:69-82, 1979.

34. Ludwig TE, McAllister JR, Lun V, Wiley JP, Schmidt TA: Diminished cartilage lubricating ability of human osteoarthritic synovial fluid deficient in proteoglycan 4: Restoration through proteoglycan 4 supplementation. *Arthritis Rheum* 64:3963-71, 2012.

35. Lukoschek M, Schaffler MB, Burr DB, Boyd RD, Radin EL: Synovial membrane and cartilage changes in experimental osteoarthrosis. *J Orthop Res* 6:475-92, 1988.

36. McCarty WJ, Cheng JC, Hansen BC, Yamaguchi T, Masuda K, Sah RL: The biophysical mechanisms of altered hyaluronan concentration in synovial fluid after anterior cruciate ligament transection. *Arthritis Rheum* 64:3993-4003, 2012.

37. Momberger TS, Levick JR, Mason RM: Hyaluronan secretion by synoviocytes is mechanosensitive. *Matrix Biol* 24:510-9, 2005.

38. Nugent GE, Aneloski NM, Schmidt TA, Schumacher BL, Voegtline MS, Sah RL: Dynamic shear stimulation of bovine cartilage biosynthesis of proteoglycan 4 (PRG4). *Arthritis Rheum* 54:1888-96, 2006.

39. Nugent GE, Schmidt TA, Schumacher BL, Voegtline MS, Bae WC, Jadin KD, Sah RL: Static and dynamic compression regulate cartilage metabolism of proteoglycan 4 (PRG4). *Biorheology* 43:191-200, 2006.

40. Raleigh AR, McCarty WJ, Chen AC, Meinert C, Klein TJ, Sah RL: Synovial joints: Mechanobiology and tissue engineering of articular cartilage and synovial fluid. In: *Comprehensive Biomaterials,* ed. by P Ducheyne, Healey KE, Hutmacher DE, Grainger DE, Kirkpatrick CJ, Elsevier, 2017, 107-34.

41. Raleigh AR, Sun Y, Qian D, Temple-Wong MM, Kato K, Murata K, Firestein GS, Masuda K, Sah RL: Synovial fluid hyaluronan fluctuation in post-traumatic osteoarthritis: Dependence on the dynamic balance between biosynthesis, loss, and fluid flux *Trans Orthop Res Soc* 42:1506, 2017.

42. Reesink HL, Watts AE, Mohammed HO, Jay GD, Nixon AJ: Lubricin/proteoglycan 4 increases in both experimental and naturally occurring equine osteoarthritis. *Osteoarthritis Cartilage* 25:128-37, 2017.

43. Schmid T, Lindley K, Su J, Soloveychik V, Block J, Kuettner K, Schumacher B: Superficial zone protein (SZP) is an abundant glycoprotein in human synovial fluid and serum. *Trans Orthop Res Soc* 26:82, 2001.

44. Schmid TM, Su J-L, Lindley KM, Soloveychik V, Madsen L, Block JA, Kuettner KE, Schumacher BL: Superficial zone protein (SZP) is an abundant glycoprotein in human synovial fluid with lubricating properties. In: *The Many Faces of Osteoarthritis,* ed. by KE Kuettner, Hascall VC, Raven Press, New York, 2002, 159-61.

45. Schmidt TA, Gastelum NS, Nguyen QT, Schumacher BL, Sah RL: Boundary lubrication of articular cartilage: role of synovial fluid constituents. *Arthritis Rheum* 56:882-91, 2007.

46. Schmidt TA, Schumacher BL, Han EH, Klein TJ, Voegtline MS, Sah RL: Chemomechanical coupling in articular cartilage: IL-1a and TGF-ß1 regulate chondrocyte synthesis and secretion of proteoglycan 4. In: *Physical Regulation of Skeletal Repair,* ed. by RK Aaron, Bolander ME, American Academy of Orthopaedic Surgeons, Chicago, 2005, 151-61.

47. Schumacher BL, Block JA, Schmid TM, Aydelotte MB, Kuettner KE: A novel proteoglycan synthesized and secreted by chondrocytes of the superficial zone of articular cartilage. *Arch Biochem Biophys* 311:144-52, 1994.

48. Schumacher BL, Hughes CE, Kuettner KE, Caterson B, Aydelotte MB: Immunodetection and partial cDNA sequence of the proteoglycan, superficial zone protein, synthesized by cells lining synovial joints. *J Orthop Res* 17:110-20, 1999.

49. Schumacher BL, Schmidt TA, Voegtline MS, Chen AC, Sah RL: Proteoglycan 4 (PRG4) synthesis and immunolocalization in bovine meniscus. *J Orthop Res* 23:562-8, 2005.

50. Swann DA, Slayter HS, Silver FH: The molecular structure of lubricating glycoprotein-I, the boundary lubricant for articular cartilage. *J Biol Chem* 256:5921-5, 1981.

51. Teeple E, Elsaid KA, Fleming BC, Jay GD, Aslani K, Crisco JJ, Mechrefe AP: Coefficients of friction, lubricin, and cartilage damage in the anterior cruciate ligament-deficient guinea pig knee. *J Orthop Res* 26:231-7, 2008.

52. Temple-Wong MM, Ren S, Quach P, Hansen BC, Chen AC, Hasegawa A, D'Lima DD, Koziol J, Masuda K, Lotz MK, Sah RL: Hyaluronan concentration and size distribution in human knee synovial fluid: variations with age and cartilage degeneration. *Arthritis Res Ther* 18:18, 2016.

53. Walker ER, Boyd RD, Wu DD, Lukoschek M, Burr DB, Radin EL: Morphologic and morphometric changes in synovial membrane associated with mechanically induced osteoarthrosis. *Arthritis Rheum* 34:515-24, 1991.

54. Wilder FV, Hall BJ, Barrett JP, Jr., Lemrow NB: History of acute knee injury and osteoarthritis of the knee: a prospective epidemiological assessment. The Clearwater Osteoarthritis Study. *Osteoarthritis Cartilage* 10:611-6, 2002.

55. Young AA, McLennan S, Smith MM, Smith SM, Cake MA, Read RA, Melrose J, Sonnabend DH, Flannery CR, Little CB: Proteoglycan 4 downregulation in a sheep meniscectomy model of early osteoarthritis. *Arthritis Res Ther* 8:R41, 2006.

56. Zhang D, Cheriyan T, Martin SD, Gomoll AH, Schmid TM, Spector M: Lubricin distribution in the torn human anterior cruciate ligament and meniscus. *J Orthop Res* 29:1916-22, 2011.

CHAPTER 4

SYNOVIAL FLUID : SERUM RATIO OF PROTEIN CONCENTRATION IS INCREASED IN EXPERIMENTAL OSTEOARTHRITIS AND INVERSELY CORRELATED WITH SYNOVIAL FLUID HYALURONAN CONCENTRATION

4.1 Abstract

Objective. The concentration ratio of protein in synovial fluid (SF relative to that in plasma ($k^{SF:S}$) at various M_r ($k^{SF:S}{}_{Mr}$) varies following injury or during disease and may reflect changes in synovial lining (SL) permeability. The aim of this study was to determine if $k^{SF:S}{}_{Mr}$ (1) varied with time after induction of post-traumatic osteoarthritis (PTOA) in the rabbit and (2) correlates with altered SF hyaluronan (HA) concentration ($c^{SF}{}_{HA}$). *Methods.* A rabbit model of PTOA was used to evaluate $c^{SF}{}_{HA}$ and $k^{SF:S}{}_{Mr}$ at early (d1-7) and more chronic (d14-42) time points following ACL transection (ACLT), with separate cohorts of rabbits undergoing SHAM surgery (control for the effect of surgery) at d7 and 28. SF and serum were collected, and portions of samples were analyzed for protein concentration and distribution by PAGE and SYPRO Ruby staining. $c^{SF}{}_{HA}$ and HA in M_r bins ($c^{SF}{}_{HA,2.5\text{-}7}$, $c^{SF}{}_{HA,1\text{-}2.5}$, $c^{SF}{}_{HA,0.5\text{-}1}$, $c^{SF}{}_{HA,<0.5}$) were assessed. *Results.* Compared to CTRL (0.35±0.01), ACLT $k^{SF:S}$ was higher at d1-7 post-injury (+51-55%). Ratio of high-M_r protein, $k^{SF:S}{}_{345\text{-}735}$, was higher in ACLT than Non-OP knees,

markedly soon (d1-7) post-injury (+124-230%) and in a sustained manner at d28 and 42 (+63-126%). ACLT $k^{SF:S}{}_{Mr}$ was higher vs. SHAM for the highest M_r proteins (+88% in $k^{SF:S}{}_{345\text{-}735}$) at d28, but not at d7, suggesting two different mechanisms for increased SF protein. Overall ACLT HA and total protein $k^{SF:S}$ were related, with $c^{SF}{}_{HA}$ decreased with increasing $k^{SF:S}$ (r^2=0.20). <u>*Conclusion.*</u> Alterations in $k^{SF:S}{}_{Mr}$ provide a joint-scale metric of the extent to which ACLT affects trans-synovial transport and altered SF composition during PTOA.

4.2 Introduction

In articular joints such as the knee, low-friction, low-wear lubrication is mediated by synovial fluid (SF), a viscous plasma dialysate supplemented with lubricant molecules secreted by joint cells [38]. In healthy joints, the SF biomolecular composition is in dynamic equilibrium, with molecules entering the SF via transport from plasma to SF and by local cell synthesis, and molecules leaving the SF via transport from SF to the lymphatics or by local degradation [5]. SF is encapsulated by a thin synovial lining (SL), consisting of a dense network of fibroblast-like synoviocytes (FLS) and interstitial matrix components such as collagen, laminin, and proteoglycans [2, 38]. SF is formed as blood plasma is filtered through the size-selective capillary and synovial lining (SL) "membranes"[31, 49]. Protein transport across these membranes is driven by both advective and diffusive fluxes [9, 15, 26, 32, 38]. Plasma volume (and associated protein) is driven down hydrostatic and osmotic pressure gradients from the vasculature to the SF (advective flux), and protein is driven down concentration gradients in the same direction (diffusive flux). The thin SL, 15-40 μm thick in rabbits, functions as a semi-permeable boundary that selectively permits and retains specific molecules into or within the joint space based on molecular mass (M_r) [16, 35, 42]. The SL is backed by a thicker synovial subintima (SS), which consists of a loose network of extracellular matrix molecules and includes penetrating capillaries (C) and lymphatics (L), but which provides little resistance to bidirectional blood-joint transport [17, 36, 42, 44, 49].

In healthy SF, the total protein concentration ($c^{SF}_{protein}$) is 25-28 mg/mL, roughly one-third of the total protein concentration in serum ($c^{S}_{protein}$) [13, 41]. High $c^{SF}_{protein}$ plays a key role in maintaining normal SF osmotic pressure and high viscosity [19, 28]. SF volume (V^{SF}) and the

majority of $c^{SF}_{protein}$ turn over completely in ~1 hr in normal joints, as influx (via capillaries) and efflux (via venules and lymphatics) occur continuously [23].

During arthritis progression or following injury, inflammation often induces joint swelling, SL hyperplasia, and SL immune cell infiltration [22, 30]. Resultant changes to SF volume (V^{SF}), SF hydrostatic and osmotic pressures, and SL architecture may alter the apparent permeability of the SL for certain molecules. In rabbits, manipulation of SL matrix content by digestion of protein or GAG components [47, 48] or of the SF hydrostatic or osmotic pressure by intra-articular injection of exogenous solutions [18, 21, 34] resulted in changes to net fluid and protein flux in the joint. Increased fluxes, and a decrease in the ability of the SL to selectively retain molecules, likely results in the loss of high M_r lubricants from the SF.

$c^{SF}_{protein}$ is generally increased in arthritis, especially for high molecular mass (M_r) proteins [20, 22]. Protein flux from the microvasculature to the SF (influx via capillaries) or from the SF to the lymphatics (efflux) has been analyzed using a variety of techniques, such as intra-articular injection of radio-labeled protein or albumin-binding dyes and periodic SF or lymph sampling to estimate protein efflux [43, 52, 54], or measurement of protein turnover via joint washout and SF sampling [8]. A proposed method for determining gross changes to protein influx is the SF to serum concentration ratio ($k^{SF:S}$), reflecting, in part, the size-selectivity of filtration between the joint space and capillaries [10, 20, 22]. Increases in $k^{SF:S}$, especially for proteins of high M_r ($k^{SF:S}_{Mr}$), suggest reduced molecular selectivity of the SL in arthritis [20, 22]. Regardless of measurement technique, these studies consistently show that protein flux is following joint injury or during disease progression.

One common form of osteoarthritis (OA) is initiated following traumatic joint injury, such as damage to the anterior cruciate ligament (ACL) [12]. This type of OA, termed post-

traumatic OA (PTOA), occurs in 12% of all OA cases and is especially common in young athletes [6, 40]. In PTOA, the composition of SF is altered, affecting key biophysical properties. Notably, the concentration of hyaluronan (HA, c^{SF}_{HA}), a key lubricating molecule, is decreased, more in the acute than chronic phases [1, 38]. increased SF HA is produced primarily by FLS within the SL, and contributes to the maintenance of SF osmotic pressure, viscosity, and volume [5, 38]. c^{SF}_{HA}, which in healthy rabbit joints is 2.68±0.27 mg/mL with a high M_r of 2-7 million, is reduced following ACL transection (ACLT) [39]. A high c^{SF}_{HA} is important in healthy joint function, as HA lowers the friction coefficient of articulating cartilage surfaces in a concentration-dependent manner [1, 45]. Theoretically, c^{SF}_{HA} is inversely proportional to the permeability to HA of the SF:serum interface [4].

Following ACLT in rabbit knees, permeability is variably increased [30], and may affect both c^{SF}_{HA} and $k^{SF:S}_{Mr}$. Thus, we tested the hypotheses that $k^{SF:S}_{Mr}$ is elevated following ACLT and is correlated with decreased c^{SF}_{HA}.

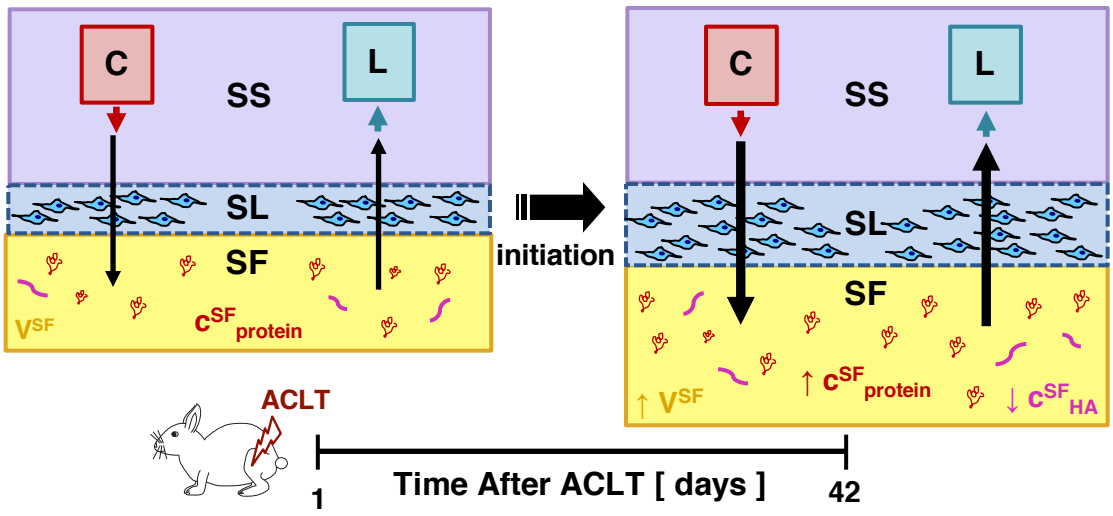

Figure 4.1: Schematic of hypothesis and specific aims for modeling synovial joint protein dynamics. Data from in vivo experiments were used to measure or calculate $c^{SF}_{protein}$, $c^{Serum}_{protein}$, and $k^{SF:S}$, and these protein-specific variables were then related to c^{SF}_{HA}. Serum protein from capillaries (C) is either allowed into the joint or restricted by the semi-permeable SL. As SF protein is removed from joint, it is transported across SL to the lymphatics (L), located in the synovial subintima (SS).

4.3 Materials and Methods

Experimental design. The study is summarized here and in **Fig. 1**, with reference to detailed methods below. 37 adult female New Zealand White (NZW) rabbits were subjected to unilateral ACLT, and knee joints were harvested at 1, 4, 7, 14, 28, and 42 days post-injury (n=6-7 per group). At harvest, serum and SF were collected from ACLT and Non-OP knees. A separate cohort of rabbits undergoing SHAM surgery were used to control for the effect of joint opening, and were sacrificed at days 7 and 28 (n=6-7 per group). In addition, SF was harvested from 30 healthy rabbits as controls (CTRL).

Rabbit SF and rabbit serum were analyzed for protein concentration in distinct molecular mass (M_r) bins using SDS-PAGE gel electrophoresis under denaturing, non-reducing conditions and protein staining. Gel images were analyzed for intensity of protein staining and compared to an M_r standard. The protein concentrations overall and within each M_r bin for SF and serum, collected from the same animal, were used to calculate the concentration ratios $k^{SF:S}$ and $k^{SF:S}{}_{Mr}$.

Statistics. Data are shown as mean±SE. The effects of (1) ACLT vs. Non-OP and time post-injury, as well as (2) ACLT vs. SHAM animal and knee operation (OP vs. Non-OP) at d7 and 28, were analyzed by 2-way repeated measures ANOVA. At each time point, differences between ACLT and Non-OP SF and between ACLT and SHAM (d7 and 28) were analyzed by paired t-test. Each ACLT, and Non-OP time point was also compared to CTRL by ANOVA and Dunnett's test. The relationships between protein $k^{SF:S}$ ($k^{SF:S}{}_{Mr}$) and $c^{SF}{}_{HA}$ ($c^{SF}{}_{HA,Mr}$) were assessed by linear regression. All statistical analyses were performed using SPSS (IBM). Results were considered significant if $P<0.05$.

Detailed experimental methods. A total of 80 adult female NZW rabbits were used in this study. All animal protocols were approved by UCSD IACUC.

Effect of ACLT in the rabbit. To examine the time course of acute injury, 50 rabbits (9-18 mos) underwent surgery for ACLT or SHAM in the right knee as described previously [30]. A drawer test was used to confirm rupture of the ACL. The left knee of rabbits was left as a contralateral Non-OP control. Following surgery, rabbits were allowed to move freely in cages and received a standard diet and water *ad libitum*. At 1, 4, 7, 14, 28, and 42 days post-ACLT and at 7 and 28 days post-SHAM, animals were euthanized via intravenous injection of pentobarbital sodium for analysis (n=6-7 rabbits per time point). Additionally, a cohort of 30 healthy rabbits (9-18 mos) were euthanized and used as a naive CTRL.

Serum and SF were harvested. After the knee joint was opened, the cut ends of the ACL, and the intact PCL, were visualized to confirm the surgical model. SF was aspirated from the parapatellar region of the knee joint using a 50 μL micro syringe and clarified by centrifugation. Whole blood was collected, allowed to clot, and centrifuged to obtain serum.

Biochemical assays. Portions of SF samples were digested with *Streptomyces hyaluronidase* (s. hy'ase) (Santa Cruz Biotech) at 10.0 U/ml in buffer (0.2M NaAc, 0.15M NaCl, 0.05M EDTA, pH 4.65) overnight at 37°C. Total protein in SF ($c^{SF}_{protein}$) and serum ($c^{S}_{protein}$) were quantified with the bicinchoninic acid (BCA) assay (Thermo Fisher Scientific). A portion of SF or serum was diluted 1:30 or 1:300 in water and assayed following the manufacturer's protocol [53].

Portions (2-4 μg protein, <2 μL SF or serum) of samples were mixed with sample buffer (62 mM tris HCl, 10% glycerol, 2% SDS, 0.0025% bromophenol blue, pH 6.8) and separated under non-reducing conditions by 4-12% PAGE with a running buffer of 0.1% SDS, Tris-glycine, pH 8.3 (Thermo Fisher Scientific). Gels were fixed in a solution of 50% methanol, 7% acetic acid and stained overnight with SYPRO Ruby stain solution (Thermo Fisher Scientific),

and imaged for blue fluorescence (STORM imager, GMI). Gel images were processed for protein distribution in M_r bins between 21, 28, 43, 70, 105, 210, 345, and 735 kd to quantify major protein bands using a custom MATLAB script by subtracting the intensities of sample buffer blanks, and then displaying on a relative scale (0 to 1) to show protein content. The linear range of the standard curve was verified using a high M_r protein (alpha-2-macroglobulin) and a protein standard with low M_r bands (Thermo). The protein concentrations overall and within each M_r bin for SF and serum, collected from the same animal, were used to calculate the concentration ratios $k^{SF:S}$ and $k^{SF:S}{}_{Mr}$.

SF samples were analyzed for the concentration and size distribution of HA. Portions of samples were treated with proteinase K (0.5 mg/mL in 0.1M sodium phosphate, 5 mM Na_2-EDTA, pH 6.5, overnight incubation at 37°C) (Sigma). Samples were boiled for 10 min to inhibit residual proteinase activity. The concentration of HA in proteinase-digested SF was determined by an ELISA-like assay using rhAggrecan (R&D Systems) for detection as described previously [53]. The size distribution of HA in SF in M_r bins, $c^{SF}{}_{HA,\,Mr}$, between 0, 0.5, 1.0, 2.5, and 7 Md was determined by separating on 1% agarose GE, Stainsall staining, densitometric imaging, and image processing [53]. SF samples were added to sample buffer (2.5% sucrose, 0.02% bromophenol blue), applied to 1% agarose, separated by horizontal electrophoresis at 100V for 70 min in TAE buffer (0.4M Tris-acetate and 0.01 M ethylenediaminetetraacetic acid, pH 8.3), fixed in 25% isopropanol, and visualized after incubation with 0.1% Stainsall reagent (Sigma). Gel images were taken on an Epson scanner (Epson America) and image processing was performed using a custom MATLAB script to determine HA distribution within M_r ranges (0.05–0.25, 0.25–0.5, 0.5–1, 1–2.5, and 2.5–7 Md) in SF samples [53]. The concentration of HA within each M_r range was calculated as the percentage of HA in that range multiplied by the overall HA

concentration or normalized secretion rate.

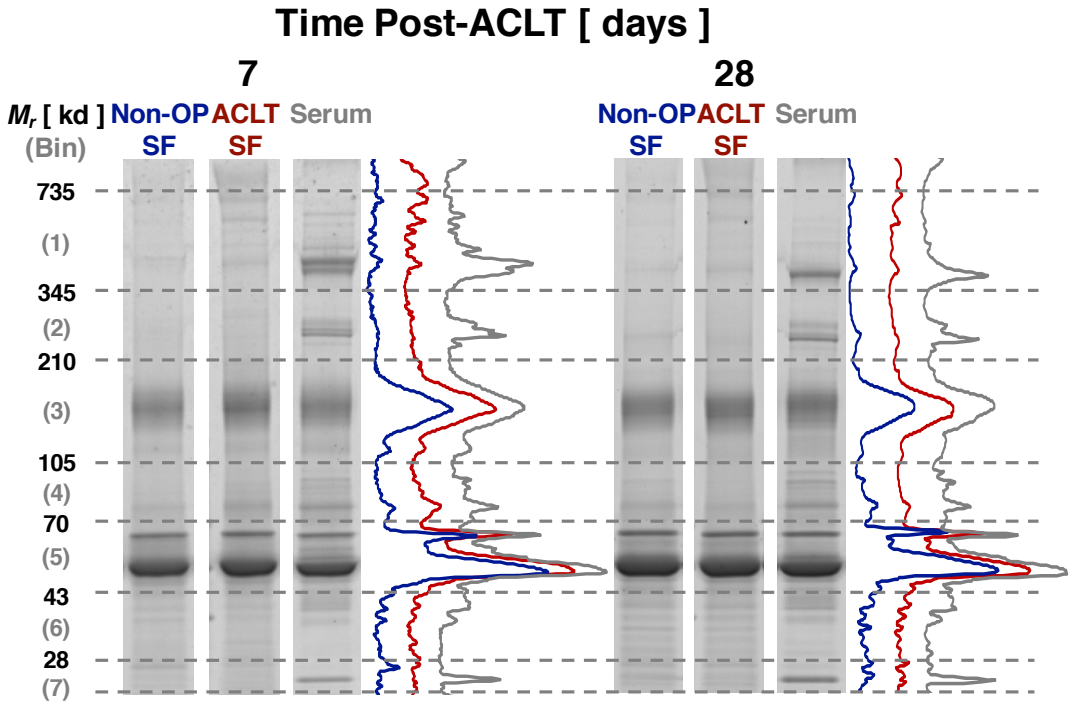

Figure 4.2: Representative SDS PAGE at 7 and 28 days post-ACLT. Non-OP SF, **ACLT** SF, and **Serum** were run in consecutive lanes on 4-12% Tris-Glycine gels. Gel images were processed for protein distribution in M_r bins between 21, 28, 43, 70, 105, 210, 345, and 735 kd to quantify major protein bands, and then displayed on a relative scale (0 to 1) to show protein content.

4.4 Results

ACLT causes time-varying changes in c^{S}_{rotein} and $c^{SF}_{protein}$**.** ACLT $c^{S}_{protein}$ was affected by time (P<0.01) (**Fig. 3A**). Compared to CTRL (53.13±0.77 mg/mL), $c^{S}_{protein}$ trended towards an increase at d14-28 (+12-13%, P=0.06-0.09), but not earlier (P=1.00).

$c^{SF}_{protein}$ was higher in ACLT knees (P<0.01) and was affected interactively by ACLT and time after surgery (P<0.05), without an effect of time (P=0.36) (**Fig. 3A**). Compared to Non-OP, ACLT $c^{SF}_{protein}$ was higher at d4, 7, and 28 post-injury (+25-72%). Compared to CTRL (18.62±0.63 mg/mL), ACLT $c^{SF}_{protein}$ was higher for all time (+22-57%, P<0.001), while Non-OP $c^{SF}_{protein}$ was not different from CTRL for the entire time course (P=0.14-1.00).

ACLT variably affects $k^{SF:S}$*, depending on* M_r**.** Total $k^{SF:S}$ was higher in ACLT knees (P<0.01) and was affected interactively by ACLT and time after surgery (P<0.05), without an effect of time (P=0.50) (**Fig. 3B**). Compared to Non-OP, ACLT $k^{SF:S}$ was higher at d4, 7, and 28 post-injury (+25-75%). Compared to CTRL (0.35±0.01), ACLT $k^{SF:S}$ was higher at d1-7 post-injury (+51-55%, P<0.001), while Non-OP $k^{SF:S}$ was not different from CTRL for the entire time course (P=0.79-1.00).

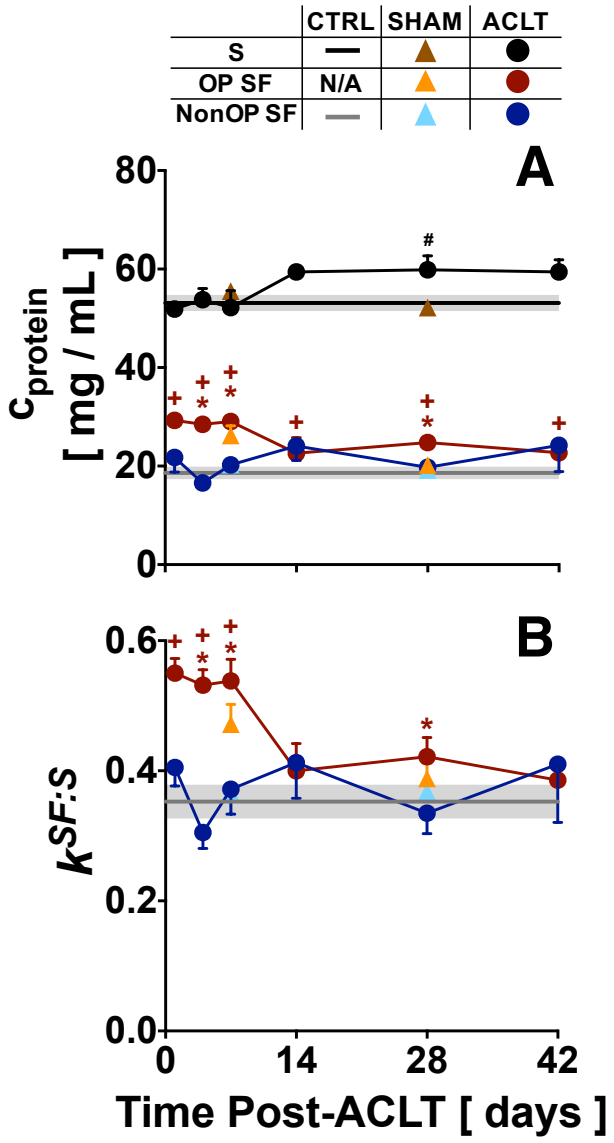

Figure 4.3: Effect of ACLT or SHAM surgery on (A) protein concentrations, $c_{protein}$, & (B) concentration ratios, $k^{SF:S}$, for SF & serum. n=4-7, *P<0.05 vs. **Non-OP**, $^{\#}$,$^{\#}P$<0.05 vs. **SHAM** for **ACLT** SF or serum. $^{+}$,$^{+}$,$^{+}$ P<0.05 vs. **CTRL** for **ACLT**, **Non-OP**, or **S**. **CTRL** values are mean±95% CI (■, n=9-16).

Depending on M_r, $k^{SF:S}{}_{Mr}$ was variably affected by ACLT at early (d1-7) and/or later (d28-42) time (**Fig. 4**). Ratio of high-M_r protein ($k^{SF:S}{}_{345-735}$, **Fig. 4A**) was affected by ACLT (P<0.001) but not by time (P=0.49), with an interaction effect (P<0.05). $k^{SF:S}{}_{345-735}$ was higher in ACLT than Non-OP knees, markedly soon (d1-7) post-injury (+124-230%, P<0.05) and in a sustained manner at d28 and 42 (+63-126%, P<0.05). Compared to CTRL (0.21±0.01), ACLT $k^{SF:S}{}_{345-735}$ was higher at d4, 7, 28, and 42 post-injury (+82-122%, P<0.05) with a trend at d14 (+77%, P=0.08), while Non-OP $k^{SF:S}{}_{345-735}$ was different from CTRL only at d14 (+87%, P<0.05).

Ratio of mid-M_r protein ($k^{SF:S}{}_{210-345}$, **Fig. 4B**) was affected by ACLT (P<0.001) with trends towards effects of time (P=0.11) and interaction (P=0.18). $k^{SF:S}{}_{210-345}$ was higher in ACLT than Non-OP knees at d4 and 28 (+62-96%, P<0.01), with a trend at d7 and 42 (+35-44%, P=0.05-0.06). Compared to CTRL (0.21±0.02), ACLT $k^{SF:S}{}_{210-345}$ was higher at d4 and 7 post-injury (+21-63%, P<0.05), while Non-OP $k^{SF:S}{}_{210-345}$ was not different from CTRL for the entire time course (P=0.54-1.00).

Ratios of low-to-mid-range M_r protein ($k^{SF:S}{}_{105-210}$ and $k^{SF:S}{}_{70-105}$, **Fig. 4C, D**) were each affected by ACLT (P<0.001) and variably with time (P=0.22 and P<0.05, respectively), with an interactive effect in both M_r ranges (P<0.05). $k^{SF:S}{}_{105-210}$ was higher in ACLT vs Non-OP knees soon (d4, 7) post-ACLT (+52%-54%, P<0.05) with a trend at d1 (+55%, P=0.05), but not later (P=0.87-0.93, d14, 42), although there was a trend at d28 (+19%, P=0.06). $k^{SF:S}{}_{70-105}$ was higher in ACLT knees both soon (+48-62% vs Non-OP, d1-7, P<0.05) and later (+43% vs Non-OP, d28, P<0.05) post-injury. Compared to CTRL (0.36±0.02), ACLT $k^{SF:S}{}_{105-210}$ was higher at d1-7 and post-injury (+54-74%, P<0.05), while Non-OP $k^{SF:S}{}_{105-210}$ was not different from CTRL for the entire time course (P=0.69-1.00). Compared to CTRL (0.29±0.01), ACLT $k^{SF:S}{}_{70-105}$ was

similarly higher at d1-7 post-injury (+42-90%, $P<0.05$), while Non-OP $k^{SF:S}_{70\text{-}105}$ was not different from CTRL for the entire time course ($P=0.62$-1.00).

Increases in $k^{SF:S}$ were also observed for select lower M_r proteins (<70 kd) (**Fig. 4E-G**). Ratios of low-M_r protein ($k^{SF:S}_{43\text{-}70}$, **Fig. 4E** and $k^{SF:S}_{21\text{-}28}$, **Fig. 4G**) were neither affected by ACLT ($P=0.66$, 0.07), nor by time ($P=0.34$, 0.27), without interaction effects ($P=0.37$, 0.06). ACLT-induced increases in these $k^{SF:S}_{Mr}$ were primarily at early time; $k^{SF:S}_{43\text{-}70}$ was higher for ACLT knees at d4 and 7 post-injury (+22-36% vs Non-OP, $P<0.05$). Compared to CTRL (0.42±0.02), ACLT $k^{SF:S}_{43\text{-}70}$ was higher at d1-7 post-injury (+29-43%, $P<0.01$), while Non-OP $k^{SF:S}_{43\text{-}70}$ was not different from CTRL for the entire time course ($P=0.16$-1.00).). $k^{SF:S}_{21\text{-}28}$ was higher for ACLT knees at d1 and 4 post-injury (+92-109% vs Non-OP, $P<0.05$). Compared to CTRL (0.29±0.03), ACLT $k^{SF:S}_{21\text{-}28}$ was higher at d1-7 post-injury (+147-154%, $P<0.001$), while Non-OP $k^{SF:S}_{21\text{-}28}$ was not different from CTRL for the entire time course ($P=0.34$-1.00).

Ratio of low-M_r protein ($k^{SF:S}_{28\text{-}43}$, **Fig. 4F**) was affected by ACLT ($P<0.01$) but not by time ($P=0.50$), with a trend towards an interaction effect ($P=0.06$). $k^{SF:S}_{28\text{-}43}$ was higher for ACLT knees at d1-7 and d28 post-injury (+24-73% vs Non-OP, $P<0.05$). Compared to CTRL (0.42±0.02), ACLT $k^{SF:S}_{28\text{-}43}$ was higher at d1-7, d28, and d42 post-injury (+101-177%, $P<0.01$), while Non-OP $k^{SF:S}_{28\text{-}43}$ was different from CTRL only at d7 (+110%, $P<0.05$).

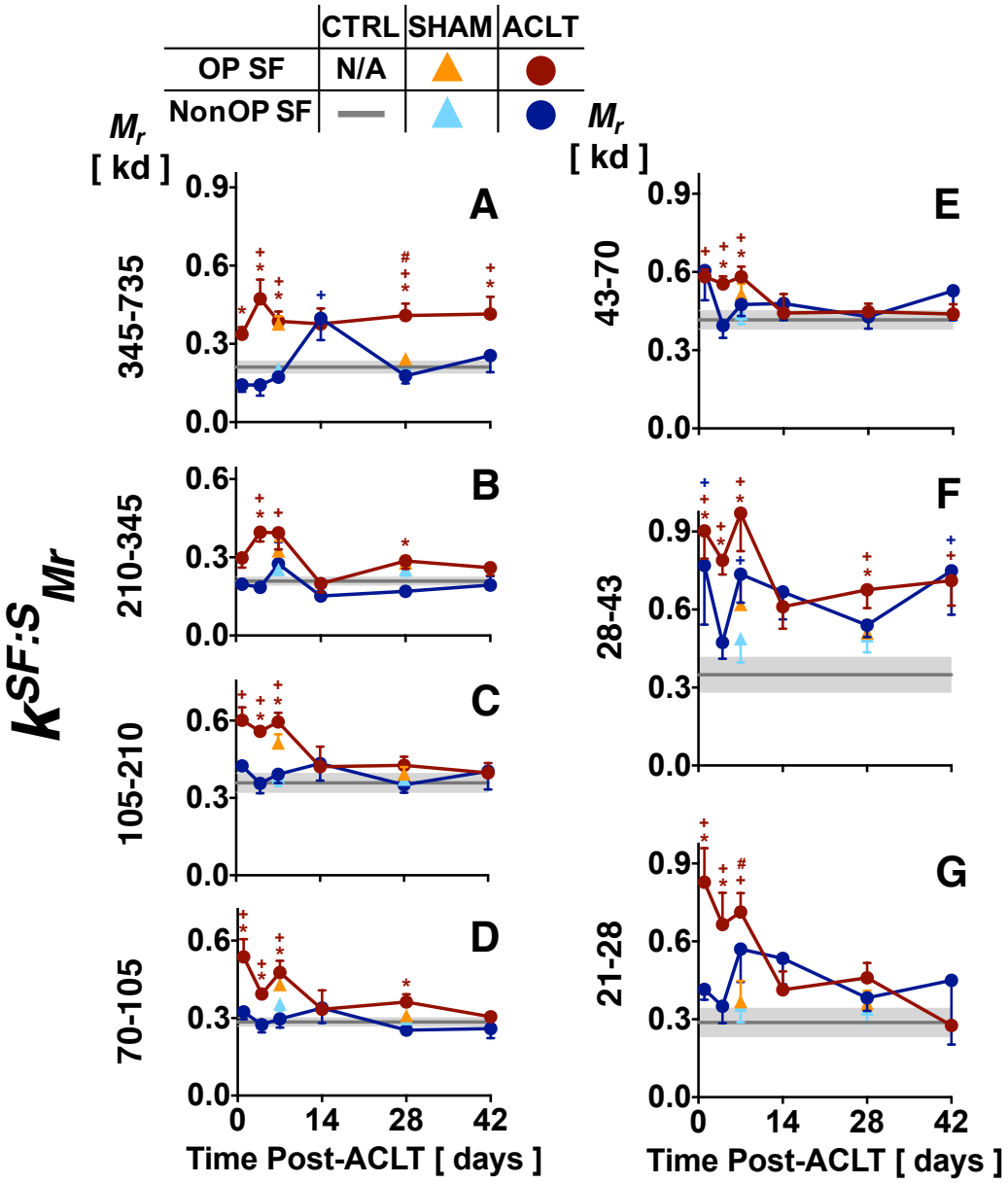

Figure 4.4: Effect of injury on $k^{SF:S}$ in different M_r ranges for ACLT and Non-OP joints: **(A)** 345-735 kd, **(B)** 210-345 kd, **(C)** 105-210 kd, (D) 70-105 kd, **(E)** 43-70 kd, **(F)** 28-43, and **(G)** 21-28 kd. Mean ± SE, n=3-7, $^{*}P<0.05$ vs. **Non-OP**, $^{\#}P<0.05$ vs. **SHAM** for **ACLT** SF or serum. $^{+}P<0.05$ vs. **CTRL** for **ACLT** and **Non-OP**. **CTRL** values are mean±95% CI (■, n=9).

SHAM surgery causes changes in $c^{S}_{protein}$, $c^{SF}_{protein}$, $k^{SF:S}$, and $k^{SF:S}_{Mr}$. SHAM $c^{S}_{protein}$ was not different from CTRL values at either d7 or d28 (P=0.27-0.78), but was decreased compared to ACLT at d28 (-15%, P<0.05), but not at d7 (P=0.40, **Fig. 3A**). $c^{SF}_{protein}$ was affected by knee (OP vs NON-OP, P<0.05), but not by surgery (ACLT vs SHAM, P=0.51) and with no interactive effect (P=0.23 **Fig. 3A**) at both d7, but with trends towards an effect of surgery (P=0.07) and an interactive effect (P=0.07) at d28. ACLT and SHAM $c^{SF}_{protein}$ were not different at d7 (P=0.24), but ACLT $c^{SF}_{protein}$ was higher at d28 (+23%, P<0.05, **Fig. 3A**). At both d7 and d28, $k^{SF:S}$ was affected by knee (P<0.05), but not by surgery (P=0.43-0.99), with trends towards an interactive effect (P=0.09-0.18, **Fig. 3B**). ACLT and SHAM $k^{SF:S}$ were not different at d7 and 28 (P=0.18-0.39).

$k^{SF:S}_{Mr}$ was affected by knee (OP vs Non-OP, P<0.05) for all high- and mid-range M_r (P<0.01) for 345-735, 210-345, 105-210, and 70-105 kd (**Fig. 4A-D)**. For lower M_r (<70 kd), there was no effect of knee (0.07-0.51) except for $k^{SF:S}_{43-70}$ and $k^{SF:S}_{28-43}$ at d7 (P<0.01, **Fig. 4E-G**). $k^{SF:S}_{Mr}$ was affected by surgery (ACLT vs SHAM) at d7 for $k^{SF:S}_{70-105}$ and at d28 for $k^{SF:S}_{345-735}$, $k^{SF:S}_{210-345}$, and $k^{SF:S}_{70-105}$ (P<0.05). There were no interaction effects between knee and surgery for $k^{SF:S}_{Mr}$ (P=0.06-0.99). At d7, ACLT $k^{SF:S}_{Mr}$ were not different from SHAM values (P=0.09-0.83) except for $k^{SF:S}_{21-28}$ (+93%, P<0.05). At d28, ACLT $k^{SF:S}_{Mr}$ was higher vs SHAM for the highest M_r proteins (+65% in $k^{SF:S}_{345-735}$, P<0.01), but values were not different than SHAM in other $k^{SF:S}_{Mr}$ (P=0.07-0.86, **Fig. 4A-G**).

Increase in ACLT $k^{SF:S}$ is correlated with decreased c^{SF}_{HA}. c^{SF}_{HA} was lower in ACLT compared to Non-OP knees (P<0.001) and affected by time (P<0.05), with an interaction effect (P<0.05, **Fig. 5A**). Compared to Non-OP, ACLT c^{SF}_{HA} was substantially lower at both early (-

51% to -64%, d4 and d7, $P<0.05$, and -51% trend at d1, $P=0.14$) and late (-47% and -33% at d28 and d42, $P<0.05$) time points post-injury. Both Non-OP and ACLT c^{SF}_{HA} were affected by time ($P<0.05$ by ANOVA and curve fits). Compared to c^{SF}_{HA} in CTRL (2.37±0.20 mg/mL), ACLT c^{SF}_{HA} was lower at all time points (-41% to –75%, $P<0.05$), while Non-OP c^{SF}_{HA} was lower only at d7 and d14 post-injury (-49% and -45%, $P<0.05$). Compared to SHAM OP knees, ACLT c^{SF}_{HA} was lower at both d7 (-73%, $P<0.001$) and d28 (-57%, $P<0.01$, Fig. **5A**).

c^{SF}_{HA} in both ACLT and Non-OP joints was comprised of primarily high M_r HA, with very little total c^{SF}_{HA} at lower M_r ranges (<1.0 Md, **Fig. 5**). c^{SF}_{HA} at high HA M_r (2.5-7.0 Md) decreased variably over time following ACLT (**Fig. 5B**). This decrease (-44% to -66% vs. Non-OP, $P<0.01$) was measured at both acute (d4, 7) and more chronic time points (d28 and d42) following injury. Compared to CTRL $c^{SF}_{HA,2.5\text{-}7}$ (1.72±0.19 mg/mL), ACLT values were decreased across all time points (-18% to -66%, $P<0.01$), but Non-OP $c^{SF}_{HA,2.5\text{-}7}$ was not ($P=0.19$-1.00, **Fig. 5B**), though there was a trend at d14 ($P=0.05$). For mid-range HA M_r (1.0-2.5 Md), ACLT c^{SF}_{HA} M_r was decreased (-60% vs. Non-OP, $P<0.05$) at d7 post-injury, and was also decreased at early time compared to CTRL $c^{SF}_{HA,1\text{-}2.5}$ values of 0.34±0.05 mg/mL (-68% to -69%, d1-7, **Fig. 5C**). For HA in the lowest M_r ranges (<1.0 Md), ACLT c^{SF}_{HA} M_r was increased (+51-83% vs. Non-OP, $P<0.05$) at d28 post-injury (**Fig. 5D,E**).

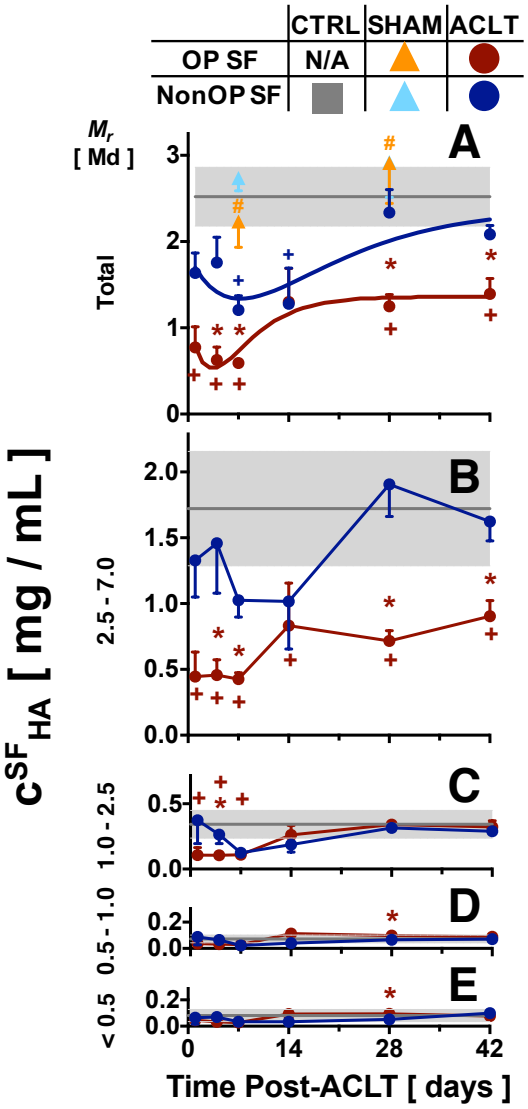

Figure 4.5: Effect of ACLT on HA concentration (c^{SF}_{HA}) and M_r distribution in SF from ACLT and Non-OP knees. c^{SF}_{HA} distribution **(A)** overall, and in **(B)** 2.5-7.0, **(C)** 1.0-2.5, **(D)** 0.5-1.0, and **(E)** < 0.5 Md ranges. Mean±SE, n=3-6, *P<0.05. $^{+}$,^{+}P<0.05 for **ACLT** or **Non-OP** vs. **CTRL**, $^{\#}P$<0.05 for **ACLT** vs. **SHAM** OP knees. **CTRL** values are mean±95% CI (■, n=9).

For all experimental groups combined, HA and total protein $k^{SF:S}$ were related, with c^{SF}_{HA} decreased with increasing $k^{SF:S}$ (r^2=0.20, P<0.001, **Fig. 6A**). The relationship between $k^{SF:S}$ and $c^{SF}_{HA,Mr}$ varied with M_r. $c^{SF}_{HA,2.5\text{-}7\ Md}$, $c^{SF}_{HA,1\text{-}2.5\ Md}$, $c^{SF}_{HA,0.5\text{-}1\ Md}$, and $c^{SF}_{HA,<0.5\ Md}$ all decreased with increasing $k^{SF:S}$ (r^2=0.28, 0.26, 0.11, and 0.06, respectively, P<0.05, **Fig. 6B-E**), with slopes decreasing with decreasing $c^{SF}_{HA,Mr}$.

$c^{SF}_{HA,Mr}$ and total protein $k^{SF:S}_{Mr}$ were also related, with c^{SF}_{HA} generally decreased with increasing $k^{SF:S}_{Mr}$ (**Tables 1, 2**). r^2 and m (slope) values tended to be highest for total c^{SF}_{HA}, and decrease with decreasing $c^{SF}_{HA,Mr}$, though the dependence on $k^{SF:S}$ depended on M_r (**Tables 1, 2**). For example, $c^{SF}_{HA,1.0\text{-}2.5}$ and $c^{SF}_{HA,0.5\text{-}1.0}$ did not depend on $k^{SF:S}_{345\text{-}735}$ (P=0.07, 0.71), but did depend on $k^{SF:S}$ of lower M_r (**Table 1**), with variable slopes across $k^{SF:S}_{Mr}$ (**Table 2**).

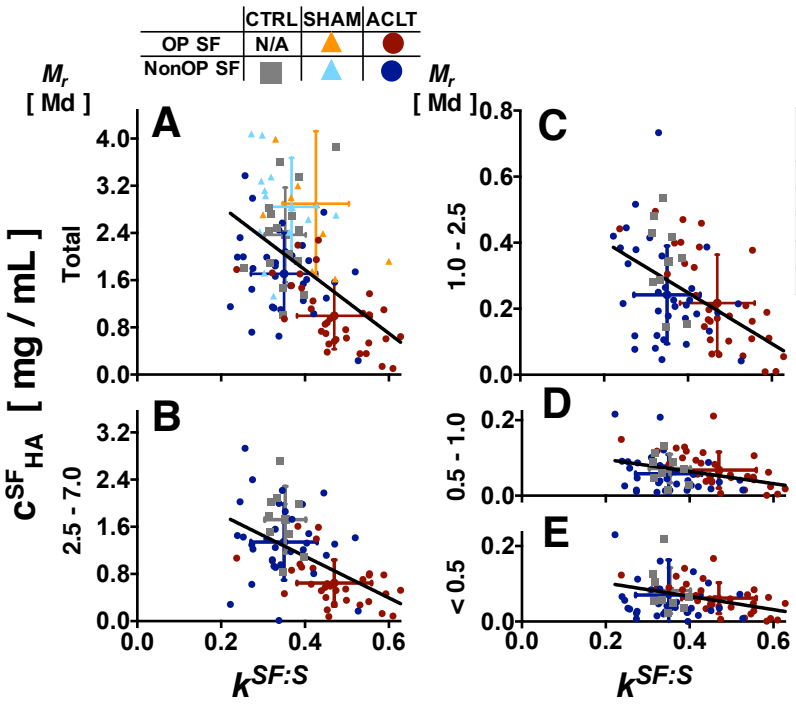

F

$c^{SF}_{HA,Mr}$ [Md]	Grp	p-value	r^2	m	b'
total	all	<0.0001	0.20	-4.76	3.36
2.5-7	all	<0.0001	0.28	-3.52	2.04
1-2.5	all	<0.0001	0.26	-0.77	0.49
0.5-1.0	all	<0.01	0.11	-0.16	0.13
<0.5	all	<0.05	0.06	-0.17	0.13

Figure 4.6: Correlation between $k^{SF:S}$ & (A) total c^{SF}_{HA}, (B) $c^{SF}_{HA,2.5\text{-}7.0}$, (C) $c^{SF}_{HA,1.0\text{-}2.5}$, (D) $c^{SF}_{HA,0.5\text{-}1.0}$, & (E) $c^{SF}_{HA,<0.5}$ for ACLT, Non-OP, CTRL, SHAM OP, & SHAM Non-OP. n=9-33/grp, mean±SD for groups. **(F)** Table of r^2 and best fit values for regression lines for all groups combined. b' values are adjusted to account for the $k^{SF:S}$ and c^{SF}_{HA} values of CTRL samples.

Table 4.1: *P*-values and r^2 for select correlations between $k^{SF:S}{}_{Mr}$ and $c^{SF}{}_{HA,Mr}$ for all groups. n=9-33/group.

	$k^{SF:S}{}_{Mr}$									
	345-735 kd		**210-345 kd**		**105-210 kd**		**70-105 kd**		**43-70 kd**	
$c^{SF}{}_{HA}$ **[mg / mL]**	***P*-value**	**r^2**	***P*-value**	**r^2**	***P*-value**	**r^2**	***P*-value**	**r^2**	***P*-value**	**r^2**
2.5 -7 Md	<0.0001	0.298	0.001	0.158	<0.0001	0.348	<0.0001	0.310	0.005	0.111
1.0-2.5 Md	0.067	0.049	0.002	0.132	<0.0001	0.292	<0.0001	0.188	0.001	0.151
0.5-1.0 Md	0.709	0.002	0.030	0.068	0.026	0.072	0.079	0.045	0.385	0.011

Table 4.2: m and b' values for select correlations between $k^{SF:S}{}_{Mr}$ and $c^{SF}{}_{HA,Mr}$ for all groups. n=9-33/group. b' values are adjusted to account for the $k^{SF:S}$ and $c^{SF}{}_{HA}$ values of CTRL samples.

	$k^{SF:S}{}_{Mr}$									
	345-735 kd		**210-345 kd**		**105-210 kd**		**70-105 kd**		**43-70 kd**	
$c^{SF}{}_{HA}$ **[mg / mL]**	**m**	**b'**	**m**	**b'**	**m**	**b'**	**m**	**b'**	**m**	**b'**
2.5 -7 Md	-2.53	1.31	-2.39	1.16	-3.16	2.12	-3.53	1.88	-1.69	1.42
1.0-2.5 Md	-0.208	0.470	-0.495	0.469	-0.657	0.509	-0.623	0.493	-0.446	0.486
0.5-1.0 Md	0.012	0.120	-0.101	0.123	-0.093	0.128	-0.087	0.126	-0.035	0.123

4.5 Discussion

In this study, a quantitative metric ($k^{SF:S}_{Mr}$) is defined, relating altered protein content in different M_r ranges to decreased c^{SF}_{HA} in a rabbit model of PTOA (**Fig. 1**, **Table 1**). The variables $c^{SF}_{protein}$ and $c^{S}_{protein}$ were measured directly from *in vivo* data, and were used to calculate the SF to serum protein ratio $k^{SF:S}$. This ratio was then compared to measured c^{SF}_{HA} and $c^{SF}_{HA,Mr}$ to determine whether increased SF protein content is correlated with decreased lubricant concentration, and thus decreased SF function [46]. $k^{SF:S}_{Mr}$ can be assessed using small (<2 μL) quantities of SF and serum and standard biochemical methods, and thus is a convenient marker for SL remodeling following injury. Because transport both into and out of the joint space depends on SL membrane properties, an increase in transport of large M_r proteins into the joint from the capillaries has negative implications for the ability of SL to retain high M_r molecules secreted into SF by resident joint cells, such as HA. At early time points (d1-7), ACLT $k^{SF:S}$ was increased vs. CTRL and Non-OP values, both for total $k^{SF:S}$ and that in all M_r ranges (**Fig. 3A**, **Fig. 4A-G**). This elevation is likely due to joint opening and acute inflammation, as these metrics were not different for ACLT vs. SHAM, but did vary by surgery (OP vs. Non-OP) at d7 for most M_r ranges (**Figs. 3**, **4**). At later time points post-injury, $k^{SF:S}$ was elevated for high (210-735 kd, **Fig. 4A-B**) and mid-range (70-210 kd) M_r (**Fig. 4C-D**), suggesting more chronic alterations to SL membrane properties during PTOA progression. Particularly for $k^{SF:S}_{345\text{-}735}$, there was a substantial increase in ACLT values compared to SHAM, suggesting an additional mechanism independent of inflammation responsible for altered SL properties.

The SF to serum protein ratios calculated in this study may be affected by a number of factors. Generalized protein staining in distinct M_r bins may be confounded if a large portion of protein measured in SF is secreted by cells resident within the joint space, as increased signal

intensity stemming from biosynthesis would overestimate SF protein influx from the capillaries. However, protein compositional analysis of discrete bands via mass spectrometry suggests that protein evaluated in $k^{SF:S}$ calculations are of a plasma dialysate, and not a native synovial, origin (data not shown). Additionally, the primary native joint protein, proteoglycan-4 (PRG4, also referred to as lubricin) [14] exists at concentrations ~20-270 μg/mL in rabbits [11, 37], an order of magnitude lower than the $c^{SF}_{protein}$ considered in the present study. Increased $c^{SF}_{protein}$ may also occur if V^{SF} decreases but the total mass of protein is relatively constant, increasing $k^{SF:S}$ since the plasma volume is assumed constant. However, in previous studies in the rabbit model of PTOA, V^{SF} was substantially higher in ACLT vs. CTRL by 250-500% [39], suggesting that if protein mass were constant, $c^{SF}_{protein}$ would be much lower. Because $c^{SF}_{protein}$ (and $k^{SF:S}$) are markedly higher in ACLT knees, the elevation in SL apparent permeability predicted by $k^{SF:S}$ values is likely an underestimation, due to dilution effects in SF.

While $c^{SF}_{protein}$, $c^{S}_{protein}$, and $k^{SF:S}$ have been previously evaluated in human knees in normal and pathological states [20, 22, 33, 51], to our knowledge this is the first time $k^{SF:S}$ has been extended to cover a broad range of M_r and has been related to changes in c^{SF}_{HA}. The $c^{SF}_{protein}$, $c^{S}_{protein}$, and $k^{SF:S}$ presented in this study for a rabbit model of PTOA are similar to prior analyses in humans. $c^{SF}_{protein}$ in normal knees is 25-28 mg/mL, compared to $c^{S}_{protein}$ measurements of ~70 mg/mL [13, 41]. The measures for $c^{SF}_{protein}$ (18.62 ± 0.63 mg/mL) and $c^{S}_{protein}$ (53.13 ± 0.77 mg/mL) in CTRL rabbit knees in the present study are slightly lower than values previously reported for rabbit $c^{SF}_{protein}$ (23.0 ± 0.4 mg/mL), but are comparable to rabbit $c^{S}_{protein}$ estimates (55.1 ± 0.1 mg/mL) [19]. In healthy human knees, $k^{SF:S}$ was 0.23±0.09 for low M_r proteins (~40 kd) and much lower (0.03±0.03) for high M_r proteins ~ 800 kd [20]. In patients with OA, $k^{SF:S}$ was increased both for low M_r (to 0.64±0.13) and high M_r (0.28±0.09) proteins, and these ratios

were more pronounced in knees of patients with inflammatory conditions such as rheumatoid arthritis (RA) and gout [20, 33]. These measures have similar trends and values to those in the present study (**Fig. 4**), with increased $k^{SF:S}$ occurring with decreased M_r and during disease progression.

A likely cause of increased $k^{SF:S}$ is altered SL matrix content and organization, and thus altered permeability, during PTOA progression. Following ACLT, increased FLS proliferation [26, 30, 50] and immune cell influx [3, 30] can lead to changes in the SL barrier function, making it more permeable to large macromolecules such as protein. Additionally, the large V^{SF} noted post-injury[58] can also stretch out the SL tissue and dilute the matrix biopolymers, changing the effective pore size and surface area of the SL [25, 27, 34]. If the effective pore size of the SL is increased, it may lead to lower retention of high-M_r SF lubricants in pathological states.

The lubricant HA forms entangled networks at high c^{SF}_{HA} and M_r, and thus plays an important role in the maintenance of SF volume and protein content in the presence of pressure gradients, such as during knee flexion and extension [7, 29]. Due to high M_r HA outflow buffering in joints, SL permeability is a function of c^{SF}_{HA}, especially that immediately contiguous with the SL [24]. Decreases in c^{SF}_{HA}, and chiefly that of high M_r, have functional implications not only for decreased joint lubrication and viscosity, but also for altered joint transport. The increase in apparent SL permeability reduces c^{SF}_{HA}, but the decrease in HA further increases permeability, acting as a positive feedback mechanism.

These results collectively implicate functionally-relevant increases in $k^{SF:S}$ for high M_r protein at early and late times after ACLT. The inverse relationship between $k^{SF:S}$ and c^{SF}_{HA} (**Fig. 3**) suggests that increased $k^{SF:S}$ reflects increased permeability, which in turn is at least partially responsible for the decrease in SF HA lubricant concentration during PTOA. The similar effects

of ACLT and SHAM at d7, but differences at d28, suggest that increases in $k^{SF:S}$ early (d1-7) after injury are due in part to an acute inflammatory response, whereas the sustained increase in $k^{SF:S}$ at later (≥ 28 days) time points may reflect SL remodeling. Therapeutics that target the increased biomolecular flux following injury or during disease progression should focus on limiting the immune response and joint effusions (for early time) and restoring SL matrix organization (for chronic time). Changes to $k^{SF:S}_{Mr}$ provide a joint-scale metric of the extent to which PTOA affects trans-synovial transport and, thus, a basis for altered SF composition in OA.

4.6 Acknowledgments

This chapter, in full, will be submitted to *Arthritis & Rheumatology*. The dissertation author was the primary author and thanksco-authors Julian J. Garcia, Barbara L. Schumacher, Shingo Miyazaki, Junichi Yamada, Gary S. Firestein, Koichi Masuda, and Robert L. Sah. This work was supported by research grants from the National Institutes of Health (R01 AR055637, T32 AR060712), the Department of Defense (DOD OR13085), the UC San Diego Frontiers of Innovation Scholarship Program, and the San Diego Fellowship.

The authors thank Dr. Samuel Ward for use of CTRL rabbit tissue.

4.7 References

1. Antonacci JM, Schmidt TA, Serventi LA, Cai MZ, Shu YL, Schumacher BL, McIlwraith CW, Sah RL: Effects of equine joint injury on boundary lubrication of articular cartilage by synovial fluid: role of hyaluronan. *Arthritis Rheum* 64:2917-26, 2012.

2. Bartok B, Firestein GS: Fibroblast-like synoviocytes: key effector cells in rheumatoid arthritis. *Immunol Rev* 233:233-55, 2010.

3. Benito MJ, Veale DJ, FitzGerald O, van den Berg WB, Bresnihan B: Synovial tissue inflammation in early and late osteoarthritis. *Ann Rheum Dis* 64:1263-7, 2005.

4. Blewis ME, Lao BJ, Jadin KD, McCarty WJ, Bugbee WD, Firestein GS, Sah RL: Semi-permeable membrane retention of synovial fluid lubricants hyaluronan and proteoglycan 4 for a biomimetic bioreactor. *Biotechnol Bioeng* 106:149-60, 2010.

5. Blewis ME, Nugent-Derfus GE, Schmidt TA, Schumacher BL, Sah RL: A model of synovial fluid lubricant composition in normal and injured joints. *Eur Cell Mater* 13:26-39, 2007.

6. Brown TD, Johnston RC, Saltzman CL, Marsh JL, Buckwalter JA: Posttraumatic osteoarthritis: a first estimate of incidence, prevalence, and burden of disease. *J Orthop Trauma* 20:739-44, 2006.

7. Coleman PJ, Scott D, Mason RM, Levick JR: Characterization of the effect of high molecular weight hyaluronan on trans-synovial flow in rabbit knees. *J Physiol* 514 (Pt 1):265-82, 1999.

8. Coleman PJ, Scott D, Ray J, Mason RM, Levick JR: Hyaluronan secretion into the synovial cavity of rabbit knees and comparison with albumin turnover. *J Physiol* 503 (Pt 3):645-56, 1997.

9. Curry F: Mechanics and thermodynamics of transcapillary exchange. In: *Handbook of Physiology,* ed. by ERaC Michel, American Physiological Society, Bethesda, 1984, 309-74.

10. Decker B, McKenzie BF, McGuckin WF, Slocumb CH: Comparative distribution of proteins and glycoproteins of serum and synovial fluid. *Arthritis Rheum* 2:162-77, 1959.

11. Elsaid KA, Jay GD, Warman ML, Rhee DK, Chichester CO: Association of articular cartilage degradation and loss of boundary-lubricating ability of synovial fluid following injury and inflammatory arthritis. *Arthritis Rheum* 52:1746-55, 2005.

12. Gelber AC, Hochberg MC, Mead LA, Wang NY, Wigley FM, Klag MJ: Joint injury in young adults and risk for subsequent knee and hip osteoarthritis. *Ann Intern Med* 133:321-8, 2000.

13. Holley HL, Patton FM, Pigman W, Platt D: An electrophoretic study of normal and post-mortem human and bovine synovial fluids. *Arch Biochem Biophys* 64:152-63, 1956.

14. Ikegawa S, Sano M, Koshizuka Y, Nakamura Y: Isolation, characterization and mapping of the mouse and human PRG4 (proteoglycan 4) genes. *Cytogenet Cell Genet* 90:291-7, 2000.

15. Kedem O, Katchalsky A: Thermodynamic analysis of the permeability of biological membranes to non-electrolytes. *Biochim Biophys Acta* 27:229-46, 1958.

16. Knight AD, Levick JR: The density and distribution of capillaries around a synovial cavity. . *Q J Exp Physiol* 68:629-44, 1983.

17. Knight AD, Levick JR: Morphometry of the ultrastructure of the blood-joint barrier in the rabbit knee. *Q J Exp Physiol* 69:271-88, 1984.

18. Knight AD, Levick JR, McDonald JN: Relation between trans-synovial flow and plasma osmotic pressure, with an estimation of the albumin reflection coefficient in the rabbit knee. *Q J Exp Physiol* 73:47-65, 1988.

19. Knox P, Levick JR, McDonald JN: Synovial fluid--its mass, macromolecular content and pressure in major limb joints of the rabbit. *Q J Exp Physiol* 73:33-45, 1988.

20. Kushner I, Somerville JA: Permeability of human synovial membrane to plasma proteins. Relationship to molecular size and inflammation. *Arthritis Rheum* 14:560-70, 1971.

21. Levick JR: Contributions of the lymphatic and microvascular systems to fluid absorption from the synovial cavity of the rabbit knee. *J Physiol* 306:445-61, 1980.

22. Levick JR: Permeability of rheumatoid and normal human synovium to specific plasma proteins. *Arthritis Rheum* 24:1550-60, 1981.

23. Levick JR: Synovial fluid and trans-synovial flow in stationary and moving normal joints. In: *Joint loading: biology and health of articular structures* ed. by HJ Helminen, Kiviranta I, Säämänen AM, Tammi M, Paukkonen K, Wright & Sons, Bristol, 1987, 149-86.

24. Levick JR: Synovial Fluid. Determinants of volume turnover and material concentration. In: *Articular cartilage and osteoarthritis,* ed. by KE Kuettner, Schleyerbach R, Peyron JG, Hascall VC, Raven Press, New York, 1992, 529-41.

25. Levick JR: An analysis of the interaction between interstitial plasma protein, interstitial flow, and fenestral filtration and its application to synovium. *Microvasc Res* 47:90-125, 1994.

26. Levick JR: Microvascular architecture and exchange in synovial joints. *Microcirculation* 2:217-33, 1995.

27. Levick JR, McDonald JN: Ultrastructure of transport pathways in stressed synovium of the knee in anaesthetized rabbits. *J Physiol* 419:493-508, 1989.

28. Levick JR, McDonald JN: Fluid movement across synovium in healthy joints: role of synovial fluid macromolecules. *Ann Rheum Dis* 54:417-23, 1995.

29. Lu Y, Levick JR, Wang W: Concentration polarization of hyaluronan on the surface of the synovial lining of infused joints. *J Physiol* 561:559-73, 2004.

30. McCarty WJ, Cheng JC, Hansen BC, Yamaguchi T, Masuda K, Sah RL: The biophysical mechanisms of altered hyaluronan concentration in synovial fluid after anterior cruciate ligament transection. *Arthritis Rheum* 64:3993-4003, 2012.

31. McDonald JN, Levick JR: Effect of extravascular plasma protein on pressure-flow relations across synovium in anaesthetized rabbits. *J Physiol* 465:539-59, 1993.

32. Patlak CS, Goldstein DA, Hoffman JF: The flow of solute and solvent across a two-membrane system. *J Theor Biol* 5:426-42, 1963.

33. Pejovic M, Stankovic A, Mitrovic DR: Determination of the apparent synovial permeability in the knee joint of patients suffering from osteoarthritis and rheumatoid arthritis. *Br J Rheumatol* 34:520-4, 1995.

34. Price FM, Levick JR, Mason RM: Changes in glycosaminoglycan concentration and synovial permeability at raised intra-articular pressure in rabbit knees. *J Physiol* 495 (Pt 3):821-33, 1996.

35. Price FM, Levick JR, Mason RM: Glycosaminoglycan concentration in synovium and other tissues of rabbit knee in relation to synovial hydraulic resistance. *J Physiol (Lond)* 495:803-20, 1996.

36. Price FM, Mason RM, Levick JR: Radial organization of interstitial exchange pathway and influence of collagen in synovium. *Biophys J* 69:1429-39, 1995.

37. Raleigh AR, Cravotta MJ, Garcia JJ, Schumacher BL, Kato K, Firestein GS, Masuda K, Sah RL: Decreased synovial fluid proteoglycan-4 concentration in ACL-transected knee joints is due to dynamic imbalance in biosynthesis, clearance, and effusion. *OARSI 2018 World Congress*:204, 2018.

38. Raleigh AR, McCarty WJ, Chen AC, Meinert C, Klein TJ, Sah RL: Synovial joints: Mechanobiology and tissue engineering of articular cartilage and synovial fluid. In: *Comprehensive Biomaterials,* ed. by P Ducheyne, Healey KE, Hutmacher DE, Grainger DE, Kirkpatrick CJ, Elsevier, 2017, 107-34.

39. Raleigh AR, Sun Y, Qian D, Temple-Wong MM, Kato K, Murata K, Firestein GS, Masuda K, Sah RL: Synovial fluid hyaluronan fluctuation in post-traumatic osteoarthritis: Dependence on the dynamic balance between biosynthesis, loss, and fluid flux *Trans Orthop Res Soc* 42:1506, 2017.

40. Roos H, Adalberth T, Dahlberg L, Lohmander L: Osteoarthritis of the knee after injury to the anterior cruciate ligament or meniscus: the influence of time and age. *Osteoarthritis Cartilage* 3:261-7, 1995.

41. Ropes MW, Rossmeisl EC, Bauer W: The origin and nature of normal human synovial fluid. *J Clin Invest* 19:795-9, 1940.

42. Sabaratnam S, Arunan V, Coleman PJ, Mason RM, Levick JR: Size selectivity of hyaluronan molecular sieving by extracellular matrix in rabbit synovial joints. *J Physiol* 567:569-81, 2005.

43. Sabaratnam S, Mason RM, Levick JR: Inside-out cannulation of fine lymphatic trunks used to quantify coupling between transsynovial flow and lymphatic drainage from rabbit knees. *Microvasc Res* 64:1-13, 2002.

44. Sabaratnam S, Mason RM, Levick JR: Molecular sieving of hyaluronan by synovial interstitial matrix and lymphatic capillary endothelium evaluated by lymph analysis in rabbits. *Microvasc Res* 66:227-36, 2003.

45. Schmidt TA, Gastelum NS, Nguyen QT, Schumacher BL, Sah RL: Boundary lubrication of articular cartilage: role of synovial fluid constituents. *Arthritis Rheum* 56:882-91, 2007.

46. Schmidt TA, Sah RL: Effect of synovial fluid on boundary lubrication of articular cartilage. *Osteoarthritis Cartilage* 15:35-47, 2007.

47. Scott D, Coleman PJ, Abiona A, Ashhurst DE, Mason RM, Levick JR: Effect of depletion of glycosaminoglycans and non-collagenous proteins on interstitial hydraulic permeability in rabbit synovium. *J Physiol* 511 (Pt 2):629-43, 1998.

48. Scott D, Coleman PJ, Mason RM, Levick JR: Glycosaminoglycan depletion greatly raises the hydraulic permeability of rabbit joint synovial lining. *Exp Physiol* 82:603-6, 1997.

49. Scott D, Levick JR, Miserocchi G: Non-linear dependence of interstitial fluid pressure on joint cavity pressure and implications for interstitial resistance in rabbit knee. *Acta Physiol Scand* 179:93-101, 2003.

50. Sellam J, Berenbaum F: The role of synovitis in pathophysiology and clinical symptoms of osteoarthritis. *Nat Rev Rheumatol* 6:625-35, 2010.

51. Simkin PA: Synovial permeability in rheumatoid arthritis. *Arthritis Rheum* 22:689-96, 1979.

52. Simkin PA: Synovial perfusion and synovial fluid solutes. *Ann Rheum Dis* 54:424-8, 1995.

53. Temple-Wong MM, Ren S, Quach P, Hansen BC, Chen AC, Hasegawa A, D'Lima DD, Koziol J, Masuda K, Lotz MK, Sah RL: Hyaluronan concentration and size distribution in human knee synovial fluid: variations with age and cartilage degeneration. *Arthritis Res Ther* 18:18, 2016.

54. Wallis WJ, Simkin PA, Nelp WB: Protein traffic in human synovial effusions. *Arthritis Rheum* 30:57-63, 1987.

CHAPTER 5

SELECT VISCOSUPPLEMENT THERAPIES DECREASE EXPERIMENTAL & THEORETICAL MEASURES OF LUBRICANT LOSS FROM THE SYNOVIAL JOINT IN A RABBIT MODEL OF POST-TRAUMATIC OSTEOARTHRITIS

5.1 Abstract

The lubricant function of synovial fluid (SF) is diminished after injury, often because of decreases in the concentrations of hyaluronan (HA, c^{SF}_{HA}) and proteoglycan-4 (PRG4, c^{SF}_{PRG4}). Following ACL transection in a rabbit model of post-traumatic osteoarthritis, the effects of intra-articular injection of viscosupplements (HA, PRG4, or the combination) on SF and SL composition over a 28-day time course were evaluated. c^{SF}_{HA} and c^{SF}_{PRG4} dynamics can be attributed to different biological (synthesis) but similar biophysical (transport) mechanisms. c^{SF}_{HA} was decreased at early times for all groups (-37% to -56% vs. CTRL), but at d28 had recovered to CTRL levels in knees treated with PRG4 and HA+PRG4, despite the large SF volume (V^{SF}) in these knees. A portion of the increase in c^{SF}_{HA} in these joints is likely due to increased HA synthesis, as *HA synthase* expression (+181-212%) and the number of synoviocytes ($N^{SL,FLS}$, +249-313%) were substantially increased at d28. c^{SF}_{PRG4} was similarly decreased early (-53% to -60%) for joints treated with PRG4 and HA+PRG4, likely due to a similar dilution lubricant mass

by V^{SF}. By d28, c^{SF}_{PRG4} had recovered to CTRL values for these joints, although the increase in c^{SF}_{PRG4} is likely not due to increased synthesis, as *PRG4* expression was decreased at d28 (-74% to -89%). c^{SF}_{HA} and c^{SF}_{PRG4} may be increased at d28 in select groups (PRG4, HA+PRG4, and HA alone for c^{SF}_{PRG4}) due to a reduction in lubricant efflux from the joint: $k^{SF:S}$, and specifically that for highest M_r proteins, $k^{SF:S}_{435\text{-}735}$, was reduced in joints treated with lubricants compared to those treated with saline (-34% to -60%). The restoration of SF lubricant concentrations by d28 post-ACLT in PRG4 and HA+PRG4 groups suggests that PRG4 IA injections, either alone or in combination with high-M_r HA, may be effective in maintaining lubricant concentrations, and therefore SF function, post-injury.

5.2 Introduction

In synovial joints such as the knee, a lubricious synovial fluid (SF) helps to reduce wear and friction between articulating cartilage surfaces contact during joint loading [45]. Following naturally-occurring injury [10, 14], during arthritis progression [53], or in experimental models of joint injury [15, 16, 61], the composition, and thus the function, of SF changes, accelerating joint deterioration. Such synovial joint injury has been used in model systems of anterior cruciate ligament (ACL) transection (ACLT) [11, 38, 46]. ACLT advances cartilage deterioration and hastens the development of osteoarthritis (OA), through mechanisms that may involve deficient SF lubrication [18, 64].

Two major SF lubricant components are hyaluronan (HA) and proteoglycan-4 (PRG4) [45, 54, 55]. The normal concentration of HA in SF (c^{SF}_{HA}) is 1-4 mg/mL, of which most (>70%) is of high molecular mass (M_r, 2-7 Md). PRG4, also known as superficial zone protein (SZP), lubricin, and megakaryocyte stimulating factor (MSF), is a ~300 kd mucinous glycoprotein [24, 50, 54, 55, 60], found at concentrations (c^{SF}_{PRG4}) ranging from 130-450 μg/mL in knee joints [16, 51]. The values of c^{SF}_{HA} and c^{SF}_{PRG4} are functionally important, as HA and PRG4 lower the friction coefficient and mechanical interaction of articulating cartilage surfaces in a concentration-dependent manner [3, 30, 37, 52]. Following joint injury [3, 5, 48] or joint surgery [20], as well as during aging and OA progression [37, 63], c^{SF}_{HA} decreases, while variable PRG4 concentrations have been reported [3-5, 14, 16]. The lubricating- and lubricant-deficient SF are restored *in vitro* by the addition of high-concentration and high-M_r HA alone, or in combination with, PRG4 [3, 35, 52]. Combined HA and PRG4 supplementation may be useful since the combination of these molecules can lubricate cartilage better than either alone [29, 52].

SF is encapsulated within the synovial cavity by a thin synovial lining (SL) and articular cartilage (AC) [6, 45]. The SL acts as a membrane, allowing selective passage of molecules between the SF joint space and underlying synovial subintima (SS) microvasculature and lymphatics [34]. Because the fluid and protein components of SF pass through capillary and SL "membranes" in series, SF is considered ultrafiltrate of plasma, supplemented with lubricants secreted by resident joint cells [8, 33, 45]. The SL contains 1-3 layers of fibroblast- and macrophage-like synoviocytes (FLS and MLS), with FLS producing lubricant components of the SF [7, 25]. HA is produced by HA synthases (HAS), which exist as three different isoforms, HAS1, HAS2, and HAS3 [47, 59]. These synthases span the fibroblast-like synoviocyte (FLS) plasma membrane, where they produce and secrete HA. The SL, with its relatively large surface area and high FLS cell density [21], is the primary source of SF HA. PRG4 is secreted by chondrocytes in the AC [54], FLS in the SL [55], as well as cells in the meniscus [56, 66] and joint ligaments [31].

Previously, the effect of intra-articular (IA) HA [57, 58, 65] or PRG4 [17, 22, 23] alone, or in combination [62], in animal models of PTOA has been evaluated. HA (0.8-1.5 Md, 10-15 mg/mL, 5 weekly injections) reduced cartilage degeneration scores [57, 65] and moderately improved c^{SF}_{HA} [58]. PRG4 (200-450 μg/mL, injected 1-3 times per week for 4 weeks) reduced cartilage degeneration scores [17, 22, 23], reduced indices of collagen breakdown [62], and improved c^{SF}_{PRG4} [62] in injured joints. However, quantitative SF profiling to assess efficacy of these therapeutics on dynamic SF lubricant composition is limited, as many prior studies were conducted in small animal models and relied on SF dilution by lavage sampled only at the time of sacrifice.

Here, we sought to elucidate the time-course of SF lubricant concentration following

injury and serial viscosupplement administration, and determine whether SF lubricant concentration is correlated with SL properties. In the rabbit ACLT model of PTOA, the aims of the current study were to evaluate (1) the effect of serial IA viscosupplementation on SF lubricant composition at various times post-injury, and (2) attribute altered c^{SF}_{HA} and c^{SF}_{PRG4} to biological and/or biophysical mechanisms.

5.3 Materials and Methods

Experimental design. The study is summarized here and in **Fig. 1**, with reference to detailed methods below. 49 adult female New Zealand White (NZW) rabbits were subjected to unilateral ACLT [11, 38] in the R knee. ACLT knees were injected with (1) saline (300 μL), (2) HA (Synvisc, 8 mg/mL, 300 μL), (3) rhPRG4 (0.5 mg/mL, 300 μL), or (4) HA and rhPRG4 (Synvisc at 8 mg/ml and rhPRG4 at 0.5 mg/mL, 350 μL) at 7, 14, and 21 days post-injury, following uniform injections of saline (300 μL) at days 2 and 4 (n=12-13 per group). At each injection time point, serum and SF were collected from ACLT knees. Joints were harvested at day 28 post-injury, and serum, SF, lavage fluids, and SL were collected from ACLT and Non-OP knees. In addition, SF, serum, and/or SL were harvested from 64 healthy rabbits as controls (CTRL).

Rabbit SF was analyzed for volume (V^{SF}), concentrations of the lubricants hyaluronan (c^{SF}_{HA}) and proteoglycan-4 (c^{SF}_{PRG4}). Rabbit SF and rabbit serum were analyzed for protein concentration in distinct molecular mass (M_r) bins using SDS-PAGE gel electrophoresis under denaturing, non-reducing conditions and protein staining. Gel images were analyzed for intensity of protein staining and compared to an M_r standard. The protein concentrations overall and within each M_r bin for SF and serum, collected from the same animal, were used to calculate the concentration ratios $k^{SF:S}$ and $k^{SF:S}_{Mr}$. Synovial lining was analyzed for total cells ($N^{SL,FLS}$) and gene expression of hyaluronan synthase (*HAS*) and proteoglycan-4 (*PRG4*).

Statistics. Data are shown as mean±SE. At each time point, the effects of therapy were analyzed by 1-way ANOVA with Tukey post-hoc testing. Groups were compared to CTRL values using ANOVA with Dunnett's test. At day 28, differences between ACLT and Non-OP samples were analyzed by paired *t*-test. The relationships between protein $k^{SF:S}$ ($k^{SF:S}_{Mr}$) and c^{SF}_{HA}

($c^{SF}_{HA,Mr}$) were assessed by linear regression. All statistical analyses were performed using SPSS (IBM). Results were considered significant if $P<0.05$.

Detailed experimental methods. A total of 113 adult female NZW rabbits were used in this study. All animal protocols were approved by UCSD IACUC.

Effect of lubricant therapy following ACLT in the rabbit. To examine the time course of acute injury, 43 rabbits (9-20 mos) underwent surgery for ACLT in the right knee as described previously [38]. A drawer test was used to confirm rupture of the ACL. The left knee of rabbits was left as a contralateral Non-OP control. Following surgery, rabbits were allowed to move freely in cages and received a standard diet and water *ad libitum*.

Synvisc (10 mg/mL, Sanofi) and rhPRG4 (1.5 mg/mL, Lubris, LLC, Framingham, MA) [1, 49] were obtained from manufacturers. Prior to injection, viscosupplements were mixed with injection-grade sterile water to obtain final concentrations of 8 mg/mL (Synvisc) and 0.5 mg/mL (rhPRG4). At 2 and 4 days post-ACLT, right knees were injected with saline (300 μL). At 7, 14, and 21 days post-ACLT, right knees were injected with a therapy (n=12-13 rabbits per group): (1) saline (300 μL), (2) HA (Synvisc, 8 mg/ml, 300 μL), (3) rhPRG4 (0.5 mg/ml, 300 μL), or (4) HA and rhPRG4 (Synvisc at 8 mg/mL and rhPRG4 at 0.5 mg/mL, 350 μL). Prior to injections, rabbits were anesthetized, and the right hind limb was shaved and cleaned. Blood and neat SF samples were collected as described above. Joints were injected with therapy and flexed 10 times.

At day 28 post-injury, animals were euthanized via intravenous injection of pentobarbital sodium for analysis. Additionally, a cohort of 64 healthy rabbits (6-18 mos) were euthanized and used as a naive CTRL. At the time of sacrifice, synovial lining were harvested from ACLT and Non-OP knees. After the knee joint was opened, the cut ends of the ACL, and the intact PCL,

were visualized to confirm the surgical model. SF was aspirated from the parapatellar region of the knee joint using a 50 μL micro syringe and clarified by centrifugation. Then, lavage fluid was collected by injecting 500 μL sterile saline (23G syringe), flexing and extending the knee joint 10 times, and aspirating. Synovial and lavage fluids were centrifuged for clarification of cells and debris prior to storage. SF (V^{SF}) and lavage (V^{LAV}) volumes were estimated from fluid masses, assuming a density of ~1 g/mL [28]. Whole blood was collected, allowed to clot, and centrifuged to obtain serum. SL was dissected from medial and lateral gutters and immediately submerged and stored in Qiazol (Qiagen).

Hyaluronan assays. SF samples were analyzed for the concentration and size distribution of HA. Portions of samples were treated with proteinase K (0.5 mg/mL in 0.1M sodium phosphate, 5 mM Na_2-EDTA, pH 6.5, overnight incubation at 37°C) (Sigma). Samples were boiled for 10 min to inhibit residual proteinase activity. The concentration of HA in proteinase-digested SF was determined by an ELISA-like assay using rhAggrecan (R&D Systems) for detection as described previously [63]. The size distribution of HA in SF in M_r bins, $c^{SF}{}_{HA,\,Mr}$, between 0, 0.5, 1.0, 2.5, and 7 Md was determined by separating on 1% agarose GE, Stainsall staining, densitometric imaging, and image processing [63]. SF samples were added to sample buffer (2.5% sucrose, 0.02% bromophenol blue), applied to 1% agarose, separated by horizontal electrophoresis at 100V for 70 min in TAE buffer (0.4M Tris-acetate and 0.01 M ethylenediaminetetraacetic acid, pH 8.3), fixed in 25% isopropanol, and visualized after incubation with 0.1% Stainsall reagent (Sigma). Gel images were taken on an Epson scanner (Epson America) and image processing was performed using a custom MATLAB script to determine HA distribution within M_r ranges (0.05–0.25, 0.25–0.5, 0.5–1, 1–2.5, and 2.5–7 Md) in SF samples [63]. The concentration of HA within each M_r range was calculated as the

percentage of HA in that range multiplied by the overall HA concentration or normalized secretion rate.

Protein assays. Portions of SF samples were digested with *Streptomyces hyaluronidase* (s. hy'ase) (Santa Cruz Biotech) at 10.0 U/mL in buffer (0.2M NaAc, 0.15M NaCl, 0.05M EDTA, pH 4.65) overnight at 37°C. Total protein in SF ($c^{SF}_{protein}$) and serum ($c^{S}_{protein}$) were quantified with the bicinchoninic acid (BCA) assay (Thermo Fisher Scientific). A portion of SF or serum was diluted 1:30 or 1:300 in water and assayed following the manufacturer's protocol [63].

Portions (2-4 μg protein, <2 μL SF or serum) of samples were mixed with sample buffer (62 mM tris HCl, 10% glycerol, 2% SDS, 0.0025% bromophenol blue, pH 6.8) and separated under non-reducing conditions by 4-12% PAGE with a running buffer of 0.1% SDS, Tris-glycine, pH 8.3 (Thermo Fisher Scientific). Gels were fixed in a solution of 50% methanol, 7% acetic acid and stained overnight with SYPRO Ruby stain solution (Thermo Fisher Scientific), and imaged for blue fluorescence (STORM imager, GMI). Gel images were processed for protein distribution in M_r bins between 20, 28, 43, 70, 105, 210, 345, and 735 kd to quantify major protein bands using a custom MATLAB script by subtracting the intensities of sample buffer blanks, and then displaying on a relative scale (0 to 1) to show protein content. The linear range of the standard curve was verified using a high M_r protein (alpha-2-macroglobulin) and a protein standard with low M_r bands (Thermo). The protein concentrations overall and within each M_r bin for SF and serum, collected from the same animal, were used to calculate the concentration ratios $k^{SF:S}$ and $k^{SF:S}_{Mr}$.

PRG4 in digested SF and in conditioned media was analyzed using a western blot assay with mouse monoclonal antibody 9G3 (anti-PRG4, Millipore) [2] to detect a glycosylated

epitope within the mucin domain of the PRG4 molecule. Portions of digested SF equivalent to 0.10-0.30 μl of SF were added to sample buffer (0.5X TAE, 0.05% SDS, 4.9% glycerol, 0.05% bromophenol blue), applied to 2% agarose gels (Lonza, Rockland, ME), separated by horizontal electrophoresis (42 mAmps for 30 min, followed by 84 mAmps for 60 min) on 2% agarose gels (3 mm thick) in TAE buffer (0.4M Tris-acetate and 0.01 M ethylenediaminetetraacetic acid, pH 8.3) with 0.1% SDS. Proteins were transferred to membranes overnight (100 mAmps) in transfer buffer (6.25mM tris, 0.048M glycine, 0.025% SDS, pH 8.3), blocked with 5% milk and 0.1% Tween in 1X PBS, and probed with either a nonspecific IgG or 9G3 (0.002 μg/mL) overnight at 4C. Membranes were rinsed extensively (0.1% PBS-Tween) and incubated with goat anti-mouse conjugated to horseradish peroxidase (0.007 μg/mL) for 1 hr at room temperature. Following the addition of ECL-Plus (Thermo Fisher Scientific), membranes were imaged for blue fluorescence (STORM imager, GMI). Intensity of staining was quantified in a custom MATLAB program. The PRG4 in SF was quantified with the use of standards of PRG4 from human SF.

FLS Estimates. $N^{SL,FLS}$, the number of FLS in the SL, was estimated from DNA in discs harvested from ACLT SL at 28 days post-ACLT (n=10-13/grp) and converted to total SL FLS based on estimates for SL surface area [27, 32]. After dissection as described above, discs (3 mm diameter) were harvested and lyophilized. Following overnight digestion in a solution of proteinase K (Roche, 0.5 mg/mL) at 60°C in PBE (100 mM sodium phosphate, 5 mM Na2EDTA, pH 7.1), samples were assayed using PicoGreen reagent (Invitrogen) [40]. Fluorescence was measured with an excitation wavelength of 480 nm and emission wavelength of 520 nm in a spectrofluorimetric plate reader (SpectraMax Gemini, Molecular Devices). Fluorescence values were converted o ng DNA using sandards of calf thymus DNA (Sigma) in the same buffer solution as samples. DNA content was normalized to determine cell number (7.8

pg DNA/cell) [26, 42]. Cells per SL disc were scaled to cells per joint SL ($N^{SL,FLS}$) using calculations of SL area based on the expected ratio of V^{SF} to tissue (cartilage and SL) area in CTRL joints (0.1 mm) [8, 27, 32]. The area of the SL (A^{SL}=6.7 cm^2) was estimated from simplified joint geometry and prior studies [27, 32].

Gene expression assays. *HAS* and *PRG4* gene expression was analyzed in SL from ACLT, Non-OP, and CTRL knees using qPCR. SL was submerged in liquid nitrogen and pulverized. RNA was isolated from SL using QIAzol reagent (Qiagen) and the RNeasy Mini Kit with a DNAse I incubation step (Qiagen). RNA was quantified using a QIAxpert spectrophotometer (Qiagen). RNA (1000 ng) was reverse transcribed using the QuantiTect Reverse Transcription Kit (Qiagen). Real-time qPCR was carried out on a Rotor-Gene Q platform with SYBR green reporter (Qiagen) using rabbit-specific primers for HA synthase 2 (*HAS2*), proteoglycan-4 (*PRG4*), glyceraldehyde 3-phosphate dehydrogenase (*GAPDH*), and ribosomal protein S18 (*RPS18*) from Qiagen. Amplification curves were converted to absolute copy numbers (CN) of gene transcripts using standard curves. The expected PCR product size was confirmed by electrophoresis. Data are reported as CN ratio of gene of interest to the geometric mean of *GAPDH* and *RPS18*. SL expression of *HAS2* is presented, as previous studies in a similar NZW cohort indicated that *HAS1* and *HAS3* expression in the SL were below the limit of detection [46].

5.4 Results

SF hyaluronan composition and M_r is differentially affected by therapy following ACLT. ACLT c^{SF}_{HA} was affected by therapy at d14 and d28 (P<0.05), but not earlier (P=0.41-0.68, **Fig. 1A**). At d14, c^{SF}_{HA} from PRG4 and HA+PRG4 groups was higher than that of HA alone (+41-42%, P<0.05). At d28, c^{SF}_{HA} from the HA+PRG4 group was higher than that of saline (+61%, P<0.05). Compared to CTRL (2.37±0.20 mg/mL), c^{SF}_{HA} was decreased at d7 and d14 for all therapies (-37% to -56%, P<0.001). At d28, only saline and HA only groups were decreased (-29% to -35%, P<0.05), while PRG4 and HA+PRG4 therapies were not different from CTRL (P=0.06-1.00). Non-OP c^{SF}_{HA} did not vary by group (P=0.08, **Fig. 1F**). For pairs of ACLT and Non-OP knees at d28, c^{SF}_{HA} was decreased in ACLT knees treated with PRG4 (-20%, P<0.05), but not for other groups (P=0.16-0.46).

c^{SF}_{HA} in both ACLT and Non-OP joints was comprised of primarily high M_r HA, with very little total c^{SF}_{HA} at lower M_r ranges (<1.0 Md, **Fig. 1**). c^{SF}_{HA} at high HA M_r (2.5-7.0 Md) decreased variably over time following ACLT (**Fig. 1B**). Compared to CTRL $c^{SF}_{HA,2.5\text{-}7}$ (1.72±0.19 mg/mL), ACLT values were decreased for all groups at d7 and d14 (-39% to -66%, P<0.001), but only for saline and HA injections at d28 (-33% to -45% vs. CTRL, P<0.05, **Fig. 1B**). At d28, ACLT $c^{SF}_{HA,2.5\text{-}7}$ in knees treated with PRG4 or HA+PRG4 were not different from CTRL (P=0.14-0.98), and $c^{SF}_{HA,2.5\text{-}7}$ from the HA+PRG4 group was higher than that of saline (+52%, P<0.05). Non-OP $c^{SF}_{HA,2.5\text{-}7}$ did not vary by group (P=0.32, **Fig. 1G**). For pairs of ACLT and Non-OP knees at d28, $c^{SF}_{HA,2.5\text{-}7}$ was decreased in ACLT knees treated from all groups (-32% to -39%, P<0.05) compared to $c^{SF}_{HA,2.5\text{-}7}$ in the contralateral Non-OP knee. For mid-range HA M_r (1.0-2.5 Md), compared to CTRL $c^{SF}_{HA,1\text{-}2.5}$ values of 0.34±0.05 mg/mL, ACLT c^{SF}_{HA} M_r was decreased only at d7 for joints treated with PRG4 or HA+PRG4 (-47% to -52% vs. CTRL,

$P<0.01$, **Fig. 1C**). For HA in the lowest M_r ranges (<0.5 Md), ACLT c^{SF}_{HA} M_r for joints treated with saline was increased (+68% vs. CTRL, $P<0.05$) at d14 post-injury (**Fig. 1E**).

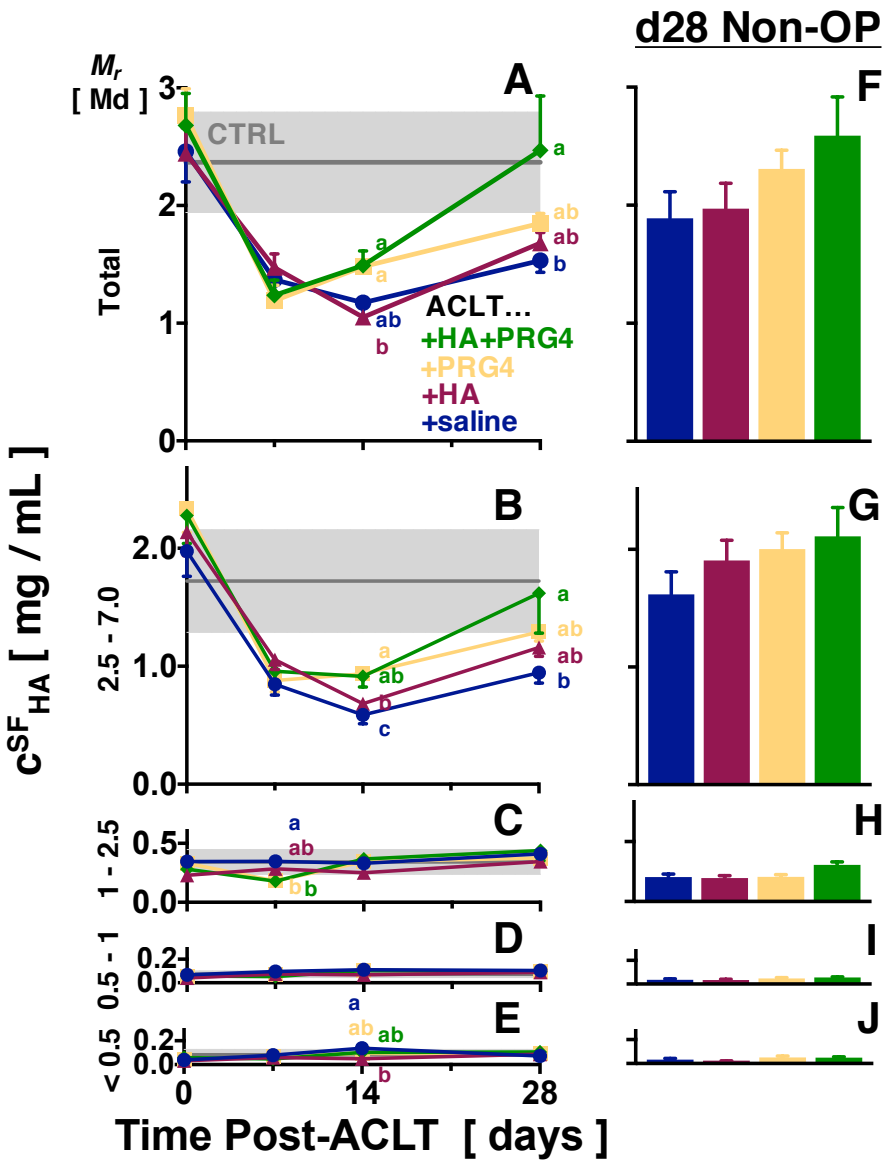

Figure 5.1: Effect of therapy on HA concentration (c^{SF}_{HA}) and M_r distribution in SF from ACLT knees. ACLT c^{SF}_{HA} distribution **(A)** overall, and in **(B)** 2.5-7.0, **(C)** 1.0-2.5, **(D)** 0.5-1.0, and **(E)** < 0.5 Md ranges. Non-OP day 28 c^{SF}_{HA} distribution **(F)** overall, and in **(G)** 2.5-7.0, **(H)** 1.0-2.5, **(I)** 0.5-1.0, and **(J)** < 0.5 Md ranges. Mean±SE, n=11-13, *P<0.05. CTRL values are mean±95% CI (■, n=9=16).

SF proteoglycan-4 composition is differentially affected by therapy following ACLT. ACLT c^{SF}_{PRG4} was affected by group at d14 and d28 post-injury (P<0.05, **Fig. 2A**). At d14, c^{SF}_{PRG4} in joints treated with HA+PRG4 was decreased compared to joints treated with HA alone (-46%, P<0.05). At d28, c^{SF}_{PRG4} from joints treated with PRG4 was increased compared to joints treated with saline (+44%, P<0.05). Compared to CTRL (159.6±13.97 μg/mL), c^{SF}_{PRG4} was decreased at d14 for joints treated with PRG4 and HA+PRG4 (-53% to -60%, P<0.001), and at d28 was decreased for joints treated with saline (-47%, P<0.01).

Serum and SF total protein concentration is variably affected by therapy following ACLT. ACLT $c^{S}_{protein}$ was affected by group at d7, 14, and 28 (P<0.01, **Fig. 2B**). At d7, $c^{S}_{protein}$ was increased in joints treated with PRG4 compared to those treated with saline or HA+PRG4 (+10-17%, P<0.01), and $c^{S}_{protein}$ this PRG4 group was increased at d14 and d28 compared to all other groups (+9-19%, P<0.01). Compared to CTRL (53.1±0.8 mg/mL), ACLT $c^{S}_{protein}$ was increased for rabbits treated with PRG4 at d7, 14, and 28 (+13-22%, P<0.001).

ACLT $c^{SF}_{protein}$ was affected by group at d28 (P<0.05), but there were no differences between individual groups (**Fig. 2B**). ACLT $c^{SF}_{protein}$ was not affected by group at other time points (P=0.13-0.71). Compared to CTRL (18.6±1.2 mg/mL), ACLT $c^{SF}_{protein}$ was increased in all treated knees at d7, 14, and 28 (+51-70%, P<0.001), but not at d0 (P=0.55). For pairs of ACLT and Non-OP knees at d28, $c^{SF}_{protein}$ was increased in ACLT knees in all groups (+23-62%, P<0.05, **Fig. 2D**).

SF to serum ratio is affected by therapy following ACLT. ACLT $k^{SF:S}$ was affected by group at d7, 14, and 28 (P<0.01, **Fig. 2C**). At d7, there were no differences in $k^{SF:S}$ between individual groups (P=0.07-1.00). At d14, $k^{SF:S}$ was increased in ACLT joints treated with HA compared to those treated with PRG4 (+16%, P<0.01). At d28, $k^{SF:S}$ was increased in ACLT

joints treated with saline compared to those treated with all lubricant therapies (+15-22%, $P<0.01$). Compared to CTRL (0.35±0.01), ACLT $k^{SF:S}$ was increased for rabbits treated with all therapies at d7, 14, and 28 (+33-66%, $P<0.001$). For pairs of ACLT and Non-OP knees at d28, $k^{SF:S}$ was increased in ACLT knees in all groups (+15-81%, $P<0.05$, **Fig. 2E**).

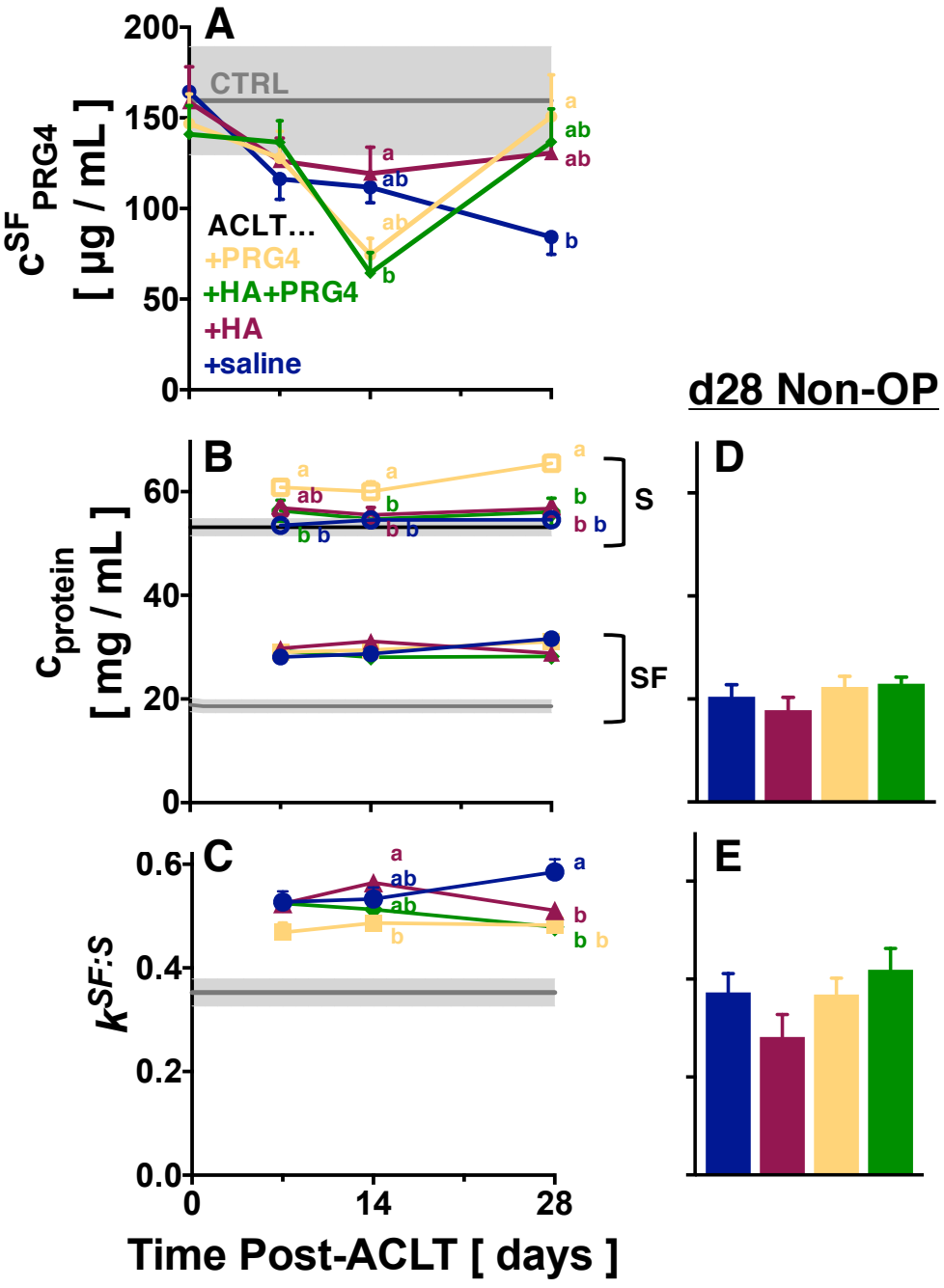

Figure 5.2: Effect of lubricant therapy on (A) c^{SF}_{PRG4}, (B) concentration ratios, $k^{SF:S}$, for SF & serum, & (C) protein concentrations, $c_{protein}$ following ACLT. Non-OP day 28 **(D)** $c^{SF}_{protein}$ and **(E)** $k^{SF:S}$. Mean±SE, n=5-13, different letters denote $P<0.05$ for 1wANOVA across groups. CTRL values are mean±95% CI (■, n=16-31).

V^{SF} and total lubricant mass were variably affected by therapy following ACLT. ACLT V^{SF} was affected by group at d7 and d14 post-injury (P<0.05, **Fig. 3A**), but not at d28 (P=0.78). Notably, at d14, V^{SF} was increased in joints treated with PRG4 and HA+PRG4 compared to those with treated with saline alone (+132-171%, P<0.05), and was also increased in joints treated with HA+PRG4 vs. HA alone (+58%, P<0.05). Compared to CTRL (25.6±2.7 μl), V^{SF} was increased in all treatment groups but saline at d7 (+929-1455%, P<0.001), and for all treatment groups at 14 and 28 post-injury (+1054-3039%, P<0.001), but not at d0 (P=0.39). For pairs of ACLT and Non-OP knees at d28, V^{SF} was increased in ACLT knees in all groups (+1903-3234%, P<0.05, data not shown).

ACLT m^{SF}_{HA} was affected by group at d14 (P<0.001, **Fig. 3B**). At this intermediate time point, compared to joints treated with saline, m^{SF}_{HA} was higher in those treated with HA, PRG4, and HA+PRG4 (+48-252%, P<0.001). Compared to CTRL (60.3±0.2 μg), m^{SF}_{HA} was higher in all treatment groups but saline (P=0.52) at d7 (+549-714%, P<0.001), and for all treatment groups at d14 and d28 post-injury (+474-1922%, P<0.05), but not at d0 (P=0.34). For pairs of ACLT and Non-OP knees at d28, m^{SF}_{HA} was increased in ACLT knees in all groups (+1516-2634%, P<0.05, data not shown).

ACLT m^{SF}_{PRG4} was affected by group at d7 post-injury (P<0.05, **Fig. 3C**). m^{SF}_{PRG4} from joints treated with PRG4 or HA+PRG4 were increased compared to joints treated with saline alone (+65-68%, P<0.05). Compared to CTRL (3.14±0.74 μg), m^{SF}_{PRG4} was increased at d7 for joints treated with HA, PRG4, and HA+PRG4 (+969-1574%, P<0.001), at d14 for all groups (+1053-1883%, P<0.001), and at d28 for joints treated with saline and HA+PRG4 (+963-2174%, P<0.001). There was no difference from CTRL m^{SF}_{PRG4} for all groups at d0 (P=0.60).

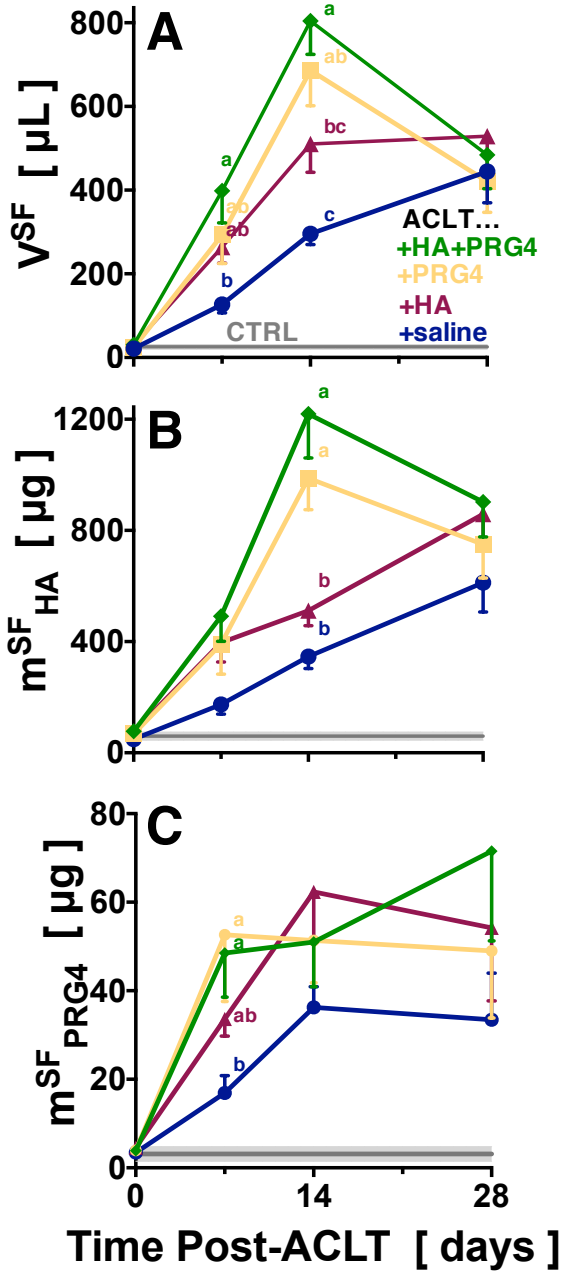

Figure 5.3: Effect of therapy on V^{SF}, m^{SF}_{HA}, and m^{SF}_{PRG4} following ACLT. Non-OP day 28 **(F)** V^{SF} and **(E)** m^{SF}_{HA}. Mean±SE, n=5-13/grp, different letters denote $P<0.05$ for 1wANOVA across groups. CTRL values are mean±95% CI (■, n=10=26).

SL permeability is differentially affected by therapy following ACLT. $k^{SF:S}$ was variably affected by therapy following ACLT, depending on protein M_r range (**Fig. 4**). In high M_r bins (345-735 kd), $k^{SF:S}$ was affected by group at d14 and d28 (P<0.05) but not at d7 (P=0.38, **Fig. 4A**). At d14, $k^{SF:S}_{345\text{-}735}$ was increased in joints treated with HA compared to those treated with PRG4 and HA+PRG4 (+18-19%, P<0.05). At d28, $k^{SF:S}_{345\text{-}735}$ was increased in joints treated with saline compared to those treated with HA, PRG4, or HA+PRG4 (+34-60%, P<0.05). For pairs of ACLT and Non-OP knees at d28, $k^{SF:S}_{345\text{-}735}$ was increased in ACLT knees in all groups (+53-117%, P<0.05, data not shown). In mid-range M_r bins (105-210 kd), $k^{SF:S}$ was not affected by group at any time point (P=0.05-0.47, **Fig. 4B**). For pairs of ACLT and Non-OP knees at d28, $k^{SF:S}_{105\text{-}210}$ was increased in ACLT knees in all groups (+39-57%, P<0.01, data not shown). In low M_r bins (20-28 kd), $k^{SF:S}$ was affected by group at d14 and d28 (P<0.01) but not at d7 (P=0.90, **Fig. 4A**). At d14, $k^{SF:S}_{20\text{-}28}$ was increased in joints treated with saline, HA, and HA+PRG4 compared to those treated with PRG4 alone (+19-28%, P<0.05). At d28, $k^{SF:S}_{20\text{-}28}$ was increased in joints treated with saline compared to those treated with HA, PRG4, or HA+PRG4 (+47-53%, P<0.05). For pairs of ACLT and Non-OP knees at d28, $k^{SF:S}_{20\text{-}28}$ was increased in ACLT knees in all groups (+24-84%, P<0.05, data not shown) except for saline, for which there was a trend towards an ACLT increase at d28 (+36%, P=0.06).

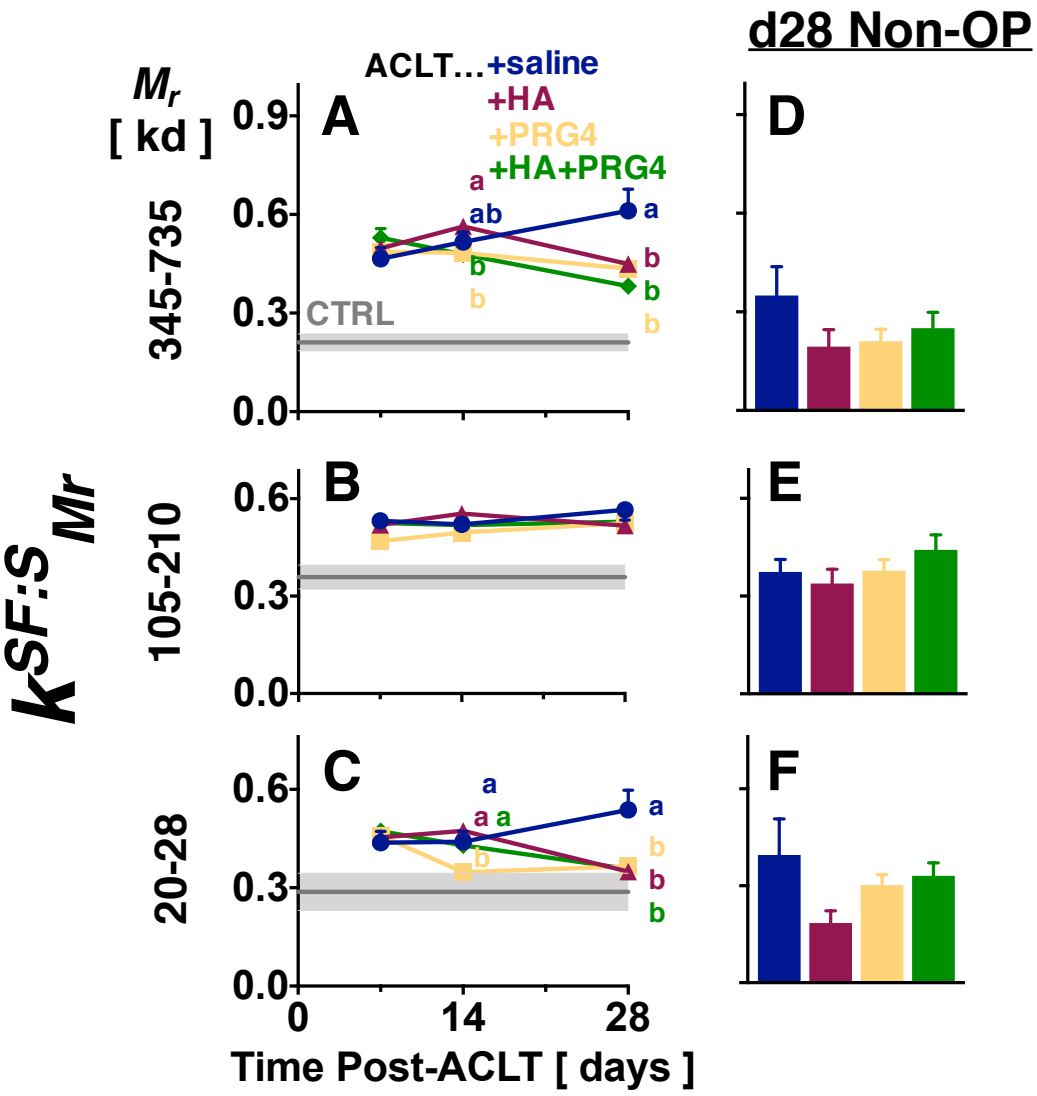

Figure 5.4: Effect of lubricant therapy on ACLT $k^{SF:S}$ in different M_r ranges: (A) high (345-735 kd), **(B)** mid-range (210-345 kd), and **(C)** low (20-28 kd). Non-OP d28 $k^{SF:S}$ in **(D)** 345-735 kd, **(E)** 210-345 kd, and **(F)** 20-28 kd ranges**.** Mean±SE, n=11-13, different letters denote $P<0.05$ for 1wANOVA across groups. CTRL values are mean±95% CI (■, n=14).

Increase in ACLT $k^{SF:S}$ is correlated with decreased c^{SF}_{HA} for certain groups. For all groups combined, HA and total protein $k^{SF:S}$ were related, with c^{SF}_{HA} decreased with increasing $k^{SF:S}$ (r^2=0.17, P<0.0001, **Fig. 5A**). The relationship between ACLT $k^{SF:S}$ and $c^{SF}_{HA,Mr}$ varied with M_r. $c^{SF}_{HA,2.5\text{-}7\ Md}$ decreased with increasing $k^{SF:S}$ (r^2=0.17, P<0.0001, **Fig. 5B-D**), but $c^{SF}_{HA,1\text{-}2.5\ Md}$, $c^{SF}_{HA,0.5\text{-}1\ Md}$, and $c^{SF}_{HA,<0.5Md}$ did not (P=0.10-0.68).

$N^{SL,FLS}$ was variably affected by therapy following ACLT, but not HAS2 and PRG4 expression. ACLT $N^{SL,FLS}$ was affected by group at d28 post-injury (P<0.05, **Fig. 6A**). Joints treated with PRG4 and HA+PRG4 were increased compared to those treated with saline (+82-87%, P<0.05). Compared to CTRL (48.8±10.5 million cells), $N^{SL,FLS}$ was increased in all treatment groups (+249-313%, P<0.001) except for saline, for which there was a trend towards an increase (+121%, P=0.10). Neither SL *HAS2* nor *PRG4* gene expression were affected by treatment group at d28 (P=0.17-0.96, **Fig. 6B,C**). Compared to CTRL SL *HAS2* expression (0.004±0.001), values were increased in all treatment groups (181-212%, P<0.001). Compared to CTRL SL *PRG4* expression (2.30±0.17), values were decreased for all treatment groups (-74% to-89%, P<0.001).

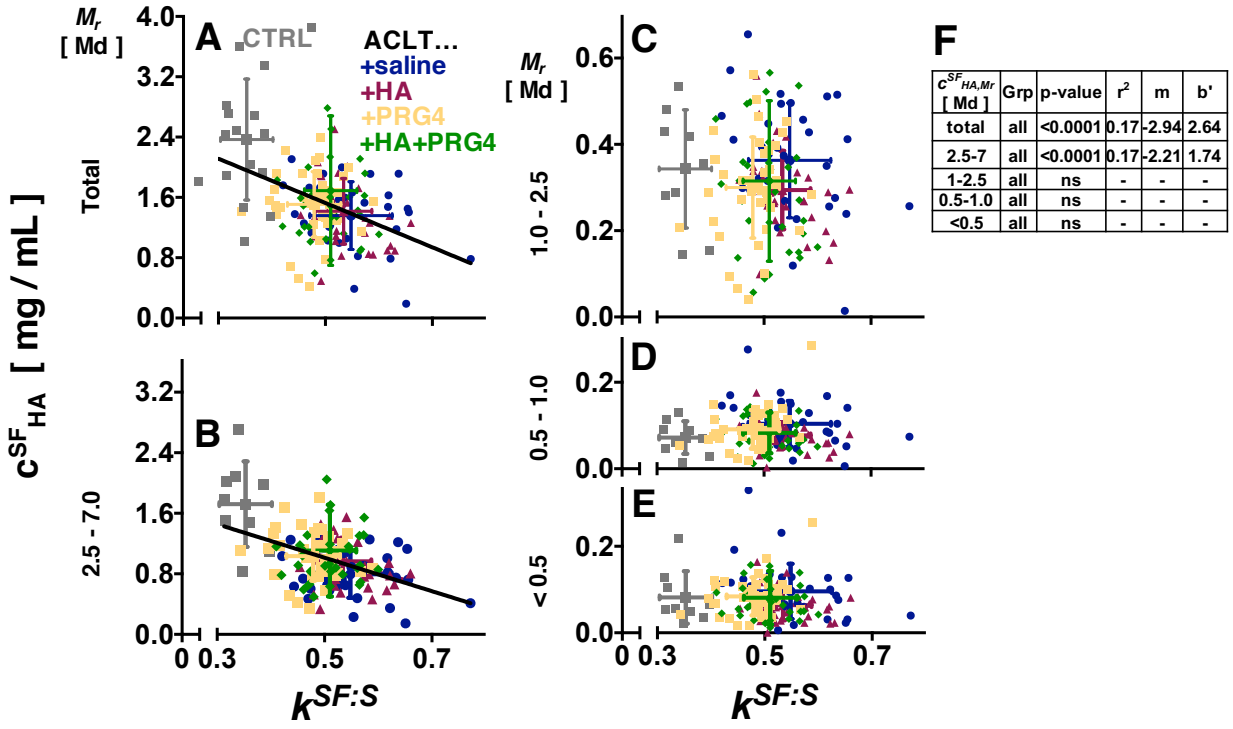

$c^{SF}_{HA,Mr}$ [Md]	Grp	p-value	r^2	m	b'
total	all	<0.0001	0.17	-2.94	2.64
2.5-7	all	<0.0001	0.17	-2.21	1.74
1-2.5	all	ns	-	-	-
0.5-1.0	all	ns	-	-	-
<0.5	all	ns	-	-	-

Figure 5.5: Correlation between $k^{SF:S}$ & (A) total c^{SF}_{HA}, (B) $c^{SF}_{HA,2.5\text{-}7.0}$, (C) $c^{SF}_{HA,1.0\text{-}2.5}$, (D) $c^{SF}_{HA,0.5\text{-}1.0}$, & (E) $c^{SF}_{HA,<0.5}$ for all experimental groups combined. n=31-39/grp, large symbols are for group mean±SD. **(F)** Table of r^2 and best fit values for regression lines. b' values are adjusted to account for the $k^{SF:S}$ and c^{SF}_{HA} values of CTRL samples (n=9-16).

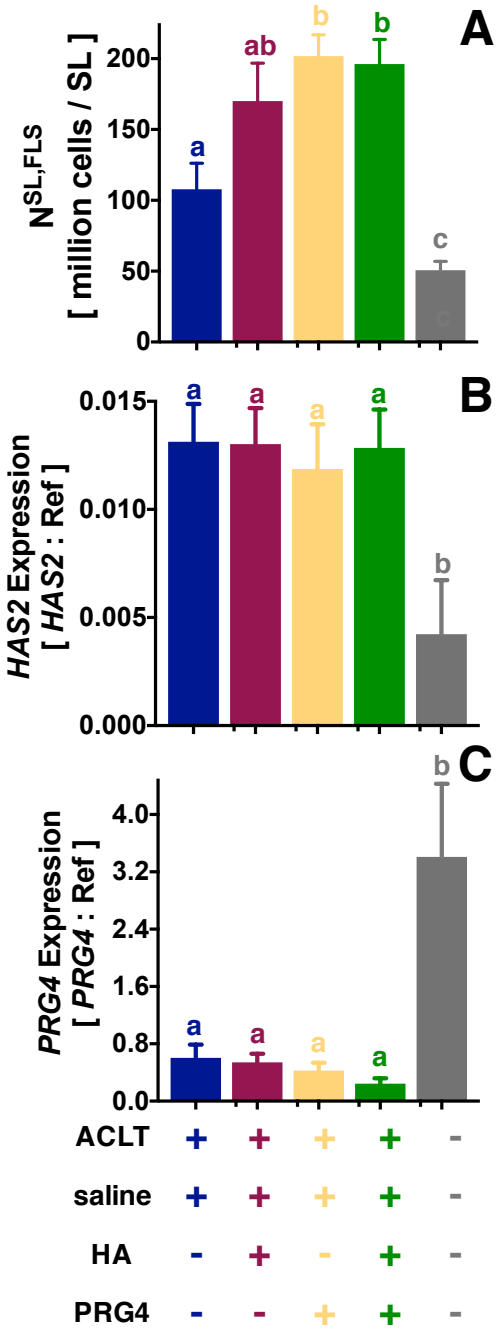

Figure 5.6: Effect of therapy on $N^{SL,FLS}$ and lubricant gene expression. **(A)** $N^{SL,FLS}$, **(B)** *HAS2*, and **(C)** *PRG4* expression. Mean±SE, n=11-13, different letters denote $P<0.05$ for 1wANOVA across groups. CTRL values are mean±95% CI (■, n=11-21).

5.5 Discussion

In this study, the effects of intra-articular lubricant therapy on SF composition and SL properties were evaluated. Following ACLT, V^{SF} increased substantially by d28 (+1054-3039% vs. CTRL, **Fig. 3A**). The time-course of changes to V^{SF} depended on IA injection, with V^{SF} reaching a peak at d14 for injections of PRG4 and HA+PRG4 (+132-171% vs. saline) before decreasing by d28; in contrast, V^{SF} from knees treated with saline or HA continually increased over the 28 days. This increase in V^{SF} reduced the concentrations of lubricants to some extent, as expected (dilution effects) [43, 46]. c^{SF}_{HA} was decreased at d7 and d14 for all groups (-37% to -56% vs. CTRL, **Fig. 1A**), but at d28 had recovered to CTRL levels in knees treated with PRG4 and HA+PRG4, despite the large V^{SF} in these knees (**Fig. 3A**). This recovery in c^{SF}_{HA} is likely due to a combination of biological and biophysical factors. m^{SF}_{HA} was increased in all groups at d28 (+914-1480% vs. CTRL, **Fig. 3B**), likely due to an increase in HA synthesis, as *HAS2* expression was substantially increased in all treatment groups at d28 (+181-212% vs. CTRL, **Fig. 6B**) as well as an increase in the number of FLS producing HA ($N^{SL,FLS}$, +249-313% vs. CTRL, **Fig. 6A**). c^{SF}_{HA} was also likely increased at d28 in select groups (PRG4, HA+PRG4) due to a reduction in HA efflux from the joint; $k^{SF:S}$, and specifically that for highest M_r proteins evaluated, $k^{SF:S}_{435\text{-}735}$, were reduced in joints treated with lubricants compared to those treated with saline (-34% to -60% vs. saline, **Fig. 2C**, **3A**). Thus, the recovery of CTRL c^{SF}_{HA} in certain viscosupplement joints can be attributed to a combination of measured (increased cell density and *HAS2* expression) and theoretical (decreased efflux) joint changes.

Similarly, c^{SF}_{PRG4} was decreased early (-53% to -60% vs. CTRL, d14, **Fig. 2A**) for joints treated with PRG4 and HA+PRG4, likely due to the substantial dilution of m^{SF}_{PRG4} (**Fig. 3C**) by V^{SF} (**Fig. 3A**). By d28, c^{SF}_{PRG4} had recovered to CTRL values for these joints. The increase in

c^{SF}_{PRG4} is likely not due to increased synthesis (as it is for HA), as *PRG4* expression was decreased across all groups at d28 (-74% to -89%, **Fig. 6C**), to a greater extent than was the increase in $N^{SL,FLS}$ vs. CTRL (**Fig. 6A**). For groups treated with PRG4 and HA+PRG4, c^{SF}_{PRG4} may be restored by a viscosupplement-mediated decrease in apparent SL permeability (as suggested by $k^{SF:S}$ data). Notably, c^{SF}_{PRG4} in joints treated with HA alone was not different from CTRL at any time point, suggesting that exogenous HA reduced PRG4 loss from the joint. In summary, c^{SF}_{HA} and c^{SF}_{PRG4} dynamics can be attributed to different biological (synthesis) but similar biophysical (transport) mechanisms. The restoration of these SF lubricant concentrations from an early decrease post-ACLT by IA injection of PRG4 alone or HA+PRG4 suggests that such therapies may be effective in maintaining lubricant concentrations, and therefore functionality [16, 45, 52], post-injury.

The variables measured in this study may be affected by a number of factors. The experimental assessment of SF dynamics compared ACLT, Non-OP, and CTRL knees. In this study, a paired, contralateral limb study design was employed to take advantage of intra-subject consistency. However, there are limitations with using an internal control, including potential systemic effects of local injury. However, since Non-OP joints were only sampled at d28, acute inflammation-mediated systemic effects are not expected to affect measurements in these knees. In ACLT knees, multiple injections likely caused minor inflammation, as evidenced by increased $c^{S}_{protein}$, $c^{SF}_{protein}$, and V^{SF} in these knees (**Fig. 2B, Fig. 3A**). One limitation of the study is that some joint tissues (cartilage, meniscus, ligaments) were not evaluated for cellular or biomolecular changes following injury. In addition to SF, SL was analyzed for biochemical changes (increases in $N^{SL,FLS}$, changes in *HAS2* and *PRG4* expression) because it is a major contributor of HA [46] and PRG4 [43] in SF, as well as a barrier to molecular efflux from the joint [12, 44]. The

analyses here focus on SF and SL dynamics, as these joint tissues are most likely to be targeted by therapies.

ACLT-induced changes in, and effect of IA therapies on, the joint variables c^{SF}_{HA} and c^{SF}_{PRG4} (both initially decreased and then increased with select treatments, **Fig. 1, Fig. 2A**), V^{SF} (substantially increased, **Fig. 3A**), $k^{SF:S}_{Mr}$ (initially increased and then decreased with select therapies, **Fig. 2B,C, Fig. 4**), $N^{SL,FLS}$ (substantially increased, **Fig. 6A**), and SL *HAS2* and *PRG4* expression (increased and decreased, respectively, **Fig. 6B, C**) were consistent with, and extended, prior analyses in different model systems at limited time points. In rabbits, c^{SF}_{HA} and c^{SF}_{PRG4} have been reported as ~2.5 mg/mL [38] and ~280 μg/mL [16], with reduced c^{SF}_{HA} and c^{SF}_{PRG4} measured following acute injury [16, 38, 46], similar to the values and trends noted here. A large increase in V^{SF} was also noted in previous studies (+70-1100%) of rabbit knees following acute injury [35, 38]. $k^{SF:S}$ has previously been studied following ACLT in rabbits (without therapeutic intervention) in our lab, with increased $k^{SF:S}$ in ACLT knees, especially for proteins in high (345-735 kd) and low (20-28 kd) protein bins [44], similar to the trends measured here (**Fig. 2C**, **4**). While the increases in $k^{SF:S}_{Mr}$ here are much larger than previously noted in rabbits following ACLT, minor inflammation induced by serial injections increased $c^{SF}_{protein}$ (**Fig. 2B**), likely causing associated increases in $k^{SF:S}_{Mr}$ (**Fig. 4**). An increase in $N^{SL,FLS}$ (**Fig. 6A**) in models of experimental OA has been shown previously [9, 36], although the mechanism for this proliferation is still unclear. Increased *HAS2* expression (**Fig. 6B**) following injury may be due to biochemical (cytokine) and mechanical (stretch) factors. During joint inflammation, cytokines are released and include IL-1β and TNF-α [19], both of which induce *HAS* expression and HA secretion in cultured FLS [7, 47]. Additionally, FLS are mechano-sensitive, and large increases in V^{SF} due to joint swelling cause stretch [39], and may induce FLS to secrete more HA [13, 41]

and proliferate (increasing $N^{SL,FLS}$). Decreased *PRG4* expression (**Fig. 6C**) was also noted in rat SL at early time post-injury [15], and this decrease may be due to increased IL-1β during acute inflammation [19, 31].

Because SF lubricant function depends on c^{SF}_{PRG4} and c^{SF}_{HA} [16, 45, 52], a detailed understanding of, and ability to quantify, the underlying basis for changes during joint injury and following therapeutic administration is useful to target pathogenesis. These results collectively implicate increases in $N^{SL,FLS}$ and predicted HA secretion for the recovery of c^{SF}_{HA} in joints treated with PRG4 and HA+PRG4, as well as decreases in $k^{SF:S}$, and specifically $k^{SF:S}_{435\text{-}735}$, for the recovery of both c^{SF}_{HA} and c^{SF}_{PRG4} in these treatment groups, likely through a reduction in lubricant efflux. The SL, with its relatively large surface area [21, 27, 46] and high FLS cell density [21, 46], appears to be the primary source of both HA [46] and PRG4 [43] in the SF. Therefore, changes to SL cellularity and composition, and thus SL architecture, have implications for the maintenance of SF lubricant properties [44]. SL, in addition to SF, may serve as a target for preventing PTOA progression. While *in vivo* lubricant restoration by HA [57, 58, 65] or PRG4 [17, 22, 23] alone has been evaluated, few studies [62] have considered the potential synergistic effects of their administration in combination. The results presented here suggest that early and sequential administration of both HA and PRG4 post-injury may attenuate decreases in SF lubricant composition and function that lead to joint degeneration in PTOA.

5.6 Acknowledgments

This chapter, in full, will be submitted to *Osteoarthritis and Cartilage*. The dissertation author was the primary author and thanks co-authors Julian J. Garcia, Barbara L. Schumacher, Junichi Yamada, Shingo Miyazaki, Raeek Rahman, Rebecca L. Drake, Gary S. Firestein, Robert L. Sah, and Koichi Masuda. This work was supported by research grants from the National Institutes of Health (R01 AR055637, T32 AR060712), the Department of Defense (DOD OR13085), the UC San Diego Frontiers of Innovation Scholarship Program, and the San Diego Fellowship.

The authors thank Dr. Samuel Ward and Dr. Gregory Heldt for use of CTRL rabbit tissue.

5.7 References

1. Abubacker S, Dorosz SG, Ponjevic D, Jay GD, Matyas JR, Schmidt TA: Full-length recombinant human proteoglycan 4 interacts with hyaluronan to provide cartilage boundary lubrication. *Ann Biomed Eng* 44:1128-37, 2016.

2. Ai M, Cui Y, Sy MS, Lee DM, Zhang LX, Larson KM, Kurek KC, Jay GD, Warman ML: Anti-lubricin monoclonal antibodies created using lubricin-knockout mice immunodetect lubricin in several species and in patients with healthy and diseased joints. *PLoS One* 10:e0116237, 2015.

3. Antonacci JM, Schmidt TA, Serventi LA, Cai MZ, Shu YL, Schumacher BL, McIlwraith CW, Sah RL: Effects of equine joint injury on boundary lubrication of articular cartilage by synovial fluid: role of hyaluronan. *Arthritis Rheum* 64:2917-26, 2012.

4. Atarod M, Ludwig TE, Frank CB, Schmidt TA, Shrive NG: Cartilage boundary lubrication of ovine synovial fluid following anterior cruciate ligament transection: a longitudinal study. *Osteoarthritis Cartilage* 23:640-7, 2015.

5. Ballard BL, Antonacci JM, Temple-Wong MM, Hui AY, Schumacher BL, Bugbee WD, Schwartz AK, Girard PJ, Sah RL: Effect of tibial plateau frracture on lubrication function and composition of synovial fluid. *J Bone Joint Surg Am* 94:e64(1-9), 2012.

6. Bartok B, Firestein GS: Fibroblast-like synoviocytes: key effector cells in rheumatoid arthritis. *Immunol Rev* 233:233-55, 2010.

7. Blewis ME, Lao BJ, Schumacher BL, Bugbee WD, Sah RL, Firestein GS: Interactive cytokine regulation of synoviocyte lubricant secretion. *Tissue Eng Part A* 16:1329-37, 2010.

8. Blewis ME, Nugent-Derfus GE, Schmidt TA, Schumacher BL, Sah RL: A model of synovial fluid lubricant composition in normal and injured joints. *Eur Cell Mater* 13:26-39, 2007.

9. Boyd R, Walker E, Wu D, Lukoschek M, Burr DB, Radin E: Morphologic and morphometric changes in synovial membrane associated with mechanically induced osteoarthrosis. *Arthritis Rheum* 34:515-24, 1991.

10. Catterall JB, Stabler TV, Flannery CR, Kraus VB: Changes in serum and synovial fluid biomarkers after acute injury (NCT00332254). *Arthritis Res Ther* 12:R229, 2010.

11. Chang DG, Iverson EP, Schinagl RM, Sonoda M, Amiel D, Coutts RD, Sah RL: Quantitation and localization of cartilage degeneration following the induction of osteoarthritis in the rabbit knee. *Osteoarthritis Cartilage* 5:357-72, 1997.

12. Coleman PJ, Scott D, Abiona A, Ashhurst DE, Mason RM, Levick JR: Effect of depletion of interstitial hyaluronan on hydraulic conductance in rabbit knee synovium. *J Physiol* 509 (Pt 3):695-710, 1998.

13. Coleman PJ, Scott D, Ray J, Mason RM, Levick JR: Hyaluronan secretion into the synovial cavity of rabbit knees and comparison with albumin turnover. *J Physiol* 503 (Pt 3):645-56, 1997.

14. Elsaid KA, Fleming BC, Oksendahl HL, Machan JT, Fadale PD, Hulstyn MJ, Shalvoy R, Jay GD: Decreased lubricin concentrations and markers of joint inflammation in the synovial fluid of patients with anterior cruciate ligament injury. *Arthritis Rheum* 58:1707-15, 2008.

15. Elsaid KA, Jay GD, Chichester CO: Reduced expression and proteolytic susceptibility of lubricin/superficial zone protein may explain early elevation in the coefficient of friction in the joints of rats with antigen-induced arthritis. *Arthritis Rheum* 56:108-16, 2007.

16. Elsaid KA, Jay GD, Warman ML, Rhee DK, Chichester CO: Association of articular cartilage degradation and loss of boundary-lubricating ability of synovial fluid following injury and inflammatory arthritis. *Arthritis Rheum* 52:1746-55, 2005.

17. Flannery CR, Zollner R, Corcoran C, Jones AR, Root A, Rivera-Bermudez MA, Blanchet T, Gleghorn JP, Bonassar LJ, Bendele AM, Morris EA, Glasson SS: Prevention of cartilage degeneration in a rat model of osteoarthritis by intraarticular treatment with recombinant lubricin. *Arthritis Rheum* 60:840-7, 2009.

18. Gelber AC, Hochberg MC, Mead LA, Wang NY, Wigley FM, Klag MJ: Joint injury in young adults and risk for subsequent knee and hip osteoarthritis. *Ann Intern Med* 133:321-8, 2000.

19. Goldring MB: Osteoarthritis and cartilage: the role of cytokines. *Curr Rheumatol Rep* 2:459-65, 2000.

20. Grissom MJ, Temple-Wong MM, Adams MS, Tom M, Schumacher BL, McIlwraith CW, Goodrich LR, Chu CR, Sah RL: Synovial fluid lubricant properties are transiently deficient after arthroscopic articular cartilage defect repair with platelet-enriched fibrin alone and with mesenchymal stem cells. *Orthop J Sports Med* 2:2325967114542580, 2014.

21. Ingram KR, Wann AK, Angel CK, Coleman PJ, Levick JR: Cyclic movement stimulates hyaluronan secretion into the synovial cavity of rabbit joints. *J Physiol* 586:1715-29, 2008.

22. Jay GD, Elsaid KA, Kelly KA, Anderson SC, Zhang L, Teeple E, Waller K, Fleming BC: Prevention of cartilage degeneration and gait asymmetry by lubricin tribosupplementation in the rat following acl transection. *Arthritis Rheum* 64:1162-71, 2012.

23. Jay GD, Fleming BC, Watkins BA, McHugh KA, Anderson SC, Zhang LX, Teeple E, Waller KA, Elsaid KA: Prevention of cartilage degeneration and restoration of chondroprotection by lubricin tribosupplementation in the rat following anterior cruciate ligament transection. *Arthritis Rheum* 62:2382-91, 2010.

24. Jay GD, Tantravahi U, Britt DE, Barrach HJ, Cha CJ: Homology of lubricin and superficial zone protein (SZP): products of megakaryocyte stimulating factor (MSF) gene expression by human synovial fibroblasts and articular chondrocytes localized to chromosome 1q25. *J Orthop Res* 19:677-87, 2001.

25. Kiener HP, Watts GF, Cui Y, Wright J, Thornhill TS, Skold M, Behar SM, Niederreiter B, Lu J, Cernadas M, Coyle AJ, Sims GP, Smolen J, Warman ML, Brenner MB, Lee DM: Synovial fibroblasts self-direct multicellular lining architecture and synthetic function in three-dimensional organ culture. *Arthritis Rheum* 62:742-52, 2010.

26. Kim YJ, Sah RLY, Doong JYH, Grodzinsky AJ: Fluorometric assay of DNA in cartilage explants using Hoechst 33258. *Anal Biochem* 174:168-76, 1988.

27. Knight AD, Levick JR: The density and distribution of capillaries around a synovial cavity. . *Q J Exp Physiol* 68:629-44, 1983.

28. Knox P, Levick JR, McDonald JN: Synovial fluid--its mass, macromolecular content and pressure in major limb joints of the rabbit. *Q J Exp Physiol* 73:33-45, 1988.

29. Kwiecinski JJ, Dorosz SG, Ludwig TE, Abubacker S, Cowman MK, Schmidt TA: The effect of molecular weight on hyaluronan's cartilage boundary lubricating ability--alone and in combination with proteoglycan 4. *Osteoarthritis Cartilage* 19:1356-62, 2011.

30. Lee HG, Cowman MK: An agarose gel electrophoretic method for analysis of hyaluronan molecular weight distribution. *Anal Biochem* 219:278-87, 1994.

31. Lee SY, Niikura T, Reddi AH: Superficial zone protein (lubricin) in the different tissue compartments of the knee joint: modulation by transforming growth factor beta 1 and interleukin-1 beta. *Tissue Eng Part A* 14:1799-807, 2008.

32. Levick JR: The influence of hydrostatic pressure on trans-synovial fluid movement and on capsular expansion in the rabbit knee. *J Physiol* 289:69-82, 1979.

33. Levick JR: Blood flow and mass transport in synovial joints. In: *Handbook of Physiology, Section 2, The Cardiovascular System, Volume IV, The Microcirculation,* ed. by M Renkin, Michel C, The American Physiological Society, 1984, 917-47.

34. Levick JR: Synovial fluid and trans-synovial flow in stationary and moving normal joints. In: *Joint loading: biology and health of articular structures* ed. by HJ Helminen, Kiviranta I, Säämänen AM, Tammi M, Paukkonen K, Wright & Sons, Bristol, 1987, 149-86.

35. Ludwig TE, McAllister JR, Lun V, Wiley JP, Schmidt TA: Diminished cartilage lubricating ability of human osteoarthritic synovial fluid deficient in proteoglycan 4: Restoration through proteoglycan 4 supplementation. *Arthritis Rheum* 64:3963-71, 2012.

36. Lukoschek M, Schaffler MB, Burr DB, Boyd RD, Radin EL: Synovial membrane and cartilage changes in experimental osteoarthrosis. *J Orthop Res* 6:475-92, 1988.

37. Mazzucco D, Scott R, Spector M: Composition of joint fluid in patients undergoing total knee replacement and revision arthroplasty: correlation with flow properties. *Biomaterials* 25:4433-45, 2004.

38. McCarty WJ, Cheng JC, Hansen BC, Yamaguchi T, Masuda K, Sah RL: The biophysical mechanisms of altered hyaluronan concentration in synovial fluid after anterior cruciate ligament transection. *Arthritis Rheum* 64:3993-4003, 2012.

39. McCarty WJ, Masuda K, Sah RL: Fluid movement and joint capsule strains due to flexion in rabbit knees. *J Biomech* 44:2761-7, 2011.

40. McGowan KB, Kurtis MS, Lottman LM, Watson D, Sah RL: Biochemical quantification of DNA in human articular and septal cartilage using PicoGreen and Hoechst 33258. *Osteoarthritis Cartilage* 10:580-7, 2002.

41. Momberger TS, Levick JR, Mason RM: Hyaluronan secretion by synoviocytes is mechanosensitive. *Matrix Biol* 24:510-9, 2005.

42. Neuman MK, Briggs KK, Masuda K, Sah RL, Watson D: A compositional analysis of cadaveric human nasal septal cartilage. *Laryngoscope* 123:2120-4, 2013.

43. Raleigh AR, Cravotta MJ, Garcia JJ, Schumacher BL, Kato K, Firestein GS, Masuda K, Sah RL: Decreased synovial fluid proteoglycan-4 concentration in ACL-transected knee joints is due to dynamic imbalance in biosynthesis, clearance, and effusion. *OARSI 2018 World Congress* 26:730, 2018.

44. Raleigh AR, Garcia JJ, Schumacher BL, Firestein GS, Masuda K, Sah RL: Synovial fluid: Serum ratio of protein concentration is increased in experimental osteoarthritis and inversely correlated with synovial fluid hyaluronan concentration. *Trans Orthop Res Soc* 43:509, 2018.

45. Raleigh AR, McCarty WJ, Chen AC, Meinert C, Klein TJ, Sah RL: Synovial joints: Mechanobiology and tissue engineering of articular cartilage and synovial fluid. In: *Comprehensive Biomaterials,* ed. by P Ducheyne, Healey KE, Hutmacher DE, Grainger DE, Kirkpatrick CJ, Elsevier, 2017, 107-34.

46. Raleigh AR, Sun Y, Qian D, Temple-Wong MM, Kato K, Murata K, Firestein GS, Masuda K, Sah RL: Synovial fluid hyaluronan fluctuation in post-traumatic osteoarthritis: Dependence on the dynamic balance between biosynthesis, loss, and fluid flux *Trans Orthop Res Soc* 42:1506, 2017.

47. Recklies AD, White C, Melching L, Roughley PJ: Differential regulation and expression of hyaluronan synthases in human articular chondrocytes, synovial cells and osteosarcoma cells. *Biochem J* 354:17-24, 2001.

48. Reesink HL, Watts AE, Mohammed HO, Jay GD, Nixon AJ: Lubricin/proteoglycan 4 increases in both experimental and naturally occurring equine osteoarthritis. *Osteoarthritis Cartilage* 25:128-37, 2017.

49. Samsom ML, Morrison S, Masala N, Sullivan BD, Sullivan DA, Sheardown H, Schmidt TA: Characterization of full-length recombinant human Proteoglycan 4 as an ocular surface boundary lubricant. *Exp Eye Res* 127:14-9, 2014.

50. Schmid T, Lindley K, Su J, Soloveychik V, Block J, Kuettner K, Schumacher B: Superficial zone protein (SZP) is an abundant glycoprotein in human synovial fluid and serum. *Trans Orthop Res Soc* 26:82, 2001.

51. Schmid TM, Su J-L, Lindley KM, Soloveychik V, Madsen L, Block JA, Kuettner KE, Schumacher BL: Superficial zone protein (SZP) is an abundant glycoprotein in human synovial fluid with lubricating properties. In: *The Many Faces of Osteoarthritis,* ed. by KE Kuettner, Hascall VC, Raven Press, New York, 2002, 159-61.

52. Schmidt TA, Gastelum NS, Nguyen QT, Schumacher BL, Sah RL: Boundary lubrication of articular cartilage: role of synovial fluid constituents. *Arthritis Rheum* 56:882-91, 2007.

53. Schmidt TA, Sah RL: Effect of synovial fluid on boundary lubrication of articular cartilage. *Osteoarthritis Cartilage* 15:35-47, 2007.

54. Schumacher BL, Block JA, Schmid TM, Aydelotte MB, Kuettner KE: A novel proteoglycan synthesized and secreted by chondrocytes of the superficial zone of articular cartilage. *Arch Biochem Biophys* 311:144-52, 1994.

55. Schumacher BL, Hughes CE, Kuettner KE, Caterson B, Aydelotte MB: Immunodetection and partial cDNA sequence of the proteoglycan, superficial zone protein, synthesized by cells lining synovial joints. *J Orthop Res* 17:110-20, 1999.

56. Schumacher BL, Schmidt TA, Voegtline MS, Chen AC, Sah RL: Proteoglycan 4 (PRG4) synthesis and immunolocalization in bovine meniscus. *J Orthop Res* 23:562-8, 2005.

57. Shimizu C, Yoshioka M, Coutts RD, Harwood FL, Kubo T, Hirasawa Y, Amiel D: Long-term effects of hyaluronan on experimental osteoarthritis in the rabbit knee. *Osteoarthritis Cartilage* 6:1-9, 1998.

58. Smith GN, Mickler EA, Myers SL, Brandt KD: Effect of intraarticular hyaluronan injection on synovial fluid hyaluronan in the early stage of canine post-traumatic osteoarthritis. *J Rheumatol* 28:1341-6, 2001.

59. Spicer AP, McDonald JA: Characterization and molecular evolution of a vertebrate hyaluronan synthase gene family. *J Biol Chem* 273:1923-32, 1998.

60. Swann DA, Slayter HS, Silver FH: The molecular structure of lubricating glycoprotein-I, the boundary lubricant for articular cartilage. *J Biol Chem* 256:5921-5, 1981.

61. Teeple E, Elsaid KA, Fleming BC, Jay GD, Aslani K, Crisco JJ, Mechrefe AP: Coefficients of friction, lubricin, and cartilage damage in the anterior cruciate ligament-deficient guinea pig knee. *J Orthop Res* 26:231-7, 2008.

62. Teeple E, Elsaid KA, Jay GD, Zhang L, Badger GJ, Akelman M, Bliss TF, Fleming BC: Effects of supplemental intra-articular lubricin and hyaluronic acid on the progression of posttraumatic arthritis in the anterior cruciate ligament-deficient rat knee. *Am J Sports Med* 39:164-72, 2011.

63. Temple-Wong MM, Ren S, Quach P, Hansen BC, Chen AC, Hasegawa A, D'Lima DD, Koziol J, Masuda K, Lotz MK, Sah RL: Hyaluronan concentration and size distribution in human knee synovial fluid: variations with age and cartilage degeneration. *Arthritis Res Ther* 18:18, 2016.

64. Wilder FV, Hall BJ, Barrett JP, Jr., Lemrow NB: History of acute knee injury and osteoarthritis of the knee: a prospective epidemiological assessment. The Clearwater Osteoarthritis Study. *Osteoarthritis Cartilage* 10:611-6, 2002.

65. Yoshioka M, Shimizu C, Harwood FL, Coutts RD, Amiel D: The effects of hyaluronan during the development of osteoarthritis. *Osteoarthritis Cartilage* 5:251-60, 1997.

66. Zhang D, Cheriyan T, Martin SD, Gomoll AH, Schmid TM, Spector M: Lubricin distribution in the torn human anterior cruciate ligament and meniscus. *J Orthop Res* 29:1916-22, 2011.

CHAPTER 6

CONCLUSIONS

6.1 Summary of Findings

The objectives of this work were to extend the understanding of the molecular and fluid dynamics in healthy joints and in those following acute injury with or without therapeutic administration. To address these objectives, novel approaches were taken. In summary, the novel methodologies were:

(A) Refinement of a continuous-time, compartmental mass balance model incorporating fluid fluxes, and application of this model to evaluate lubricant dynamics in rabbit knees following acute injury (**Chapter 2, 3**).

(B) Application of $k^{SF:S}$ over a continuous M_r range to elucidate changes in SL barrier function in healthy and PTOA joints (**Chapter 4**).

The major findings related to the scientific objectives were:

1. The decreases in lubricant concentrations c^{SF}_{HA} and c^{SF}_{PRG4} following ACLT are driven by different biological and biophysical mechanisms (**Chapter 2, 3**).

a. c^{SF}_{HA} is decreased despite increased HA secretion by SL and proliferation of FLS due to increased SF volume (diluting the mass of HA) and a substantial and increasing HA loss (via efflux and degradation) with time.

b. c^{SF}_{PRG4} is initially unchanged despite a substantial and immediate decrease in the secretion of PRG4 by both FLS and ACH, but is decreased at more chronic times following injury as PRG4 clearance increases.

2. SL transport is affected by ACLT at both acute and chronic time points, the former may be inflammation-mediated while the latter appears to be due to a chronic remodeling of the tissue (**Chapter 4**).

   a. Overall ACLT HA and total protein $k^{SF:S}$ were related, with c^{SF}_{HA} decreased with increasing $k^{SF:S}$ (r^2=0.39).

   b. Alterations in $k^{SF:S}$ provide a joint-scale metric of the extent to which ACLT affects trans-synovial transport and may help explain mechanistically why SF composition is altered in PTOA.

3. Select viscosupplement therapies, injected serially following ACLT, appear to attenuate the chronic reduction in both c^{SF}_{HA} and c^{SF}_{PRG4} that occurs during PTOA progression (**Chapter 5**).

   a. c^{SF}_{HA} was decreased at early times for all groups (-37% to -56% vs. CTRL), but at d28 had recovered to CTRL levels in ACLT knees treated with PRG4 and HA+PRG4, despite the large V^{SF} in these knees. A portion of the increase in m^{SF}_{HA} in these joints is likely due to increased HA synthesis, as *HAS2* expression (+181-212%) and $N^{SL,FLS}$ (+249-313%) were substantially increased at d28.

b. c^{SF}_{PRG4} was similarly decreased early (-53% to -60%) for joints treated with PRG4 and HA+PRG4, likely due to a similar dilution lubricant mass by V^{SF}. By d28, c^{SF}_{PRG4} had recovered to CTRL values for these joints, although the increase in c^{SF}_{PRG4} cannot be attributed to increased synthesis, as *PRG4* expression was decreased at d28 (-74% to -89%).

c. c^{SF}_{HA} and c^{SF}_{PRG4} were likely increased at d28 in select groups (PRG4, HA+PRG4, and HA alone for c^{SF}_{PRG4}) due to a reduction in lubricant efflux from the joint: $k^{SF:S}$, and specifically that for highest M_r proteins, $k^{SF:S}_{435\text{-}735}$, was reduced in joints treated with lubricants compared to those treated with saline (-34% to -60%).

6.2 Discussion

The current work can be expanded in the future in a number of ways. The mass balance model (**Chapter 2**) can be further refined by parsing the loss term ($L^{SF}_{i,total}$) into two components: loss due to efflux ($L^{SF}_{i,efflux}$) and loss due to degradation ($L^{SF}_{i,degradation}$). $L^{SF}_{i,efflux}$ from the SF to the lymphatics (across the SL barrier) can be estimated over a similar time course as that studied in the rabbit model of PTOA using a combination of experimental and theoretical measures. Using equations for advective and diffusive efflux presented in the Introduction (**Chapter 1**), SF variables (P^{SF}, π^{SF}) can be calculated from in vivo data for V^{SF} and $c^{SF}_{protein}$, respectively [7, 13]. Variables pertaining to SL barrier function ($\sigma^{SF\,|\,L}$, $k^{SF\,|\,L}$, $p^{SF\,|\,L}$) can be estimated from prior experimental data in rabbit knees [2, 8-12, 16-18]. Finally, variables pertaining to the lymphatics (P^{L}, π^{L}, $c^{L}_{protein}$) can either be approximated from prior data (of which there is little in the rabbit model), or else measured experimentally.

Because the combined experimental-theoretical model presented in **Chapter 2** and used in **Chapters 3** and **4** relies heavily on the generation term (G^{SF}_i), measurement of synthesis *in vivo* (without the use of *in vitro* cultures to estimate rates of secretion from lubricant gene expression) can be carried out using deuterated water (^2H_2O). Mass isotopomer distribution analysis (MIDA), also known as combinatorial analysis, allows for calculation of fractional synthesis rates of polymers (including proteins and glycosaminoglycans) from a small sample of tissue following heavy water (^2H_2O) labeling [4]. In previous studies, ^2H_2O has been administered to animals via drinking water, via an initial bolus of ^2H_2O followed by administration of ^2H_2O in the drinking water (*ad libitum*) for a range of time points from several weeks up to one year. [1, 3, 14.] Once incorporated, ^2H can be used to label freshly synthesized HA and protein (including PRG4), and may therefore serve as a dynamic index of changes to the rates of lubricant synthesis following injury. Only a minimal amount of tissue would need to be harvested at each time point, as Because MIDA techniques rely on the distribution of the isotopomeric species, they are not constrained by total mass recovery of the analyte of interest [4].

Finally, experimental measures to quantify SL matrix and cellular organization and density following ACLT would be useful to help define alterations in its barrier function during PTOA progression. Because the structure and organization of SL is often disrupted during joint harvest (thus precluding traditional histology techniques), 3D imaging of a joint with SL intact will likely yield novel conclusions related to the changes in this tissue in diseased states. One such 3D imaging method is digital volumetric imaging (DVI), which has been used previously to determine chondrocyte cellularity and variation by depth in for bovine tissue at different stages of development [5, 6]. Because there is a limitation to sample size with these methods, it may be

necessary to use a different animal model of PTOA (such as mouse [15]) so that the entire joint structure can be visualized. Anticipated findings from this type of analysis (for CTRL or Non-OP vs. ACLT) include accurate measures of FLS density, SL thickness and area, and proximity of SL to vascular or lymphatic structures (affording insight into the transport pathways into and out of the synovial cavity).

In summary, the mass balance model updated and used here for dynamic *in vivo* data can be further refined to allow for more comprehensive estimates for specific loss mechanisms, particularly those pertaining to molecular efflux from the SF. These suggested model enhancements may provide additional insight into mechanisms of therapeutic intervention (such as the IA viscosupplement injections evaluated in **Chapter 5**), with special attention paid to variables governing the SF-SL boundary and its maintenance as a barrier to macromolecule transport.

6.3 References

1. Busch R, Kim Y-K, Neese RA, Schade-Serin V, Collins M, Awada M, Gardner JL, Beysen C, Marino ME, Misell LM: Measurement of protein turnover rates by heavy water labeling of nonessential amino acids. *BBA* 1760:730-44, 2006.

2. Coleman PJ, Scott D, Abiona A, Ashhurst DE, Mason RM, Levick JR: Effect of depletion of interstitial hyaluronan on hydraulic conductance in rabbit knee synovium. *J Physiol* 509 (Pt 3):695-710, 1998.

3. Decaris ML, Gatmaitan M, FlorCruz S, Luo F, Li K, Holmes WE, Hellerstein MK, Turner SM, Emson CL: Proteomic analysis of altered extracellular matrix turnover in bleomycin-induced pulmonary fibrosis. *Mol Cell Proteomics* 13:1741-52, 2014.

4. Holmes WE, Angel TE, Li KW, Hellerstein MK: Dynamic proteomics: In vivo proteome-wide measurement of protein kinetics using metabolic labeling. *Methods Enzymol* 561:219-76, 2015.

5. Jadin KD, Bae WC, Schumacher BL, Sah RL: Three-dimensional (3-D) imaging of chondrocytes in articular cartilage: growth-associated changes in cell organization. *Biomaterials* 28:230-9, 2007.

6. Jadin KD, Wong BL, Bae WC, Li KW, Williamson AK, Schumacher BL, Price JH, Sah RL: Depth-varying density and organization of chondrocyte in immature and mature bovine articular cartilage assessed by 3-D imaging and analysis. *J Histochem Cytochem* 53:1109-19, 2005.

7. Knight AD, Levick JR: Pressure-volume relationships above and below atmospheric pressure in the synovial cavity of the rabbit knee. *J Physiol* 328:403-20, 1982.

8. Knight AD, Levick JR: Effect of fluid pressure on the hydraulic conductance of interstitium and fenestrated endothelium in the rabbit knee. *J Physiol* 360:311-32, 1985.

9. Knight AD, Levick JR, McDonald JN: Relation between trans-synovial flow and plasma osmotic pressure, with an estimation of the albumin reflection coefficient in the rabbit knee. *Q J Exp Physiol* 73:47-65, 1988.

10. Levick JR: An analysis of the effect of synovial capillary distribution upon trans-synovial concentration profiles and exchange. *Q J Exp Physiol* 69:289-300, 1984.

11. Levick JR: A two-dimensional morphometry-based model of interstitial and transcapillary flow in rabbit synovium. *Exp Physiol* 76:905-21, 1991.

12. Levick JR, McDonald JN: Synovial capillary distribution in relation to altered pressure and permeability in knees of anaesthetized rabbits. *J Physiol* 419:477-92, 1989.

13. Levick JR, McDonald JN: Viscous and osmotically mediated changes in fluid movement across synovium in response to intraarticular albumin. *Microvasc Res* 47:68-89, 1994.

14. Li KW, Siraj SA, Cheng EW, Awada M, Hellerstein MK, Turner SM: A stable isotope method for the simultaneous measurement of matrix synthesis and cell proliferation in articular cartilage in vivo. *Osteoarthritis Cartilage* 17:923-32, 2009.

15. Little CB, Hunter DJ: Post-traumatic osteoarthritis: from mouse models to clinical trials. *Nat Rev Rheumatol* 9:485-97, 2013.

16. Price FM, Levick JR, Mason RM: Changes in glycosaminoglycan concentration and synovial permeability at raised intra-articular pressure in rabbit knees. *J Physiol* 495 (Pt 3):821-33, 1996.

17. Scott D, Coleman PJ, Abiona A, Ashhurst DE, Mason RM, Levick JR: Effect of depletion of glycosaminoglycans and non-collagenous proteins on interstitial hydraulic permeability in rabbit synovium. *J Physiol* 511 (Pt 2):629-43, 1998.

18. Scott D, Coleman PJ, Mason RM, Levick JR: Glycosaminoglycan depletion greatly raises the hydraulic permeability of rabbit joint synovial lining. *Exp Physiol* 82:603-6, 1997.